# OPTIMAL DETECTION AND ESTIMATION FOR ECHO RANGING IN A RANDOMLY FADING ENVIRONMENT

# OPTIMAL DETECTION AND ESTIMATION FOR ECHO RANGING IN A RANDOMLY FADING ENVIRONMENT

by

JON WEI MARK

A Thesis
Submitted to the Faculty of Graduate Studies
in Partial Fulfilment of the Requirements
for the Degree
Master of Engineering

McMaster University
March 1968

MASTER OF ENGINEERING (1968)
(Electrical Engineering)

McMaster University
Hamilton, Ontario

TITLE: OPTIMAL DETECTION AND ESTIMATION FOR ECHO RANGING IN A RANDOMLY FADING ENVIRONMENT

AUTHOR: Jon Wei Mark, B.A.Sc. (University of Toronto, 1962)

SUPERVISOR: Professor N.K. Sinha

NUMBER OF PAGES: xiv, 150

SCOPE AND CONTENTS:

A conditionally biased maximum a posteriori criterion has been used to derive an optimal estimator-demodulator for the extraction of a signal propagated through a randomly fading medium. Practical realization of the estimator-demodulator takes the form of a self-synchronized (or tracking) receiver with amplitude estimation performed at baseband.

A combination of self-synchronized demodulation-estimation-correlation detection is conjectured to be optimum for the pseudo-random signalling employed.

Signal processing gain and dynamic range have been used as criteria of signal detectability. An analytical formula for signal processing gain, taking into account the code self-noise, has been derived. System performances have been evaluated by simulating the overall tracking echo ranging system in the IBM 7040 computer.

## ABSTRACT

A self-synchronized echo ranging system with optimum utilization of signal estimation and detection strategies has been designed and simulated. A binary convolution code has been utilized to modulate the transmitter signal. The random medium is modelled by a vector sum of a fixed and a random component; the medium fading process has a Rician distribution density. A channel estimator has been derived using a maximum a posteriori probability criterion. The estimator is an adaptive processor whereby the variance of the medium fading process is recomputed during each updating cycle. The estimator attempts to provide a coherent input to the correlator. An optimum processor for the signalling described is an ordered serial estimator-correlator combination. It is conjectured that the estimator offers an improvement in signal processing gain of approximately 5 dB over and above the non-optimized system. Accompanying this is an improvement in peak-to-sidelobe ratio and in false alarm probability. A 3 bit (8 level) quantized system is conjectured to be a 'good' trade-off between degradation in system performance and simplification in system implementation.

## ACKNOWLEDGEMENTS

I wish to thank Dr. N. K. Sinha for many stimulating discussions and encouragement given during the course of this work.

Acknowledgement is also made for the financial support of the National Research Council under grant A-3374.

I would also like to express my sincere thanks and appreciation to my wife, Betty, whose patience and encouragement permitted the completion of this work with the minimum of stress.

Also finally, I would like to thank Mrs. M. Kennard and Mrs. T. Kammermayer for typing this thesis.

TABLE OF CONTENTS

TABLE OF ILLUSTRATIONS

| FIGURE | | PAGE |
|---|---|---|

## NOMENCLATURE

| | |
|---|---|
| $s(t, \{a(t_o)\})$ | - transmitted signal |
| $\{a(t_o)\}$ | - Pseudo-random code (intelligence), a time function |
| $t_o$ | - digit or subpulse duration (baud length) |
| $\omega_o$ | - Angular carrier frequency |
| W | - signal bandwidth |
| N | - Code Length |
| T | - signal duration |
| $\xi(t)$ | - reverberation |
| $\gamma(t)$ | - complex channel fading process |
| $\phi(t)$ | - random phase of fading process |
| $b_t$ | - complex target strength |
| $\delta$ | - delay rate |
| $X(t, \delta, \gamma(t), b_t, \{a(t_o)\})$ | - target echo |
| $n(t)$ | - Additive noise |
| $m(t)$ | - Corrupted intelligence |
| $m^*(t)$ | - Conditional biased estimate of m(t) |
| $\phi_{\gamma\gamma}(t, y)$ | - Covariance function of channel fading random process |
| $\phi_{nn}$ | - Covariance function of Additive noise |
| $\sigma n^2$ | - Variance of Additive noise |
| $\varepsilon(t)$ | - Incoherent fluctuation after demodulation stage |

NOMENCLATURE (Continued)

| | |
|---|---|
| $\sigma_{\varepsilon}^{2}$ | - variance of incoherent fluctuation noise after demodulation stage |
| $E_s$ | - signal energy |
| $P_a$ | - Average signal power |
| $E\{\cdot\}$ | - Expected value of |
| $G$ | - Signal processing gain |
| $r_o$ | - output signal-to-noise power ratio |
| $r_i$ | - Input signal-to-noise power ratio |

# CHAPTER I

# INTRODUCTION

Fundamental to the design of an optimum detection system is an understanding of the statistics of the random variates that make up the propagation medium. These random variates, generally known as noise in information theory, can be signal dependent or signal independent. In any echo ranging situation both signal dependent and signal independent noises may be present. The signal independent noise, generally assumed to be gaussianly distributed and both spatially and temporally white, is easy to handle both mathematically and practically.

The ambiguity function analysis introduced by Woodward [1] has been the motivating force behind modern detection system designs. Though the approach to the problems pertaining to specific issues may differ, the fundamental theory of signal design [1] remains useful. The detection problem is tractable when the corrupting influence is mainly additive noise [2], [3]. Schwartz [8] and Van Trees [9] have made significant contributions towards communication through randomly fading media.

The theme of the present thesis is to design and to simulate a one-shot statistical detection system to operate in a randomly fading environment. Attempts will be made to combine pure theoretical design philosophy with practical intuition as regards the statistics of the random medium. Though the theory presented is equally applicable to radar and ionospheric signalling, the sonar situation will be assumed tacitly in the sequel.

The signal detection system is sectioned into three major parts: the transmitter, the medium, and the receiver. The medium also includes the target or targets. In the sequel each of these parts are dealt with in detail, first presenting the theory and mathematical models, and then the system simulations on the IBM 7040 digital computer.

A detailed analysis on the detection of a stationary point target in white, gaussian noise has been made by Mark & Hicks [11]. In this thesis an extension to the detection of moving target or targets in a randomly fading environment, where the fading noise may be non-stationary but time-invariant over the observation interval under consideration, is carried out.

Our criteria for signal detectability are output signal-to-noise ratio, signal resolution, and dynamic range as specified by the peak-to-sidelobe ratio together with a false alarm probability.

Strictly from the view point of signal resolution and energy content, the wide-band pseudo-random encoding is chosen. Unless the demodulation high frequency carrier is derived from the observable the pseudo-random modulation employed is very sensitive to doppler shift. To cope with moving target(s) self-synchronized demodulation is improvised in this thesis.

A non-realizable optimum estimator-demodulator is derived in Chapter V using a conditionally biased maximum a posteriori criterion. Practical realization of the estimator is made in Chapter VI.

Since the receiver under consideration is one-shot, signal estimation takes the form of channel estimation. The objective here is to apply interpolation or smoothing on the noise processes for as long a duration as the transmission band permits. This kind of channel estimation is inherently sub-optimum as there is insufficient time available for signal adaptation.

System implementation and signal-to-noise ratio computation, together with computer simulation results, are detailed in Chapter VII. Auxiliary mathematical analyses are described in Appendices I, II, and III. Computer simulation programs are explained in detail in Appendix IV.

# CHAPTER II

## SIGNAL DETECTION PHILOSOPHY

The fundamental theory of statistical signal detection has been well documented [1], [6], [7]. None of the basic theory will be repeated in this thesis; the interested readers are referred to the references provided.

Bearing in mind that the fundamental principles of signal detection are still the springboard for every system design, a system is considered to be "good" only because of added features, namely, optimization techniques. It is well known that the detectability and resolvability of a detection system is directly proportional to the time-bandwidth product. The outstanding feature of a large time-bandwidth product signal is its compressibility, that is, a long duration signal may be compressed to enhance signal resolution, hence the name pulse compression systems.

The ambiguity function analysis first advanced by Woodward [1] is a good criterion for the discrimination against stationary point targets in respect to time delay and frequency shift. Complex targets may be thought of as made up of many point targets, associated with which are target strengths, target phases, and target separations with respect to some reference point. The complex target possesses a finite intrinsic bandwidth as viewed by the receiver. If the maximum separation between point targets is less than the reciprocal of the effective signal bandwidth, the point targets are non-resolvable. Therefore, if the effective signal bandwidth is W, point targets situated inside a range patch $\leq 1/W$ are treated as a single target.

In the case of wideband pseudo-random modulation waveforms, the signal bandwidth is given by $1/t_o$, where $t_o$ is the subpulse duration of the modulation waveform. For a modulation waveform having N subpulses the total signal duration is $T = Nt_o$. Such a modulation waveform offers a doppler resolution of $1/T$ and a time delay resolution of $1/W$. $N = WT$ is the time-bandwidth product, also known as the compression ratio, of the pseudo-random modulation waveform. High signal resolution can be achieved by maximizing the time-bandwidth product. To illustrate this point a sketch of a typical ambiguity diagram for a truncated (aperiodic) pseudo-random modulation waveform is shown in Figure 1.

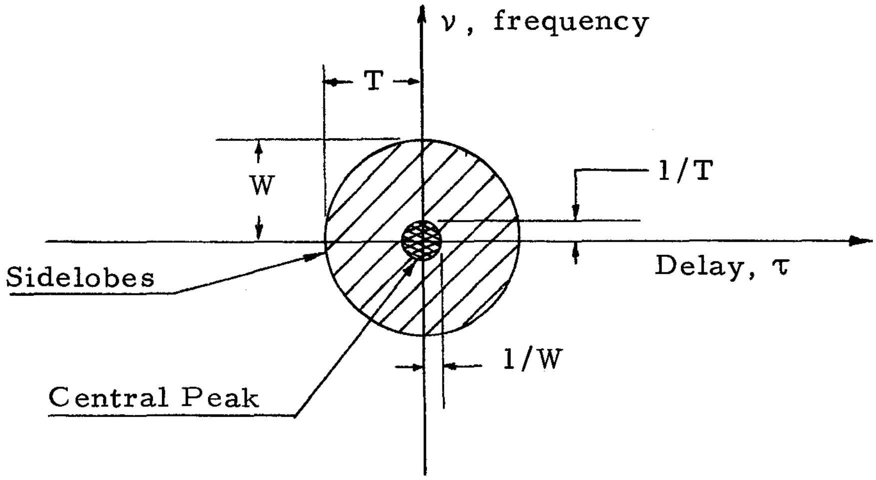


Figure 1 - Typical Two-Dimensional Ambiguity Diagram for Aperiodic Pseudo-random Waveforms

The ambiguity function is given by the envelope of the convolution integral between the incoming and the reference bandpass signals. In mathematical form the ambiguity function is represented by equation (1):

$$\chi(\tau, \nu) = \int_{-\infty}^{\infty} u^*(t) \quad v(\tau - t)\, e^{-j2\pi\nu t}\, dt \qquad (1)$$

where u(t) is the complex envelope of the received signal

v(t) is the complex envelope of the reference signal

$\nu$ = Doppler frequency

$\tau$ = time delay

The ambiguity surface is a probabilistic plot. As such the energy under it can only be re-distributed but not eliminated. Consequently, to achieve the desired form of ambiguity surface, one can only optimize the modulation waveform in such a manner that a greater percentage of the energy is centrally located within a narrow region, such that the off-centre lobes are very small in comparison with the central peak. It is well known that a random waveform possesses such a property. However, to be of use in signal encoding, the waveform must be deterministic, that is, it must be reproducible. The so called codes manufactured from basic algebraic structures are deterministic. At the same time these codes possess the random property. Reproducible codes which possess the random property are known as pseudo-random codes.

The design of an echo ranging system should constitute the following steps:-

(1) Select a suitable modulation waveform.

(2) Design a receiver which is optimum for the particular modulation waveform chosen.

(3) Take into account the noise statistics of the corrupting influences and tailor the receiver design accordingly.

(4) Select a time-bandwidth product which is most suitable for the environment involved and which satisfies the transducer or antenna transmittability requirement.

If the system is to be simulated, one adds

(5) Simulation of a statistical model of the propagation medium, including the target(s).

The tracking echo ranging system analyzed in this thesis, also referred to as a self-synchronized detection system, is shown in the functional block diagram of Figure 2. Each of the major parts, transmitter, medium, and receiver, will be analyzed in detail in subsequent chapters.

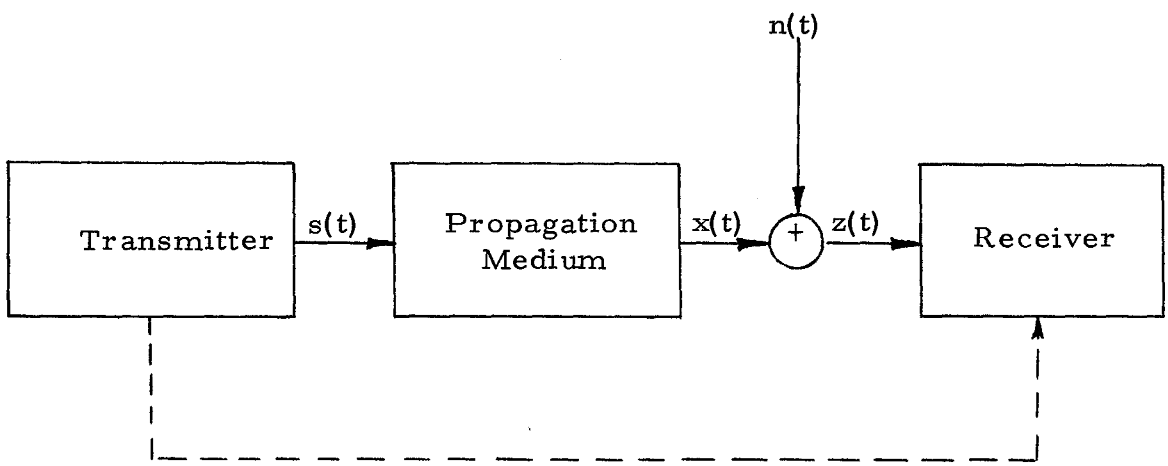


Figure 2 - Functional Block Diagram of a Detection System

# CHAPTER III

## SIGNAL ENCODING WITH BINARY CODES

The fundamental principle of binary sequence derivation and generation has been dealt with elsewhere [14], and will not be described in this thesis. For the sake of completeness, however, a short analysis of the basic coding with algebraic structures is given in Appendix I.

The binary M-sequences discussed in Appendix I have lengths given by the formula $2^n-1$. Sequences with lengths different from these, possessing similar statistical properties, may be obtained by convolving two or more sequences, as noted in Appendix I. Since coding is a tool employed in this thesis, the analysis in the sequel will mainly be concerned with signal modulation using a time function of the binary sequence. In particular the $(2^3-1) * (2^4-1)$ or 105 digit convolution code is used for computer simulation of the overall system. Where computer memory becomes a limitation the component $(2^4-1)$ or 15 digit M-sequence is employed.

The modulation process shown in Figure 3 may be thought of as phase reversal modulation or double sideband suppressed carrier amplitude modulation. The transmitted signal may be represented mathematically by*:-

(i) Phase reversal modulation:

$$s(t, \{a(t_o)\}) = \mathrm{Sin}[\,\omega_o t + \theta_o + \tfrac{\pi}{2}\{a(t_o)\}\,] \qquad (2a)$$

(ii) Double sideband suppressed carrier amplitude modulation:

$$s(t, \{a(t_o)\}) = \{a(t_o)\}\ \mathrm{Cos}(\omega_o t + \theta_o) \qquad (2b)$$

where $\{a\}$ is the binary code with $\pm 1$ amplitude.

$\omega_o$ = the carrier frequency

$\theta_o$ = initial carrier phase (will be ignored in the analysis)

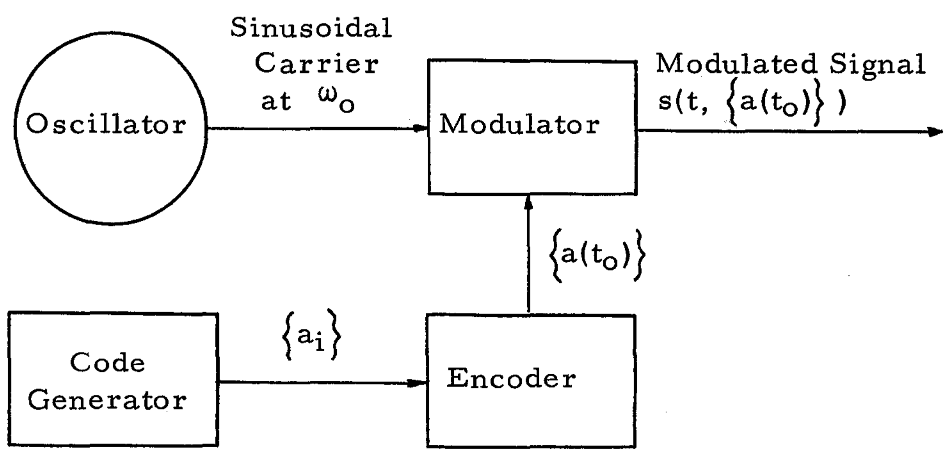


Figure 3 - Block Diagram for Signal Modulation

* Both notations will be used in subsequent chapters.

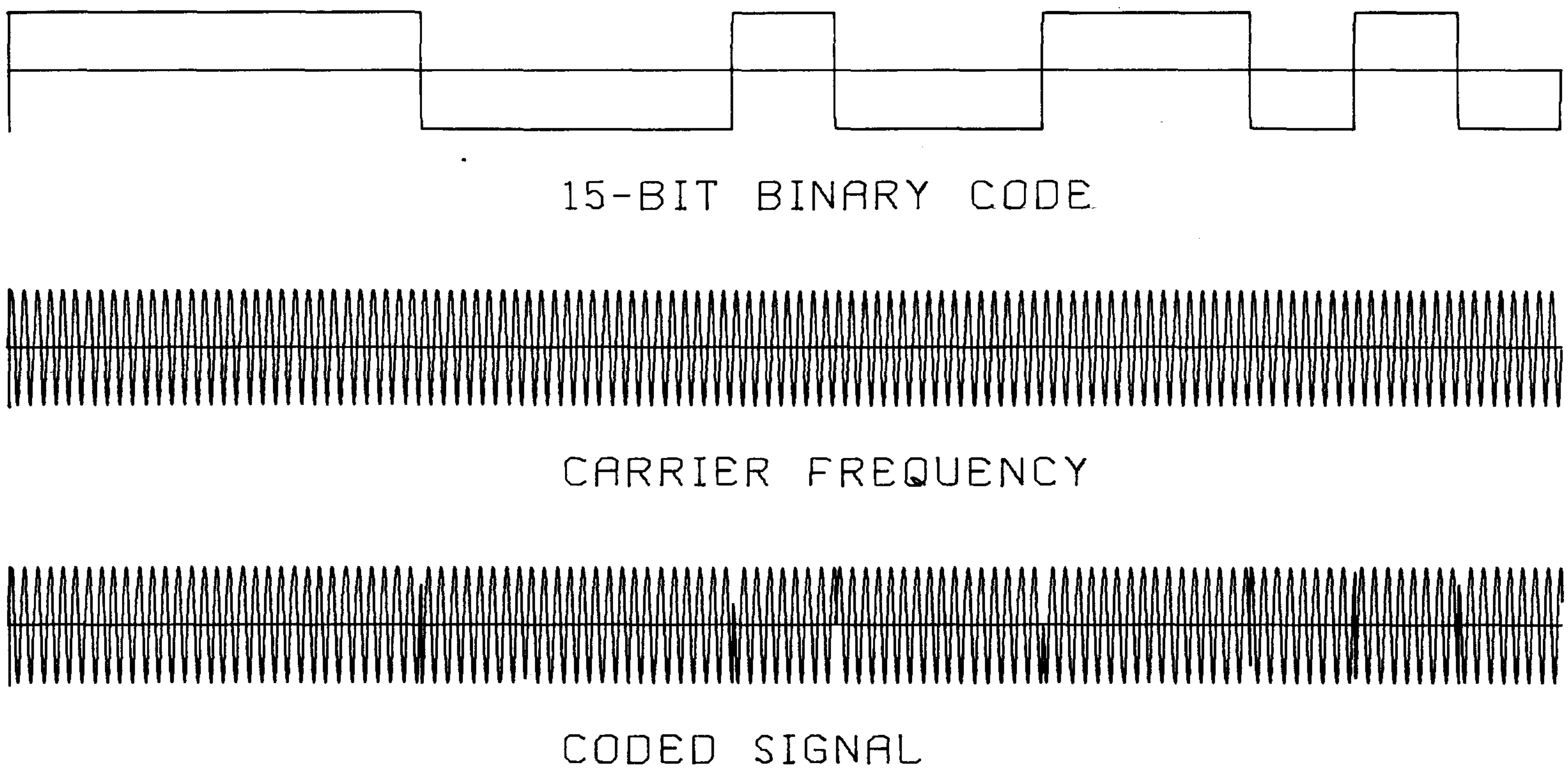


Figure 4 - SIGNAL ENCODING PROCESS

A pictorial representation of the modulation process is illustrated in Figure 4.

For the purpose of echo ranging in a sonar situation where the same transducer is employed for transmission and reception, it is desirable to use an aperiodic code. The binary sequences discussed in Appendix I are periodic in nature. To satisfy our requirement we truncate one period of the convolution code in effecting the modulation process. The truncation results in a finite signal duration but also introduces self-noise. As a result the autocorrelation function will not possess the desirable property of $\frac{1}{N-1}$ normalized off-centre lobes as noted in Appendix I. Therefore, in the absence of external interferences the fundamental limitation on dynamic range is the self-noise.

Consider, in the absence of fading and multipath effects, representing the received signal vector by

$$\underline{z} = \underline{s} + \underline{n}$$

where $\underline{s}$ = the signal vector

$\underline{n}$ = the additive noise vector.

Assumptions:-

$\underline{s}$ and $\underline{n}$ are statistically independent and $E[\ \underline{n}\ ] = 0$

To enhance signal detectability the optimum procedure is to operate on the observable by a known reference signal [11]. The cross-moment matrix between the received vector $\underline{z}$ and the reference vector $\underline{s}$ is given by

$$C_{\underline{z}\,\underline{s}} = E\left\{\underline{z} \cdot \underline{s}^T\right\}$$
$$= E\left\{\underline{s} \cdot \underline{s}^T\right\} + E\left\{\underline{n} \cdot \underline{s}^T\right\}$$
$$= C_{\underline{s}} + C_{\underline{n}\,\underline{s}} \tag{4a}$$

The superscript T denotes matrix transposition. The coherent component $C_{\underline{s}}$ is the signal second moment matrix and the incoherent component $C_{\underline{n}\,\underline{s}}$ is the cross-moment matrix between the noise vector, $\underline{n}$, and the reference signal vector, $\underline{s}$. In the one-dimensional case, the equivalent to equation (4a) is usually designated by

$$\phi_{z\,s}(\tau) = \phi_{s\,s}(\tau) + \phi_{n\,s}(\tau) \tag{4b}$$

where $\phi_{z\,s}(\tau)$ = the cross-correlation function of the observable, z(t), and the signal, s(t),

$\phi_{s\,s}(\tau)$ = the signal auto-correlation function,

$\phi_{n\,s}(\tau)$ = the cross-correlation function of the noise, n(t), and the signal, s(t).

Aside from the self-noise inherent in the signal moment matrix, $C_{\underline{s}}$, the limiting factor on signal detectability is the additive noise. This is apparent by considering the mean and the covariance of $C_{\underline{z}\,\underline{s}}$:-

$$E\left\{C_{\underline{z}\,\underline{s}}\right\} = E\left\{C_{\underline{s}} + C_{\underline{n}\,\underline{s}}\right\} = C_{\underline{s}} \tag{5a}$$

and

$$\mathrm{Cov}\left\{C_{\underline{z}\,\underline{s}}\right\} = E\left\{\left[C_{\underline{z}\,\underline{s}} - E\left\{C_{\underline{z}\,\underline{s}}\right\}\right] \cdot \left[C_{\underline{z}\,\underline{s}} - E\left\{C_{\underline{z}\,\underline{s}}\right\}\right]^T\right\}$$
$$= E\left\{C_{\underline{n}\,\underline{s}} \cdot C_{\underline{n}\,\underline{s}}^T\right\} \tag{5b}$$

With the assumption that signal and noise are statistically independent and that the noise process has zero mean, the off-diagonal elements of Cov $\{C_{\underline{z}\,\underline{s}}\}$ vanish. Since the covariance matrix represent perturbation on signal detectability, minimization of the perturbation amounts to minimizing the trace of Cov $\{C_{\underline{z}\,\underline{s}}\}$. It can be shown, by expansion of the covariance matrix of equation (5b), that

$$\text{tr Cov}\{C_{\underline{z}\,\underline{s}}\} = E_{\underline{s}} \cdot \sigma_{\underline{n}}^2$$

where $E_{\underline{s}}$ = signal energy

$\sigma_{\underline{n}}^2$ = noise variance.

For a given signal, the amount of perturbation is a direct function of the noise variance associated with the observable. If the noise variance is large in comparison to the variance of the self-noise of the signal, the environmental noise simply swamps out the self-noise. In the situation under consideration the environment is relatively noisy. Moreover, the self-noise by itself impose a negligibly small masking effect on signal detectability. Therefore, the self-noise effect will be ignored in the signal detection optimization analysis in the sequel. Vector notation offers compactness of representation; wherever feasible vector notation will be used. The signals under consideration are fundamentally scalar-valued, however. Therefore, the notation of equation (4b) will be used mostly in this thesis.

# CHAPTER IV

## STATISTICAL MODEL OF FADING MEDIUM

With the exception of the transmitted signal all interferences are random processes. Assuming a knowledge of probability theory, we define a random or stochastic process simply as a process, $x(t)$, for which repetitive observations yield a set of relations between $x$ and its argument, $t$, only in a probabilistic sense, that is, describable only by the probability moments.

In our terminology the medium includes the target(s). The channel will, therefore, be composed of a randomly fading component acting on the sum of target echo plus multipath returns, and an additive noise. The additive noise is assumed to be statistically independent from the other components. Also, each component may have a different intrinsic bandwidth. The following sections describe in detail the various components that make up the random channel.

### 4.1 Additive Noise

We shall assume that the additive noise is statistically independent of the randomly fading noise and of the multipath noise. It is assumed to be statistically stationary, Gaussian and spatially and temporally white. It is assumed to have a constant power-density, $N_o$ (watts/Hz), over some constant bandwidth, $W_n$, which at least spans the transmission band. The additive noise is assumed to have a zero mean and its variance is given by $\sigma_n^2 = W_n N_o$. The additive, gaussian noise is thus characterized by the probability density function

$$P(n) = \frac{1}{\sqrt{2\pi}\,\sigma_n} \exp\left[ - \frac{n^2}{2\,\sigma_n^2} \right] \tag{6}$$

Correspondingly the complex time function n(t) of duration T may be represented by the probability density function

$$P\left[n(t)\right] = \frac{1}{\left[ 2\pi W_n N_o \right]^{TW_n}} \exp\left[ - \frac{1}{2N_o} \int_o^T n^2(t)\,dt \right] \tag{7}$$

## 4. 2 The Random Medium

Excluding the target itself the random medium is made up of a fading noise and a multipath noise, the latter is called reverberation in sonar.* Fading is the result of scattering encountered in the propagation space between the sonar system and the desired target; reverberation is the result of scattering at the same relative locality as the desired target. The propagation phenomenon is illustrated pictorially in Figure 5.

* We note that reverberation imposes a threat to signal detectability only at observation time.

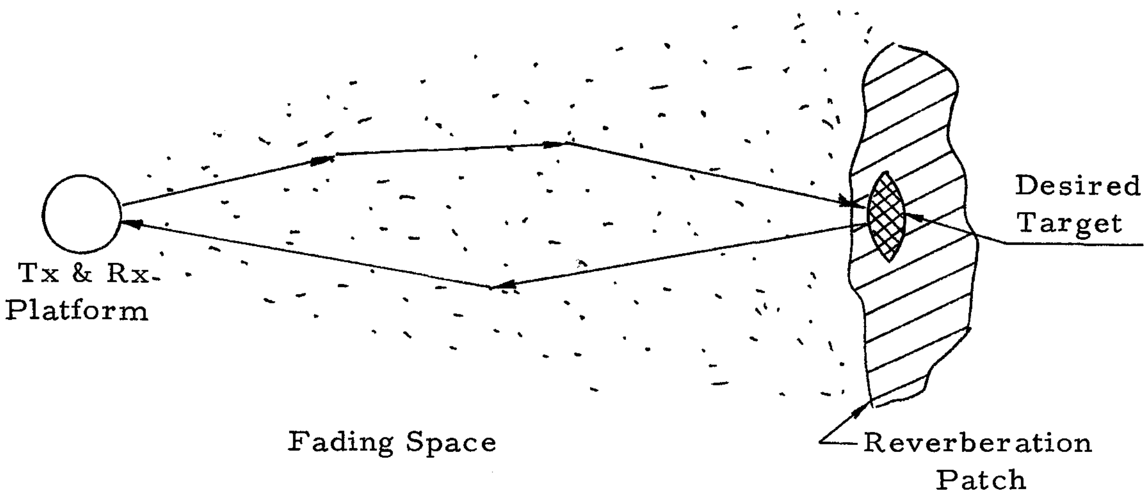


Figure 5 - A Sketch of Signal Propagation
(forward and return paths may be identical)

4.2.1 Nature of Random Medium

The propagation space is made up of an infinite number of particles of various sizes and shapes. Each of these particles poses as a scatterer in a microscopic sense. In our analysis we are only concerned with the macroscopic phenomenon, that is, the total effect of many of these tiny particles acting collectively. We shall consider a cluster of many particles as a scatterer in a macroscopic sense.

The scatterers as defined above may have motions. Also, their reflectivity properties may change with time. The scatterers are thus random variates. As such they are describable only by a set of statistics. Depending on the rapidity of the motions of the scatterers and the rate at which their reflectivities change, the random variates may be stationary, non-stationary, time-varying, or time-invariant. A time-varying channel implies very rapid change in statistics with respect to time. In this thesis the random channel is assumed to be time-invariant, though it may be stationary or non-stationary. That is, the random channel statistics are assumed to remain invariant at least for some duration longer than the time required for their computation.

Since time is a relative quantity a differentiation between the duration which describes the time-variant vs time-invariant aspect and that which describes the stationary and non-stationary aspects of the random process is in order. In dealing with the concept of stationarity we refer to some duration which is at least an order of magnitude longer than that implied in analyzing the time-variant vs time-invariant aspect. Having said this, we say a random process is stationary if it remains invariant with respect to time. That is, the statistics of the random process are determinable independent of the time origin. If the statistics depend on the origin, we say the process is non-stationary. The concept of stationarity is thus time dependent. A strictly stationary process is defined as one whose probability moments are function only of the difference in time. A process is said to be wide-sense stationary if it is covariance stationary. An important class of processes which need only be wide-sense stationary are the normal or Gaussian processes. The Gaussian process is completely determined by its first and second moments. In the real world, strictly stationary processes are most likely nonexistent. At best we would have wide-sense stationary processes. If the invariant period is short compared to the observation interval, the random process is said to be non-stationary. The non-stationary phenomenon may be due to rapid motion of the scatterers or due to truncations of a stationary process.

The stationary time-invariant channel is easy to analyze, since the channel statistics need only be computed once when estimating the signal. In a non-stationary situation the channel statistics need to be up-dated at regular intervals. In other words the system must be capable of adapting itself to the channel statistics.

### 4.2.2 Multipath Medium Characterization

In the previous section we have assumed that multipath and fading structures exist because of reflections from scatterers situated randomly in the propagation space. To characterize the fading and multipath structures mathematically we translate our observation point to the vicinity of the multipath source. In so doing we neglect the nominal range delay. This is plausible since the nominal delay contributes no useful information to our analysis.

When the signal represented by equation (2b) is transmitted the signal reflected from the $k^{th}$ scatterer may be written as

$$r_k(t) = b_k\, s(t - t_k)$$
$$= b_k \left\{a(t_o)\right\} \mathrm{Cos}\left[\,\omega_o(t - t_k) - \phi_k\,\right] \tag{8}$$

where $b_k$ = $k^{th}$ target strength

$t_k$ = the time delay of the $k^{th}$ path with respect to the observation point

$\phi_k$ = the $k^{th}$ target phase

Equation (8) is merely the transmitted signal weighted by the multipath or fading effect, $b_k\, e^{j\theta_k}$, where $\theta_k = \omega_o t_k + \phi_k$. The fading or multipath effect may be separated into two components, one fixed and one random. Then equation (8) becomes

$$r_k(t) = R_e \left\{ \left\{ a(t_o)\right\} \cdot e^{j\omega_o t} \left[\nu_k e^{-j\alpha_k} + \eta_k e^{-j\beta_k}\,\right]\right\} \tag{9}$$

where $\nu_k\, e^{-j\alpha_k}$ is the fixed component,

$\eta_k\, e^{-j\beta_k}$ is the random component.

A pictorial representation of the random variates resulting from scattering by the $k^{th}$ scatterer is illustrated in Figure 6.

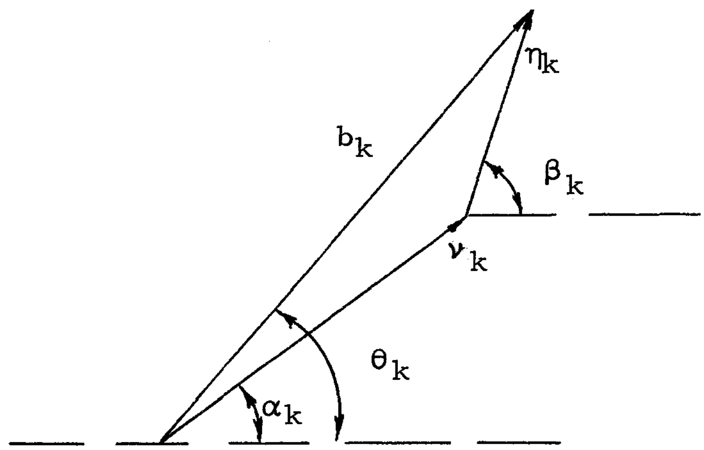


Figure 6 - Pictorial Representation of the k^th Random Path

The random variates represented by equation (9) are Rician in distribution. That is, the random variates are made up of a specular component and a random component. The specular component is given by the expectation of the random process; the random component is representable by two zero mean gaussian processes at quadrature. The envelope of the random component has a Rayleigh probability density function with mean square, $\sigma_r^2$, and its phase is uniformly distributed over the prime interval 0 - 2π. Mathematically the probability density of the random component may be represented as follows:-

$$P[\eta_k(t)] = \frac{\eta_k(t)}{\pi\sigma_r^2} e^{-\eta_k^2(t)/\sigma_r^2} \quad , \eta_k \geq 0, \ 0 \leq \beta_k \leq 2\pi \tag{10}$$

Although the phase, $\beta_k$, is uniformly distributed over the prime interval $0 \rightarrow 2\pi$, the variation in phase during an observation interval is assumed to be small in a time-invariant channel. In other words we assume that the channel does not completely scintillate the code.

The parameters which describe the random variates as a result of scattering are the amplitude, $b_k$, the phase, $\theta_k$, and the differential delay, $\tau_k$. As such the $k^{th}$ path may be completely described by their joint first-order probability density function $P_r[b_k, \theta_k, \tau_k] = P_r(\tau_k) P_r(b_k, \theta_k/\tau_k)$. Applying the cosine law to the triangle of Figure 6 we obtain:

$$\eta_k^2 = b_k^2 + \nu_k^2 - 2 b_k \nu_k \operatorname{Cos}(\theta_k - \alpha_k) \tag{11}$$

The envelope of the random component is thus expressible in terms of $b_k$, $\nu_k$, $\theta_k$ and $\alpha_k$, accounting for the specular component. Using equation (11), equation (10) may be modified to yield an expression which describes the joint density function of amplitude and phase of the sum of a fixed vector and a vector with Rayleigh distributed amplitude and completely random phase:

$$P_r[b_k, \theta_k/\tau_k] = \frac{b_k}{\pi\sigma_k^2} \exp\left[-\frac{b_k^2 + \nu_k^2 - 2b_k \nu_k \operatorname{Cos}(\theta_k - \alpha_k)}{\sigma_k^2}\right]$$

$$0 \leq b_k < \infty, \ -\pi \leq \theta_k - \alpha_k \leq \pi \tag{12}$$

The probability density representation of equation (12) is due originally to Rice [4]. The overall fading effect is given by the product of contributions from scatterers in the propagation space. The gross multipath structure is given by the sum of contributions from paths in the vicinity of the desired target. If there are L scatterers in the propagation space the overall fading effect is given by

$$\gamma(t) = \prod_{i=1}^{L} c_i \, e^{-j\phi_i} \quad . \tag{13}$$

We assume the random variates causing fading are non-time-dispersive. As such the fading effect may be thought of as a multiplicative noise. The gross multipath effect is representable by

$$\xi(t) = \sum_{k=1}^{M} b_k \, e^{-j\theta_k} \tag{14}$$

where M is the number of multipaths.

If the probing signal is s(t), the total multipath reflection will be

$$\begin{aligned} r(t) &= \xi(t)\, s(t-\tau) \\ &= \sum_{k=1}^{M} b_k \, s(t-\tau_k)\, e^{-j\phi_k} \\ &= \sum_{k=1}^{M} b_k \left\{ a(t_o) \right\} \operatorname{Cos}\left[ \omega_o(t-\tau_k) - \phi_k \right] \\ &= \sum_{k=1}^{M} r_k(t) \end{aligned} \tag{15}$$

where $r_k(t)$ is given by equation (8).

The fading effect represented by equation (13) and the multipath effect by equation (14) are present only when the signal is present. Because the multipath effect is represented in the manner by equation (15) the corrupting interference imposed by it is known as signal dependent noise, or reverberation in sonar terminology. The effect of fading is to reduce the target echo amplitude and may be to scintillate the target echo. The integrability of the code at observation time is entirely dependent on the degree of fading.

Assumption: The ensemble correlation of the fading process, for a stationary interval, obeys the following equation:

$$E\ [\gamma(\tau)\ \cdot\ \gamma^*(\lambda)] = \rho(\tau)\ \delta(\tau-\lambda),$$

where $E[\cdot]$ is the ensemble expectation, $\delta(\cdot)$ is a delta function, and $\rho(\tau)$ is the correlation coefficient of the fading process.

## 4.3 The Target

The target echo may be viewed as the (M + 1)th multipath. It differs from the other multipaths only in target strength, phase and separation. If a target is complex, it may be made up of more than one high-light. The coefficient of reflection of the target or its high-lights may be considerably larger than those of the undesired multipaths, though the total multipath effect of M undesired scatterers may be significant.

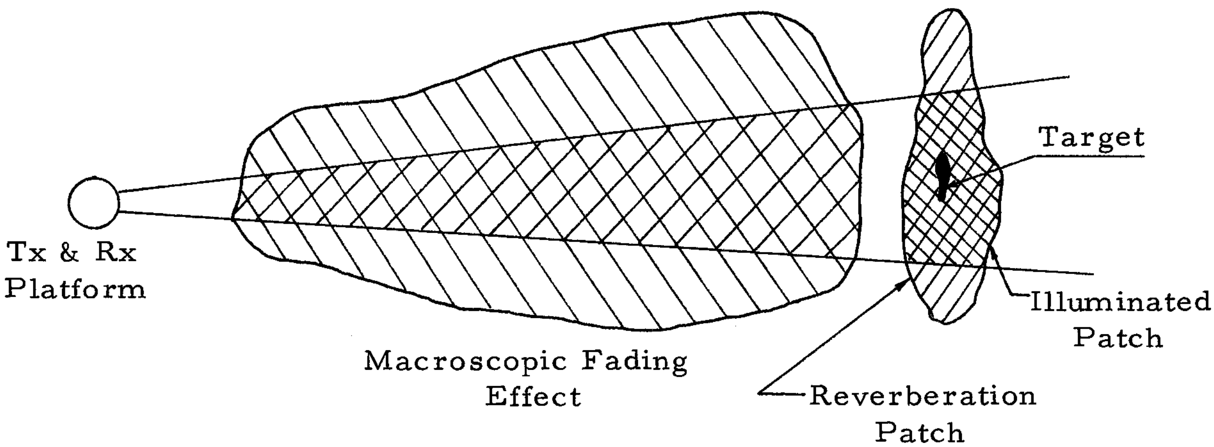


Figure 7 - Target Illumination of Tx-Rx Beams
(The Tx & Rx Beams are Assumed Identical here)

The target illumination by the Tx-Rx beams is illustrated in Figure 7. The multipath effect, including the target, may be represented by:-

$$\zeta(t) = |b_t| \left\{a(t_o)\right\} \mathrm{Cos}\left[\omega_o(t - \tau_t) - \phi_t\right]$$

$$+ \sum_{k=1}^{M} b_k \left\{a(t_o)\right\} \mathrm{Cos}\left[\omega_o(t - \tau_k) - \phi_k\right] \qquad (16)$$

where $|b_t|$ = the desired target strength (magnitude)*

$\phi_t$ = the desired target phase

$\tau_t$ = target differential delay

* the complex target strength is represented by $b_t = |b_t| \, e^{-j\phi_t}$

All other parameters are as previously defined. Equation (16) is in turn weighted by the medium fading, so that the observed signal is representable by:-

$$
\begin{aligned}
z(t) &= \gamma(t) \cdot \zeta(t) + n(t) \\
&= \gamma(t) \; |b_t| \left\{a(t_o)\right\} \cos\left[\omega_o(t - \tau_t) - \phi_t\right] \\
&\quad + \sum_{k=1}^{M} b_k \left\{a(t_o)\right\} \cos\left[\omega_o(t - \tau_k) - \phi_k\right] \\
&\quad + n(t) \qquad (17)
\end{aligned}
$$

where n(t) is the additive white gaussian noise discussed in section 4. 1.

The effect of reverberation is most significant when the target is either stationary or is moving at the same speed as the reverberation patch. When the target speed is much greater than that of the reverberation patch, the reverberation effect is minimal. Let $\delta$ represent the delay rate due to the target and $\delta'$, the delay rate due the reverberation patch. then equation (17) may be written as:-

$$
\begin{aligned}
z(t) &= \gamma(t) \; |b_t| \left\{a(t_o)\right\} \mathrm{Cos}\left[\omega_o(1 - \delta)\, t - \phi_t\right] \\
&\quad + \sum_{k=1}^{M} b_k \left\{a(t_o)\right\} \cdot \mathrm{Cos}\left[\omega_o(1 - \delta')\, t - \phi_k\right] \\
&\quad + n(t) \qquad (18)
\end{aligned}
$$

The desired target moves out of the reverberation influence when $\delta >> \delta'$, as the energy concentration of the target and the reverberation patch occur at different frequency bands.

Although the individual multipaths obey a Rayleigh or Rician distribution, the distribution of reverberation depends largely on the population density of the scatterers that make up the gross reverberation structure. If the multipaths are sparingly populated, i. e. M not very large, the distribution density of reverberation may be described by a Poisson probability density function. In the limit as M becomes infinitely large reverberation takes the form of a Gaussian process.

Unless the sonar system is operating at Homing ranges, reverberation does not appear to be a limiting factor in system performance. If anything which limits the system performance at all, in the author's opinion, it is the fading effect $\Upsilon(t)$. For this reason the reverberation aspect will not be dealt with thoroughly in this thesis. The interested readers are referred to the references cited [2], [3]. When reverberation is insignificant, equation (18) reduces to:-

$$z(t) = \Upsilon(t)\, b_t \left\{a(t_o)\right\} \text{Cos}\, \left[\omega_o\,(1-\delta)t\right] + n(t)$$

$$= m(t)\, \text{Cos}\, \left[\omega_o(1-\delta)t\right] + n(t) \qquad (19a)$$

where we have let $m(t) = \Upsilon(t)\ b_t \left\{a(t_o)\right\}$ to be the corrupted intelligence. $\Upsilon_t(t)$ and $b_t$ are complex functions. In the notation of equation (2a) we may alternatively represent the received signal by:-

$$z(t) = \text{Sin}\left[\omega_o(1 - \delta)t + \tfrac{\pi}{2} m(t)\right] \qquad (19b)$$

$\delta$ in equations (19) is the delay rate* due to target motion. Any envelope compression or stretching due to $\delta$ have been ignored.

* A treatise of the moving target is described in Appendix II.

# CHAPTER V

# SIGNAL ESTIMATION PHILOSOPHY

## 5.1 General Discussion

In Chapters II and III we have discussed the signal detection aspect, where the optimum detection strategies depend on the properties of the signal and noise. Estimation shall be defined as the problem of measuring the parameters of a target echo (signal) embedded in noise. As such it is related to the problem of detecting a signal in noise. We can expect then the optimum estimation strategies to depend on the characteristics of the signal and the noise in much the same way as the optimum detection strategies.

The discussion of signal parameter estimation in the sequel will adhere to the following conotations: An estimator is the operation (decision rule) which yields estimates from the observables, an estimate is a value or result of the estimation process.

Random processes, as the name indicates, can only be described in terms of probability moments. That is to say, we cannot say with certainty what the random process is at any particular instant of time, but we can say probably what is it over some duration of time. We therefore expect estimation to depend on time. The longer the interval available for signal estimation the better will be the estimates. Ideally we should like to have an infinite duration for making the estimates. Practically, however, the maximum time available for updating a signal estimation process is the duration in which the statistics of the process remains invariant. This duration varies depending on the stationarity of the process. At any rate, if the receiver is a one-shot receiver, as is in the present analysis, the time available for estimation may be limited by the reciprocal of the effective signal bandwidth. This is especially true since the system analyzed in this thesis is a wide-band system. The feasible form of estimation will, at best, be suboptimum, as there will be insufficient time to permit parameter adaptivity. On the other hand, if the system is continuous, the estimates obtained in the previous instant may be utilized to update computations at the present instant. We shall refer to the former as short-term estimation and the latter as long-term estimation. The former system is designed for target acquistion and is the main concern of this thesis. The latter is suitable for tracking the trajectory of the target once it has been acquired. We therefore have in estimation theory a fundamental tool for the design of adaptive systems.

## 5.2 Channel Estimation

### 5.2.1 Channel Estimation Defined

Channel estimation, in our analysis, may be categorized into two aspects; namely, amplitude and epoch estimation. Epoch estimation involves the measurement of any change of signal characteristics in the time and frequency domains. It also takes into account intersymbol interferences. This aspect of estimation will not be dealt with in this thesis. Our main concern will be amplitude estimation.

Consider the simple system shown in Figure 8.

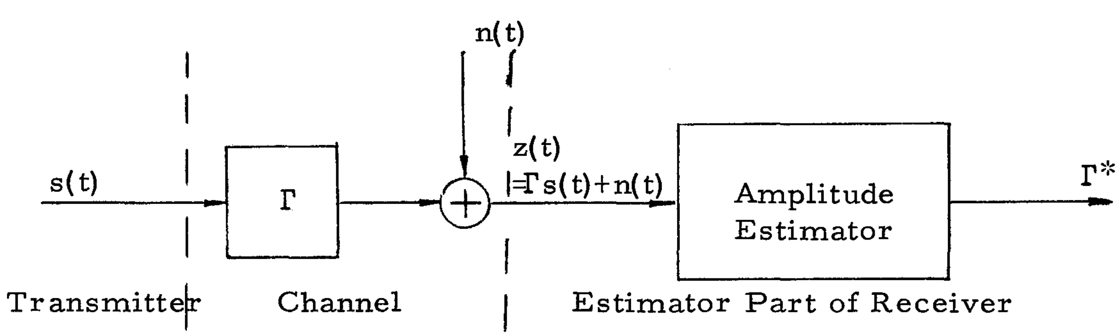


Figure 8 - A Signal-Amplitude Estimator

The channel is assumed to be a stationary time-invariant process such that $\Gamma$ may be treated as an unknown constant. The task of the estimator is to provide a measurement of the unknown channel gain $\Gamma$. We shall call this measured value the estimate, $\Gamma^*$.

The channel output is of the form

$$z(t) = \Gamma\, s(t) + n(t) \qquad (20a)$$

where $\Gamma$ is an unknown scalar. In vector notation

$$\underline{z} = \Gamma \underline{s} + \underline{n} \qquad (20b)$$

where $\underline{s}$ is the probing signal vector

$\underline{n}$ is the additive gaussian noise vector.

### 5.2.2 The Simple Amplitude Estimator

We define the signal energy by $E_s = \underline{s}^T \cdot \underline{s}$. We know the observed vector, $\underline{z}$, to contain as one of its components, the signal vector, $\underline{s}$. Since we know with certainty what the signal vector $\underline{s}$ is, the natural approach is to operate on the observed vector with the known reference signal vector. Doing this, we have

$$\underline{z}^T \cdot \underline{s} = (\Gamma \underline{s})^T \cdot \underline{s} + \underline{n}^T \cdot \underline{s}. \qquad (21)$$

Since $\Gamma$ is a scalar quantity, equation (21) may be written as:-

$$\underline{z}^T \cdot \underline{s} = \Gamma\, \underline{s}^T \cdot \underline{s} + \underline{n}^T \cdot \underline{s} \qquad (22)$$

Recognizing that the first term on the left hand side of equation (22) is the signal energy weighted by the unknown channel gain , we normalize equation (22) to obtain the estimate, $\Gamma^*$:

$$\Gamma^* = \Gamma + \frac{\underline{n}^T \cdot \underline{s}}{E_s}$$

$$= \Gamma + \Delta \qquad (23)$$

where $\Delta = \frac{\underline{n}^T \cdot \underline{s}}{E_s}$ is the perturbation on the determination of $\Gamma$. If $\underline{n}$ and $\underline{s}$ are statistically independent and if $E\left\{\underline{n}\right\} = 0$, we have

$$E\left\{\Delta\right\} = E\left\{\frac{\underline{n}^T \cdot \underline{s}}{E_s}\right\} = 0 \qquad (24)$$

and

$$E\left\{\Delta^2\right\} = E\left\{\left[\frac{\underline{n}^T \cdot \underline{s}}{E_s}\right]^2\right\}$$

$$= \frac{\sigma_n^2}{E_s} \qquad (25)$$

where $\sigma_n^2 = E\left\{\underline{n}^T \cdot \underline{n}\right\} = \int \frac{N_o}{2}\delta(\tau)d\tau = \frac{N_o}{2}$ is the variance of the additive noise. Since $\underline{n}$ is a gaussian vector, $\Delta$ is also a gaussian random variable with mean and variance given by equations (24) and (25), respectively. Hence, the estimate $\Gamma^*$ is a random variable with probability-density function given by

$$P(\Gamma^*/\Gamma) = \frac{1}{\sqrt{2\pi\sigma_n^2/E_s}} \exp\left[-\frac{(\Gamma^* - \Gamma)^2}{2\sigma_n^2/E_s}\right] \qquad (26)$$

We note that, $\sigma_n^2/E_s$ , the variance of the perturbation component, $\Delta$ , represents the noise-to-signal ratio at the input of the receiver. As $\sigma_n^2/E_s \to 0$, $\Gamma^* \to \Gamma$.
$\Gamma$ can thus be estimated precisely if it were a constant gain. The amplitude estimator has the configuration shown in Figure 9.

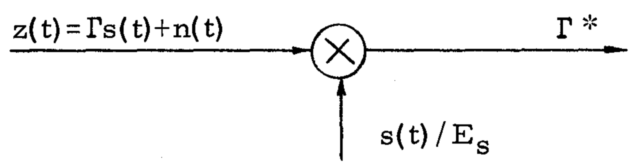


Figure 9 - The Simple Amplitude Estimator

In the sonar situation we are dealing with in this thesis, the channel gain is a random variable. As in Chapter IV, we denote the channel gain by $\gamma(t)$. The random variable, $\gamma(t)$, may have stationary or non-stationary statistics. $\gamma(t)$ is the random variate which corrupts the coherency of the intelligence $\{a(t_o)\}$.

5.3 Random Amplitude Estimation

The randomly fading phenomenon in a non-dispersive channel, as stated in Chapter IV, may be considered as multiplicative noise. The statistics of this multiplicative noise may be represented by a Rayleigh or Rician probability density function.

In the absence of reverberation we may represent the observable by equations (19)

$$z(t, \delta, \gamma(t), b_t, \{a(t_o)\}) = m(t) \cos \omega_o(t-\delta t) + n(t) \qquad (19a)$$

or

$$z(t, \delta, \gamma(t), b_t, \{a(t_o)\}) = \cos[\omega_o(t-\delta t) + m(t)] + n(t) \qquad (19b)$$

where $m(t) = \gamma(t) b_t \{a(t_o)\}$ is an explicit function of the intelligence $\{a(t_o)\}$, as defined in equations (2)

Let $z(t) = x(t) + n(t)$ (27)

Our objective is to extract from $z(t)$ an estimate of the intelligence, $m^*(t_o)$. As stated previously, to derive a set of optimum estimation strategies we need a knowledge of the characteristics of the signal and noise. This means that we need a knowledge of the probability distribution of $a(t_o)$. Therefore, an estimator is optimum only for a particular modulation waveform. Over the duration $t_o$ our intelligence is uniformly distributed. Also the target strength, $b_t$, in all cases, will be an unknown constant. We therefore conclude that the variance of $m(t)$ is in effect the variance of $\gamma(t)$. We have, in effect

$$E\{m(t)\} = \lim_{t_o \to \infty} a(t_o) \cdot b_t \cdot E\{\gamma(t)\}$$

and

$$\phi_{mm}(t_1, t_2) = E\{[m(t) - E[m(t)]]^2\} = \phi_{\gamma\gamma}(t_1, t_2)$$

where $\phi_{\gamma\gamma}(t_1, t_2)$ is the covariance function of the multiplicative noise. Since in the real world the invariant period is finite, the limit given $t_o$ is unnecessary. If $t_o$ is too short, at most it will cause the otherwise stationary process to be nonstationary. In which case the variance of multiplicative noise needs to be recomputed during each updating interval. Since $\gamma(t)$, whether it is a Rayleigh or Rician process, is representable by two orthogonal gaussian processes, m(t) may be viewed as a result of gaussianization of $a(t_o)$ by the channel.

Our criterion for the derivation of an optimal estimator will be a conditionally biased maximum likelihood estimate. For reason of compactness of representation we shall use vector notation for the analysis in the remainder of this chapter.

If $\underline{m}^*$ is the estimate, we have

$$E\left\{\underline{m}^*\right\} = \underline{m} \circ \underline{e} \tag{28}$$

where the composition $\circ$ is either + or -

We note that if the estimate is unbiased $\underline{e} = \underline{0}$.

Writing equation (28) as

$$\underline{e} = \underline{m} - E\left\{\underline{m}^*\right\} \tag{29}$$

and assuming the cost of making an error is unimodal, $\underline{e}$ may be given a multinormal probability density function. The mean and covariance of $\underline{e}$ are then

$$E\left\{\underline{e}\right\} = E\left\{\underline{m}\right\} - E\left\{\underline{m}^*\right\}$$

$$= \underline{\mu} - \underline{\mu}^* \qquad (30)$$

and
$$\mathrm{Cov}\left[\underline{e}\right] = \Phi_{\underline{e}\,\underline{e}} = E\left\{\left[(\underline{m}-\underline{\mu}^*)-(\underline{\mu}-\underline{\mu}^*)\right]\cdot\left[(\underline{m}-\underline{\mu}^*)-(\underline{\mu}-\underline{\mu}^*)\right]^T\right\}$$

$$= E\left\{(\underline{m}-\underline{\mu})\quad(\underline{m}-\underline{\mu})^T\right\}$$

$$= \mathrm{Cov}\left[\underline{m}\right] \qquad (31)$$

where $\underline{\mu} = E\left\{\underline{m}\right\}$ and $\underline{\mu}^* = E\left\{\underline{m}^*\right\}$ . Our primary objective is to put a bias on the channel perturbation, $\gamma(t)$. For ease of representation we let:- $\Phi_{\gamma\gamma} = \Phi_{mm} = \mathrm{Cov}\left[\underline{m}\right]$

Assumption:-

The vector $\underline{m}$, being an implicit function of the observable $\underline{z}$, does not depend on the estimate $\underline{m}^*$.

With the above assumption we have

$$P(\underline{m}/\underline{m}^*) = P(\underline{m})$$

Also
$$P(\underline{e}) = P(\underline{m}/\underline{m}^*) = P(\underline{m})$$

Hence
$$P(\underline{m}) = P(\underline{e}) = k_1 e^{-1/2\left[(\underline{m}-\underline{\mu}),\ \Phi^{-1}_{\gamma\gamma}(\underline{m}-\underline{\mu})\right]} \qquad (32)$$

In vector notation equation (27) becomes

$$\underline{z} = \underline{x} + \underline{n}$$

or
$$\underline{n} = \underline{z} - \underline{x}$$
where $\underline{m}$ is implicit in $\underline{x}$

Since $\underline{n}$ is a gaussian vector we have

$$P(\underline{z}/\underline{m}) = P(\underline{z}/\underline{x}) = P(\underline{n}) = k_2 e^{-1/2\left[(\underline{z}-\underline{x}),\ \Phi^{-1}_{nn}(\underline{z}-\underline{x})\right]} \qquad (33)$$

From Decision Theory the Bayes' rule is:-

$$P(\underline{m}/\underline{z}) = \frac{P(\underline{z}/\underline{m})\, P(\underline{m})}{P(\underline{z})} \qquad (34)$$

where $P(\underline{m}/\underline{z})$ = the a posteriori probability of $\underline{m}$ given $\underline{z}$ has been observed,

$P(\underline{z}/\underline{m})$ = the likelihood or forward probability of observing $\underline{z}$ given $\underline{m}$ contains the intelligence,

$P(\underline{m})$ and $P(\underline{z})$ are the marginal probabilities of $\underline{m}$ and $\underline{z}$ respectively.

Our task is to find an operator which transforms the observable $\underline{z}$ into $\underline{m}^*$. This operator will be optimum if

$$\frac{\partial}{\partial \underline{m}} P(\underline{m}/\underline{z}) = 0 \qquad (35)$$

That is, the a posteriori probability is the criterion for the optimum estimator and equation (35) is the condition for optimization. Using the condition of equation (35) on the Bayes' rule of equation (34), we have the alternate condition

$$\frac{1}{P(\underline{z})} \frac{\partial}{\partial m} \left[P(\underline{z}/\underline{m}) \cdot P(\underline{m})\right] = 0,$$

or

$$\frac{\partial}{\partial \underline{m}} \left[P(\underline{z}/\underline{m}) \cdot P(\underline{m})\right] = 0, \qquad (36)$$

since $\dfrac{1}{P(\underline{z})} \neq 0$. Since the logarithm operation possesses monotonic properties, it is appropriate to take logarithms and then partial derivatives. Doing this we have

$$\frac{\partial}{\partial \underline{m}} \ln \left[P(\underline{z}/\underline{m}) \cdot P(\underline{m})\right] = \frac{\partial}{\partial \underline{m}}\left[\ln P(\underline{z}/\underline{m}) + \ln P(\underline{m})\right] = 0 \quad (37)$$

The $\underline{m}^*$ which satisfies the above partial derivative is the optimum operator we are seeking. Using equations (32) and (33) in equation (37) we have

$$\ln P(\underline{m}) = \ln k_1 - 1/2\left[(\underline{m}-\underline{\mu}), \Phi_{\gamma\gamma}^{-1}(\underline{m}-\underline{\mu})\right],$$

$$\frac{\partial}{\partial \underline{m}} \ln P(\underline{m}) = -\Phi_{\gamma\gamma}^{-1}(\underline{m} - \underline{\mu}), \quad (38)$$

and
$$\ln P(\underline{z}/\underline{m}) = \ln k_2 - 1/2\left[(\underline{z} - \underline{x}), \Phi_{nn}^{-1}(\underline{z} - \underline{x})\right],$$

$$\frac{\partial}{\partial \underline{m}} P(\underline{z}/\underline{m}) = \Phi_{nn}^{-1}(\underline{z} - \underline{x}) \frac{\partial x}{\partial \underline{m}}, \quad (39)$$

and finally

$$\Phi_{nn}^{-1}(\underline{z} - \underline{x})\frac{\partial x}{\partial \underline{m}} - \Phi_{\gamma\gamma}^{-1}(\underline{m} - \underline{\mu}) = 0$$

or
$$\underline{m}^* = \underline{\mu} + \Phi_{nn}^{-1} \Phi_{\gamma\gamma}(\underline{z} - \underline{x})\frac{\partial \underline{x}}{\partial \underline{m}^*} \quad (40)$$

Let $\underline{g} = \Phi_{nn}^{-1}(\underline{z} - \underline{x})$. The one-dimensional equivalent is $g(y) = \int_0^{t_o} \Phi_{nn}^{-1}(z(t) - x(t))\, dt$.

Then
$$\underline{m}^* = \underline{\mu} + \Phi_{\gamma\gamma}\frac{\partial \underline{x}}{\partial \underline{m}^*} \cdot \underline{g}$$

As a function of time (the one-dimensional case),

$$m^*(t) = E\{m(t)\} + \int_0^{t_o} \Phi_{\gamma\gamma}\frac{\partial x(y, m^*(t))}{\partial m^*(t)}\, g(y)\, dy$$

But
$$g(y) = \int_0^{t_o} \Phi_{nn}^{-1}(z(t) - x(t))\, dt$$

Hence $\quad m^*(t) = E\left\{m(t)\right\} + \int_o^{t_o} \Phi_{\gamma\gamma}(t, y) \dfrac{\partial x(y, m^*(t))}{\partial m^*(t)}$

$$\cdot \left[\int_o^{t_o} \Phi_{nn}^{-1} [z(t) - x(t)]\, dt\right] dy \qquad (41)$$

We note that for white gaussian noise with spectral density $N_{o/2}$, we get

$$\Phi_{nn} = \overline{n(t_1)\; n(t_2)}$$

$$= \int N_{o/2}\; \delta(t_1 - t_2)$$

$$= N_{o/2} = \sigma_n^{\;2}$$

Hence, for this case

$$m^*(t) = E\left\{m(t)\right\} + \frac{2}{N_o} \int_o^{t_o} \Phi_{\gamma\gamma}(t, y) \frac{\partial x(y, m^*(t))}{\partial m^*(t)} [z(y) - x(y)]\; dy$$

$$\ldots (41a)$$

But x(y) is a high frequency sinusoid, so that

$\dfrac{\partial x(y,\ m^*(t))}{\partial m^*(t)} x(y)$ becomes a double carrier frequency signal, which integrates to zero over the duration $t_o$. Equation (41) then reduces to

$$m^*(t) = E\left\{m(t)\right\} + \Phi_{nn}^{-1} \int_o^{t_o} \Phi_{\gamma\gamma}(t, y) \frac{\partial x(y, m^*(t))}{\partial m^*(t)}\; z(y)\; dy$$

$$\ldots (42)$$

The second term in equation (42) manifests a demodulation process. In equation (42) we have an estimator-demodulator. Realization of equation (42) requires an initial knowledge of the expectation of the corrupted intelligence, m(t) and the covariance functions of the fading random variates and the additive, white, gaussian noise.

Since neither m(t) nor n(t) is an explicit function, we can neither compute $E\{m(t)\}$ nor $\phi_{nn}$ readily from the observable z(t). Equation (42) therefore represents a non-realizable optimum estimator-demodulator. This optimum estimator-demodulator has the configuration shown in Figure 10. A practical realization of the optimum estimator should take the form of first demodulation and then estimation. This aspect will be the subject of the next Chapter.

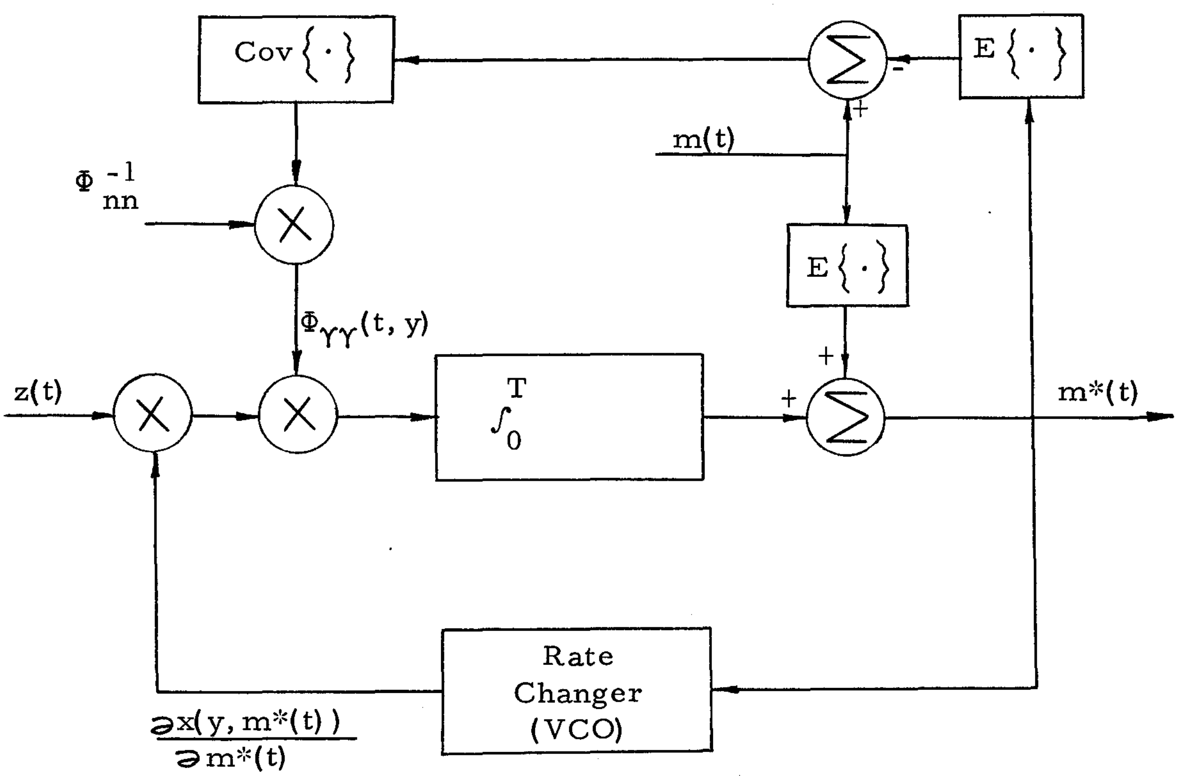


Figure 10
Optimum Non-Realizable
Estimator-Demodulator

# CHAPTER VI

# SIGNAL DECODING FOR ECHO RANGING IN A FADING ENVIRONMENT

## 6.1 Introduction

Thus far we have described the signalling techniques, the mathematical model of the randomly fading medium, and the signal detection and estimation strategies. In this chapter we analyze a practical design of an optimal echo ranging receiver for the encoded signal and the randomly fading medium described in Chapters III and IV, respectively. The theoretical aspects of signal detection and signal estimation strategies described in Chapters II and V, respectively, will be tailored to fit the practical design problem.

The receiver described in the sequel derives its demodulation frequency from the observable, $z(t)$. For this reason the receiver shall be termed a self-synchronized or tracking receiver. The receiver is theoretically capable of acquiring a moving target at any speed. However, to accommodate a large doppler frequency a correspondingly wide tracking loop bandwidth is required. It follows that more noise will be allowed to penetrate into the system, thereby deteriorating the system performance. In a practical design

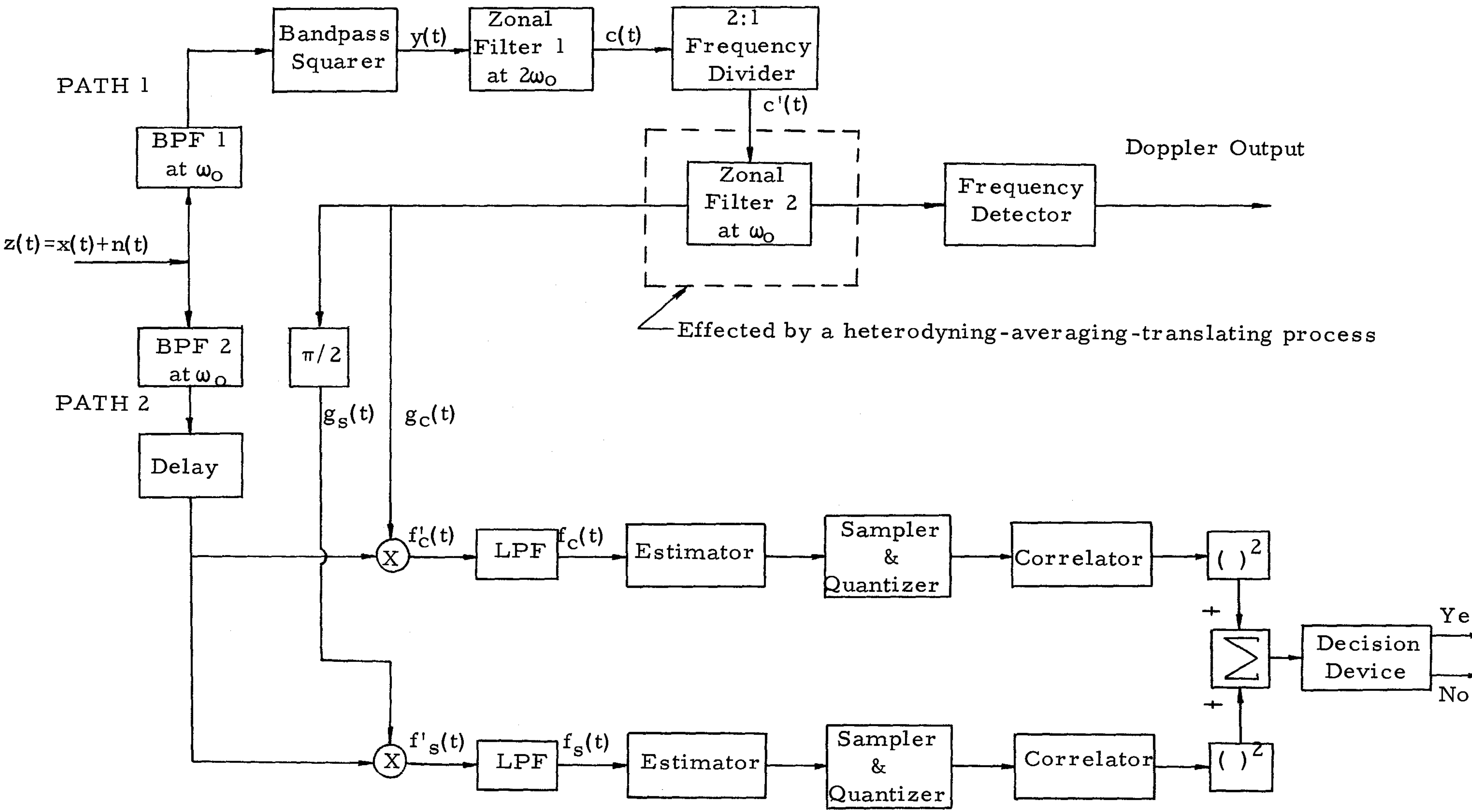


Figure 11 - An Optimum Adaptive Echo Ranging Receiver

the loop bandwidth will normally be just sufficiently big to accommodate the largest doppler shift anticipated.

The optimum self-synchronized pulse compression receiver for the signalling described in Chapter III is shown in Figure 11. If the information bandwidth and the largest doppler frequency anticipated are identical, one bandpass filter at the front end of the receiver suffices for both paths (1) and (2). The analysis of the bandpass squarer in path 1 is described in Appendix III. The second zonal filter at the carrier frequency $\omega_0$ is effected by an ordered heterodyning-averaging-translating process.

## 6.2 The Tracking One-Shot Receiver

As discussed in Chapter IV, reverberation has the same characteristics as the target echo. Since path 2 of the tracking receiver is maintained linear until the decision stage, superposition applies up to and including the correlator stage. Reverberation, if large in comparison to the desired target echo, may falsify signal detection. As in Chapter IV, we will assume reverberation to impose negligible threat on signal detection. As such we will ignore reverberation; the interferences encountered will mainly be random fading and additive, white, gaussian noise. In this respect the received signal is representable by equation (27) repeated below:-

$$z(t) = x(t) + n(t) \tag{27}$$

where $x(t) = \gamma(t)\, b_t \left\{a(t_o)\right\} \text{Cos}\, \omega_o(t - \delta t)$

is the desired target echo, as indicated in section 5. 3.

6. 2. 1 <u>Path 1</u>

Path 1 in Figure 11 is a carrier frequency regeneration process. The pertinent outputs from this path are a sinusoidal waveform at the input frequency and a doppler frequency to indicate the speed of moving target(s) if any. The sinusoidal waveform is utilized to effect quadrature demodulation at path 2 while the doppler frequency serves as a measure of target speed. Since we employ phase reversal modulation, a bandpass squarer is required to remove the modulation. As indicated in Appendix III the bandpass squarer exhibits weak signal suppression property. It is to be recognized then, for a high signal-to-noise ratio input the system will surely function properly. Our main concern, therfore, will be the low input signal-to-noise ratio cases. It is noted in Appendix III that the output signal-to-noise ratio exceeds unity when the input signal-to-noise ratio is approximately 6 db. We shall therefore concern ourselves with input signal-to-noise ratio below this figure. The especially interesting cases are the negative db input signal-to-noise ratio cases.

## 6.2.2 Zonal Filter 2

The function of this zonal filter is to limit the noise content so as to provide a relatively clean sinusoid for demodulation and, at the same time, to yield the doppler frequency, if any. * The bandwidth of the zonal filter will be sufficiently wide to accommodate the maximum anticipated doppler shift. To effect this zonal filter we employ a heterodyning-averaging-translating scheme. The filter is implemented by a two channel system at quadratures. The input to this zonal filter is given by equation (III-14).

$$\begin{aligned} c'(t) = {} & m^2(t)/2\,\mathrm{Cos}\,\omega_o(t - \delta t) \\ & + m(t)\,v_c(t)\,\mathrm{Cos}\,\omega_o(t - \delta t) - m(t)\,v_s(t)\,\mathrm{Sin}\,\omega_o(t - \delta t) \\ & + 1/2(v_c^2(t) - v_s^2(t))\,\mathrm{Cos}\,\omega_o(t - \delta t) \\ & - v_c(t) \cdot v_s(t)\,\mathrm{Sin}\,\omega_o(t - \delta t) \qquad \text{(III-14)} \end{aligned}$$

The zonal filter implementation is illustrated by the configuration of Figure 12.

* Frequency estimation, which is not dealt with in this thesis, may be introduced to optimize the carrier regeneration and Doppler determination.

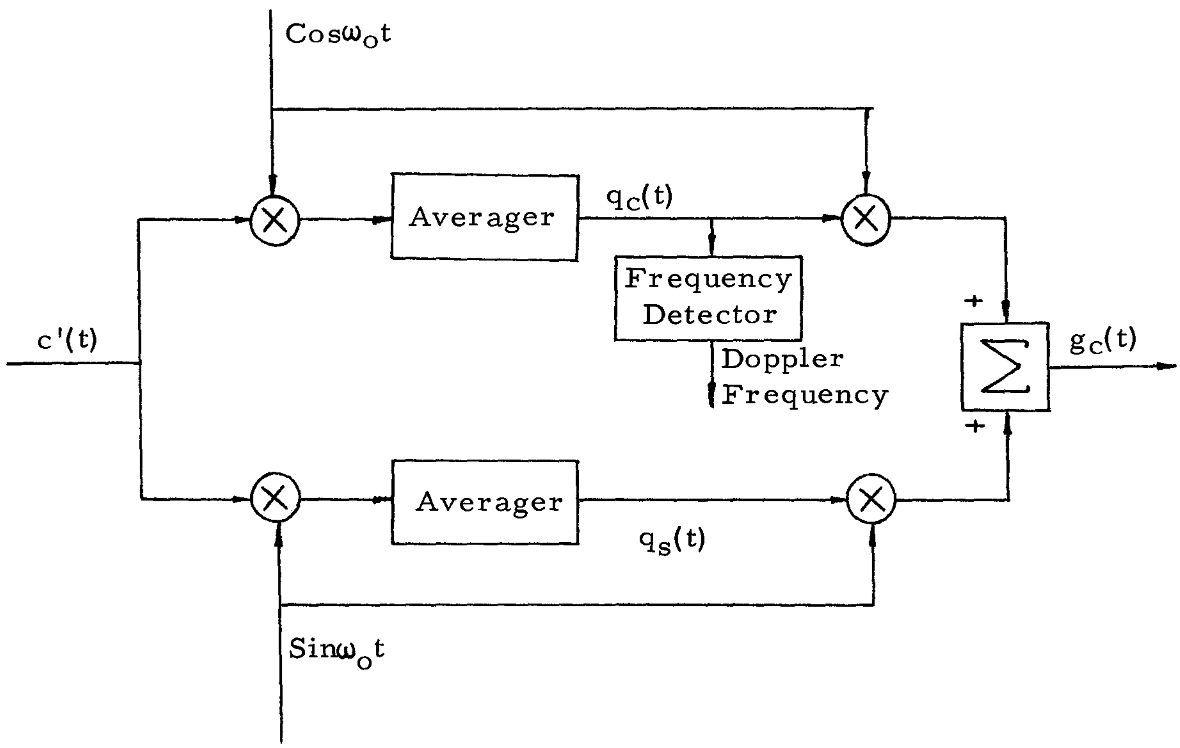


Figure 12 - Zonal Filter 2 Configuration

From Figure 12 we have, for the mixing stage:

$$
\begin{aligned}
c'(t)\,Cos\omega_o t = {} & \frac{m^2(t)}{2}Cos\left[\omega_o(t - \delta t)\right]Cos\omega_o t \\
& + m(t)v_c(t)Cos\left[\omega_o(t - \delta t)\right]\cdot\ Cos\omega_o t \\
& - m(t)v_s(t)Sin\omega_o(t - \delta t)Cos\omega_o t \\
& + 1/2(v_c{}^2(t) - v_s{}^2(t))Cos\omega_o tCos\omega_o t \\
& - v_c(t)\cdot v_s(t)Sin\omega_o(t - \delta t)Cos\omega_o t \qquad (43)
\end{aligned}
$$

and

$$c'(t)\mathrm{Sin}\omega_o t = 1/2m^2(t)\mathrm{Cos}\,\omega_o(t - \delta t)\mathrm{Sin}\omega_o t$$
$$+ m(t)v_c(t)\mathrm{Cos}\omega_o(t - \delta t)\mathrm{Sin}\omega_o t$$
$$- m(t)v_s(t)\mathrm{Sin}\omega_o(t - \delta t)\mathrm{Sin}\omega_o t$$
$$+ 1/2(v_c{}^2(t))\mathrm{Cos}\omega_o(t - \delta t)\mathrm{Sin}\omega_o t$$
$$- v_c(t) \cdot v_s(t)\mathrm{Sin}\,\omega_o(t - \delta t) \cdot \mathrm{Sin}\omega_o t \tag{44}$$

Upon averaging over some duration of time $T_o$, we have, for the in phase channel

$$q_c(t) = E\left\{\frac{m^2(t)}{4}\mathrm{Cos}\delta\omega_o t\right\}$$
$$+ E\left\{\frac{m(t)v_c(t)}{2}\mathrm{Cos}\,\delta\omega_o t\right\}$$
$$+ E\left\{-\frac{m(t)v_s(t)}{2}\mathrm{Sin}\delta\omega_o t\right\}$$
$$+ E\left\{\frac{v_c{}^2(t) - v_s{}^2(t)}{4}\mathrm{Cos}\,\delta\omega_o t\right\}$$
$$+ E\left\{- v_c(t) \cdot v_s(t)\mathrm{Sin}\delta\omega_o t\right\} \tag{45}$$

where the high frequency components have been averaged out. Similarly, we get, for the quadrature channel:

$$q_s(t) = E\left\{\frac{m^2(t)}{4}\mathrm{Sin}\delta\omega_o t\right\}$$
$$+ E\left\{\frac{m(t)\,v_c(t)}{2}\mathrm{Sin}\,\delta\omega_o t\right\}$$
$$+ E\left\{-\frac{m(t) \cdot v_s(t)}{2}\mathrm{Cos}\delta\omega_o t\right\}$$
$$+ E\left\{\frac{v_c{}^2(t) - v_s{}^2(t)}{4}\mathrm{Sin}\delta\omega_o t\right\}$$
$$+ E\left\{- 1/2v_c(t) \cdot v_s(t)\mathrm{Cos}\,\delta\omega_o t\right\} \tag{46}$$

Implicit in the derivation of equations (45) and (46) is the assumption that $T_o >> 1/2\omega_o$ and $T_o < \frac{1}{\delta\omega_o}$.

Remembering that $v_c(t)$ and $v_s(t)$ are zero mean gaussian processes and assuming $T_o$ to be sufficiently long for these random gaussian processes to average out, that is,

$$\frac{1}{T_o}\int_o^{T_o} v_c(t)\,dt \doteq \frac{1}{T_o}\int_o^{T_o} v_s(t)\,dt \doteq 0,$$

we get, for the in phase channel:

$$q_c(t) = E\left\{\frac{m^2(t)}{4}\right\} \operatorname{Cos}\delta\omega_o t + E\left\{\frac{v_c^2(t) - v_s^2(t)}{4}\right\} \operatorname{Cos}\delta\omega_o t \qquad (47)$$

and for the quadrature channel:

$$q_s(t) = E\left\{\frac{m^2(t)}{4}\right\} \operatorname{Sin}\delta\omega_o t + E\left\{\frac{v_c^2(t) - v_s^2(t)}{4}\right\} \operatorname{Sin}\delta\omega_o t \qquad (48)$$

In equations (47) and (48) we have the expected values of the random functions residing at the frequency $\delta\omega_o$. Depending on the averaging duration $T_o$ and the randomness of the functions $m^2(t)$, $v_c(t)$ and $v_s(t)$, the fluctuations may average out. Equations (47) and (48) may be illustrated by the vectorial representation shown in Figure 13.

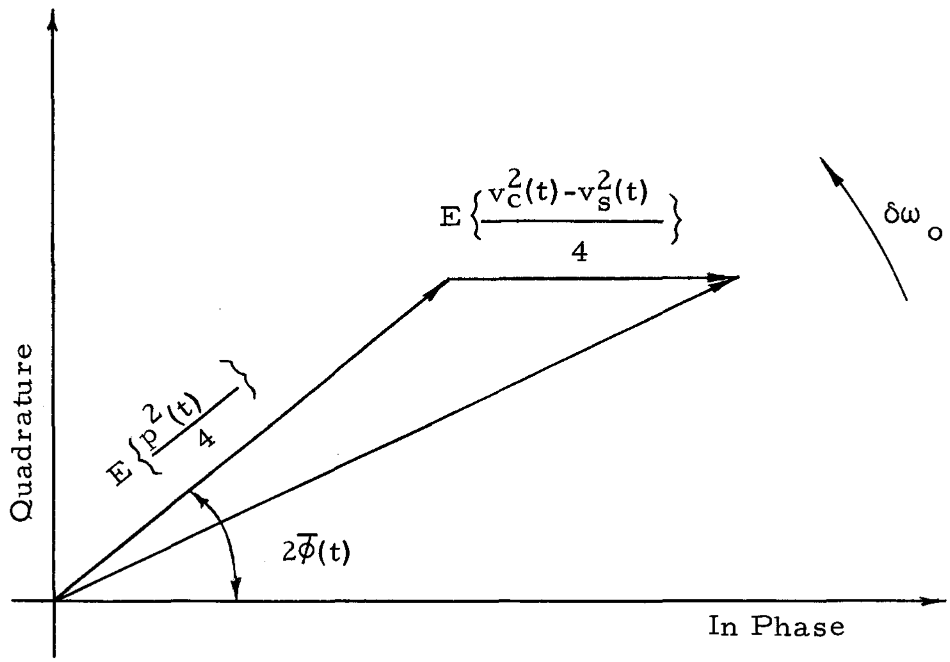


Figure 13 - Vectorial Representation For The Averaged Random Functions

The resultant vector shown in Figure 13 rotates at a rate of $\delta\omega_o$, which is the doppler frequency. Therefore, the doppler frequency may be obtained by passing the waveforms represented by either of equation (47) or (48) through a frequency detector. As indicated in Figure 12 the high frequency sinusoid required for signal demodulation is obtained by combining the two quadrature channels after frequency translation. Translating the frequency and combining, we have

$$g_c(t) = q_c(t)\,\mathrm{Cos}\,\omega_o t + q_s(t)\,\mathrm{Sin}\,\omega_o t$$

$$= E\left\{\frac{m^2(t)}{4}\right\} \mathrm{Cos}\,\delta\omega_o t\,\mathrm{Cos}\,\omega_o t + E\left\{\frac{v_c^{\,2}(t) - v_s^{\,2}(t)}{4}\right\} \cdot \mathrm{Cos}\,\delta\omega_o t\,\mathrm{Cos}\,\omega_o t$$

$$+ E\left\{\frac{m^2(t)}{4}\right\} \mathrm{Sin}\,\delta\omega_o t\,\mathrm{Sin}\,\omega_o t + E\left\{\frac{v_c^{\,2}(t) - v_s^{\,2}(t)}{4}\right\} \cdot \mathrm{Sin}\,\delta\omega_o t \cdot \mathrm{Sin}\,\omega_o t$$

$$= E\left\{\frac{m^2(t)}{4}\right\} \mathrm{Cos}\,\omega_o(t - \delta t) + E\left\{\frac{v_c^{\,2}(t) - v_s(t)}{4}\right\} \cdot \mathrm{Cos}\,\omega_o(t - \delta t) \tag{49}$$

The quadrature channel reference carrier is obtained by shifting equation (46) by $\pi/2$ radians:

$$g_s(t) = E\left\{\frac{m^2(t)}{4}\right\} \mathrm{Sin}\,\omega_o(t - \delta t) + E\left\{\frac{v_c^{\,2}(t) - v_s^{\,2}(t)}{4}\right\} \mathrm{Sin}\,\omega_o(t - \delta t) \tag{50}$$

Letting $\overline{A(t)} = E\left\{\frac{|m(t)|^2}{4}\right\}$ and $\overline{B(t)} = E\left\{\frac{v_c^{\,2}(t) - v_s^{\,2}(t)}{4}\right\}$,

we rewrite equations (49) and (50) as

$$g_c(t) = \overline{A(t)}\,\mathrm{Cos}\left[\omega_o(t - \delta t) - 2\bar{\phi}(t)\right] + \overline{B(t)}\,\mathrm{Cos}\,\omega_o(t - \delta t) \tag{51}$$

$$g_s(t) = \overline{A(t)}\,\mathrm{Sin}\left[\omega_o(t - \delta t - 2\bar{\phi}(t)\right] + \overline{B(t)}\,\mathrm{Sin}\,\omega_o(t - \delta t) \tag{52}$$

In going from equation (III-14) to equations (51) and (52) we have subjected the incoherent fluctuations to statistical averaging, thereby smoothing out the random fluctuations resulting from bandpass squaring. Because of the finite duration, $T_o$, any fluctuation with period greater than $T_o$ will remain untouched. The derived sinusoidal waveforms $g_c(t)$ and $g_s(t)$ will, therefore, still be suffering from very slow random fluctuation. However, $g_c(t)$ and $g_s(t)$ are expected to be recognizable sinusoids; the averaged slow fluctuation should impose no detrimental effect on the demodulation process at path 2. In retrospect we note that the averaging duration, $T_o$, restricts the doppler range to the bound

$$|\delta \omega_o| \max. < \frac{2\pi}{T_o} .$$

### 6.2.3 Path 2

The delay introduced in path 2 is designed to allow computation time for carrier regeneration in path 1. The signals arriving at the set of multipliers in path 2 are derived from the same observable, with those from path 1 having undergone a carrier regeneration transformation. Carrying out the multiplication indicated in path 2, Figure 11, we have

$$f'_c(t) = z(t) \cdot g_c(t), \tag{53}$$

and $$f_s'(t) = z(t) \cdot g_s(t) \tag{54}$$

Using equations (27), (51) and (52) and letting $p(t) = \text{Env}\left\{m(t)\right\}$,

we have

$$\begin{aligned}
f_c'(t) &= [\, p(t)\text{Cos}[\omega_o(t-\delta t) - \phi(t)] + v_c(t)\text{Cos}\,\omega_o(t-\delta t) - \\
&\qquad\qquad v_s(t)\text{Sin}\,\omega_o(t-\delta t)\,] \\
&\quad \cdot [\overline{A}(t)\text{Cos}[\omega_o(t-\delta t) - 2\overline{\phi}(t)] + \overline{B}(t)\text{Cos}\,\omega_o(t-\delta t)] \\
&= 1/2\, p(t)\overline{A}(t)\Big\{\text{Cos}[2\omega_o(t-\delta t) - \phi(t) - 2\overline{\phi}(t)] \\
&\qquad\qquad + \text{Cos}\,(2\overline{\phi}(t) - \phi(t)]\Big\} \\
&\quad + 1/2\, p(t)\overline{B}(t)\Big\{\text{Cos}[2\omega_o(t-\delta t) - \phi(t)] + \text{Cos}\phi(t)\Big\} \\
&\quad + 1/2\, v_c(t)\overline{A}(t)\,[\text{Cos}[2\omega_o(t-\delta t) - 2\overline{\phi}(t)] + \text{Cos}\;2\overline{\phi}(t)] \\
&\quad + 1/2\, v_c(t)\overline{B}(t)\Big\{\text{Cos}\;2\omega_o(t-\delta t) + \text{Cos}\,[o]\Big\} \\
&\quad - 1/2\, v_s(t)\overline{A}(t)\Big\{\text{Sin}[2\overline{\phi}(t)] + \text{Sin}[2\omega_o(t-\delta t) - 2\overline{\phi}(t)]\Big\} \\
&\quad - 1/2\, v_s(t)\overline{B}(t)\Big\{\text{Sin}\,[o] + \text{Sin}\;2\omega_o(t-\delta t)\Big\}
\end{aligned}$$

After low-pass filtering we get

$$\begin{aligned}
f_c(t) &= 1/2\Big\{\underbrace{p(t)\overline{A}(t)\text{Cos}[2\overline{\phi}(t) - \phi(t)] + p(t)\overline{B}(t)\text{Cos}\phi(t)}_{\text{Coherent Component}} \\
&\quad + 1/2\Big\{\underbrace{v_c(t)\overline{A}(t)\text{Cos}[2\overline{\phi}(t)] + v_c(t)\overline{B}(t) - v_s(t)\overline{A}(t)\text{Sin}\;2\overline{\phi}(t)}_{\text{Incoherent Component}}\Big\}.
\end{aligned} \tag{55}$$

Similarly,

$$\begin{aligned}
f_s(t) &= 1/2\Big\{\underbrace{-\,p(t)\overline{A}(t)\text{Sin}[2\overline{\phi}(t) - \phi(t)] + p(t)\overline{B}(t)\text{Sin}\phi(t)}_{\text{Coherent Component}}\Big\} \\
&\quad - 1/2\Big\{\underbrace{v_c(t)\overline{A}(t)\text{Sin}[2\overline{\phi}(t)] - v_s(t)\overline{A}(t)\text{Cos}[2\overline{\phi}(t)] - v_s(t)\overline{B}(t)}_{\text{Incoherent Component}}\Big\}.
\end{aligned} \tag{56}$$

It is of interest to note that by further assuming

$$\frac{1}{T_o}\int_o^{T_o} v_c^{\,2}(t)\;dt \doteq \frac{1}{T_o}\int_o^{T_o} n^2(t)\;dt$$

$$\frac{1}{T_o}\int_o^{T_o} v_s^{\,2}(t)\;dt \doteq \frac{1}{T_o}\int_o^{T_o} n^2(t)\;dt$$

we have $\overline{B}(t) = 1/4\left\{\frac{1}{T_o}\int_o^{T_o} v_c^{\,2}(t)\;dt - \frac{1}{T_o}\int_o^{T_o} v_s^{\,2}(t)\;dt\right\} \doteq 0$

With this latter assumption equations (55) and (56) reduce to the simpler forms:-

$$\begin{aligned} f_c(t) &= 1/2\,p(t)\overline{A}(t)\,\mathrm{Cos}[\,2\phi(t)\;-\phi\,(t)] \\ &\quad + 1/2\,v_c(t)\overline{A}(t)\,\mathrm{Cos}[\,2\overline{\phi}(t)] - 1/2\,v_s(t)\overline{A}\,(t)\mathrm{Sin}\,[2\phi(t)\,] \\ &= 1/2\overline{A}(t)\Big\{p(t)\,\mathrm{Cos}[\,2\overline{\phi}(t) - \phi(t)\,] \\ &\qquad + v_c(t)\,\mathrm{Cos}\,[2\overline{\phi}(t)\,] - v_s(t)\,\mathrm{Sin}[\,2\overline{\phi}(t)]\Big\}, \quad (57) \end{aligned}$$

and

$$\begin{aligned} f_s(t) &= 1/2\overline{A}(t)\Big\{p(t)\mathrm{Sin}[\,\phi(t) - 2\overline{\phi}(t)] \\ &\qquad - v_c(t)\mathrm{Sin}\,[2\overline{\phi}(t)\,] - v_s(t)\,\mathrm{Cos}[\,2\overline{\phi}(t)]\Big\}. \quad (58) \end{aligned}$$

Implicit in the coefficient p(t) of the coherent components in equations (57) and (58) is the randomly fading envelope, $\mathrm{Env}\{\gamma(t)\}$, the complex target strength $b_t$, and the intelligence $\{a(t_o)\}$. It is noted that equations (55) and (56), or (57) and (58), are baseband waveforms, that is, there is no frequency content other than that implicit in the intelligence $\{a(t_o)\}$. The perturbations which mask the intelligence are all wide-band random processes which are subject to statistical averaging. To enhance the comprehension of the intelligence $\{a(t_o)\}$, we estimate the random function P(t), hopefully, to average out the incoherent fluctuations and the perturbations inherent in the fading factor, $\gamma(t)$. We shall tailor the theoretical optimum estimator derived in Chapter V to a practically realizable configuration for the system under consideration. The optimization process presented in the sequel will, therefore, necessarily be sub-optimum. We shall assume the analysis up to equations (57) and (58) holds. Therefore, equations (57) and (58) are the signals we wish to estimate.

## 6.3 The Channel Estimator

The necessity for signal estimation, as stated in Chapter V, arises from the fact that the processes corrupting the signal intelligence are random in nature. Since the code, $\{a_i(t_o)\}_{i = 1, 2, \ldots, N}$, itself is random, it is not feasible to estimate the whole code. We therefore resort to estimate the digits. Partitioning the code into individual digits, we represent the corrupted intelligence, on a digit basis, by

$$P(t) = \text{Env}\{m(t)\} = \text{Env}\{\gamma(t) \quad b_t\} \cdot a(t_o) \qquad (59)$$

where $a(t_o)$ is a single digit or subpulse of duration $t_o$. Since the in phase and the quadrature channels have similar statistics it suffices to implement identical estimators in both channels. We will, therefore, concern ourselves with the in phase channel only in analyzing the practical channel estimator.

Using equation (59) in equation (57), we have

$$f_c(t) = 1/2\overline{A}(t)\left\{\mathrm{Env}[\gamma(t)]\cdot b_t\cdot a(t_o)\mathrm{Cos}\,[2\phi(t)-\phi(t)] + v_c(t)\mathrm{Cos}[2\overline{\phi}(t)] - v_s(t)\mathrm{Sin}\,[2\phi(t)]\right\}$$

$$= \alpha(t) + \varepsilon\,(t) \qquad (60)$$

where $\alpha(t) = 1/2\overline{A}(t)\mathrm{Env}[\gamma(t)]\cdot b_t\cdot a(t_o)\mathrm{Cos}\,[2\phi(t)-\phi(t)]$

is the corrupted intelligence,

$$\varepsilon(t) = 1/2\overline{A}(t)\,[v_c(t)\mathrm{Cos}[2\phi(t)] - v_s(t)\mathrm{Sin}[2\overline{\phi}(t)]]$$

is the incoherent noise. The mean and variance of the incoherent noise are

$$E\{\varepsilon(t)\} = 1/2\overline{A}(t)\mathrm{Cos}\,[2\overline{\phi}(t)]E\{v_c(t)\} - 1/2\overline{A}(t)\mathrm{Sin}[2\overline{\phi}(t)]\cdot E\{v_s(t)\} = 0$$

and

$$\sigma_\varepsilon^2 = E\{\varepsilon^2(t)\} = \left[\frac{\overline{A}(t)}{2}\right]^2\left\{\mathrm{Cos}^2[2\overline{\Phi}(t)]E[v_c^2(t)] + \mathrm{Sin}^2[2\overline{\phi}(t)]E[v_s^2(t)]\right\}$$

$$= \left[\frac{\overline{A}(t)}{2}\right]^2\sigma_n^2$$

since

$$E[v_c^2(t)] = E[v_s^2(t)] = \sigma_n^2$$

is the noise variance at the system input. Thus the variance, $\sigma_\varepsilon^2$, of the incoherent additive noise at the demodulation stage is simply the additive noise variance at the input weighted by a constant scalar. But the same weighting is also applied to the signal term. Therefore the signal-to-noise ratio at the demodulation stage, from the mathematical viewpoint, is the same as that at the system input. We note also that since $n(t)$ is Gaussianly distributed $\varepsilon(t)$ is also.

Except for a translation in frequency equation (60) is similar to equation (27). Therefore the analysis in Chapter V subsequent to equation (27) holds. By substituting $f_c(t)$ for $z(t)$, $\alpha(t)$ for $x(t)$, and $\varepsilon(t)$ for $n(t)$ in the optimal estimator of equation (41a), we get the following optimal estimator for the system under consideration:-

$$\alpha^*(t) = E\left\{\alpha(t)\right\} + 1/\sigma_\varepsilon^2 \int_o^{t_o} \sigma_\alpha^2(t, y)[f_c(y) - \alpha^*(y)]\, dy$$

$$= E\left\{\alpha(t)\right\} + \frac{1}{K\sigma_n^2} \int_o^{t_o} \sigma_\alpha^2(t, y)[f_c(y) - \alpha^*(y)]\, dy \tag{61}$$

where $\sigma_\varepsilon^2 = K\sigma_n^2$ and $\sigma_\alpha^2(t, y) = \phi_{\alpha\alpha}(t, y)$.

The estimate, $\alpha^*(t)$, is thus obtained by updating the expectation of $m(t)$. We have

$$E\left\{f_c(t)\right\} = E\left\{\alpha(t)\right\} = E\left\{\varepsilon(t)\right\}$$
$$= E\left\{\alpha(t)\right\}. \tag{62}$$

It is thus mathematically satisfying to obtain $E\left\{\alpha(t)\right\}$.

Taking second moment of $f_c(t)$, we have

$$E\left\{f_c^{\,2}(t)\right\} = E\left\{[\,\alpha(t) + \varepsilon(t)]^2\right\}$$

$$= E\left\{\alpha^2(t)\right\} + E\left\{\varepsilon^2(t)\right\}$$

$$E\left\{f_c^{\,2}(t)\right\} - [\,E\left\{f_c(t)\right\}]^2 = E\left\{\alpha^2(t)\right\} - [E\ \alpha(t)\,]^2 + E\left\{\varepsilon^2(t)\right\}$$

$$= \sigma_\alpha^{\,2} + \sigma_\varepsilon^2$$

$$\doteq \sigma_\gamma^2 + \sigma_\varepsilon^2$$

$$\doteq \sigma_\gamma^2 + K\sigma_n^{\,2}\ . \qquad (63)$$

Using equations (62) and (63) in equation (61) we get the optimal estimator configuration shown in Figure 14.

In regard to the optimal adaptive estimator of equation (61) we make the following interesting observations:-

(i) $\sigma_\gamma^2(t, y)$ is the variance of the fading random variates. If the channel has stationary statistics, $\sigma_\gamma^2(t, y) = \sigma_\gamma^2$. If the channel has non-stationary statistics, $\sigma_\gamma^2(t, y)$ depends on the time origin and needs to be computed for each updating process.

(ii) The ratio $\sigma_\gamma^2(t, y)/\sigma_n^{\,2}$ represents a multiplicative noise-to-additive noise power ratio. The updating components is more significant when $\sigma_\gamma^2(t, y) > \sigma_n^{\,2}$

(iii) Neither $\alpha(t)$ nor $\varepsilon(t)$ is an observable; therefore explicit computations for $E\left\{\alpha(t)\right\}$, $\sigma_\gamma^2(t, y)$ and $\sigma_\varepsilon^2$ impose some difficulty.

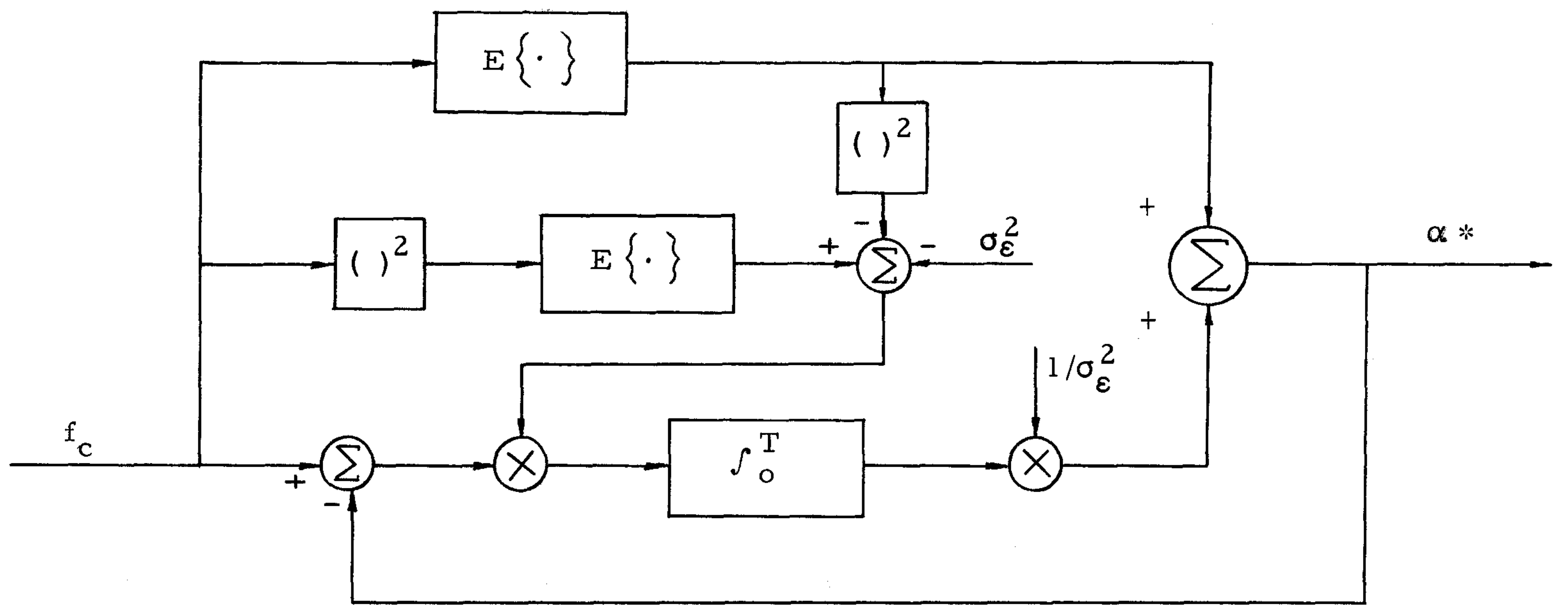


Figure 14 - Optimal Adaptive Estimator

(iv) To implement the optimal adaptive estimator of Figure 14, we need only a knowledge of $\sigma_\varepsilon^2$. Real channels usually have stationary time invariant additive noise; $\sigma_\varepsilon^2$, therefore, can be measured before hand. The optimal adaptive estimator can, therefore, be realized; the optimality is dependent on the estimation duration $t_o$, however.

## 6.4 The Correlator

The correlator may be derived using a maximum likelihood criterion. The derivation and realization of the cross-correlator has been described elsewhere [11] and will not be repeated in this thesis. The following comments as regards the correlator, however, are in order.

(1) The derivation of the correlator is based on the maximum likelihood criterion. As such its implementation bears a direct relationship to the code chosen for signal encoding in Chapter III.

(2) The correlator output signal-to-noise ratio, signal resolution, and dynamic range are detectability criteria of system performance.

(3) The correlator is representable by the equation

$$R_{\alpha^* a} = \sum_{j=1}^{N} \sum_{i=1}^{N} \alpha_j^*(t_o) \cdot a_i(t_o) \qquad (63)$$

where $\left\{\alpha_{-j}^{*}(t_o)\right\}$ = is the overall estimator output for an interval $T = Nt_o$

$\left\{a_i(t_o)\right\}$ = is the reference sequence.

Equation (63) is simply illustrated in Figure 15a.

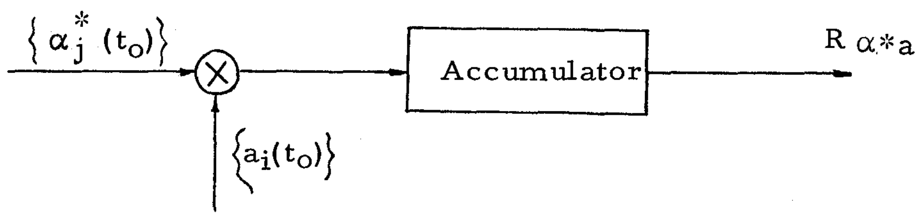


Figure 15a - The Cross-Correlator

Identical correlators are employed for the in-phase and the quadrature channels. The final system output is a combination of these:

$$\psi = \left\{ [R_{\alpha_c^{*} a}]^2 + [R_{\alpha_s^{*} a}]^2 \right\}^{1/2} \tag{64}$$

The above equation is illustrated in Figure 15b.

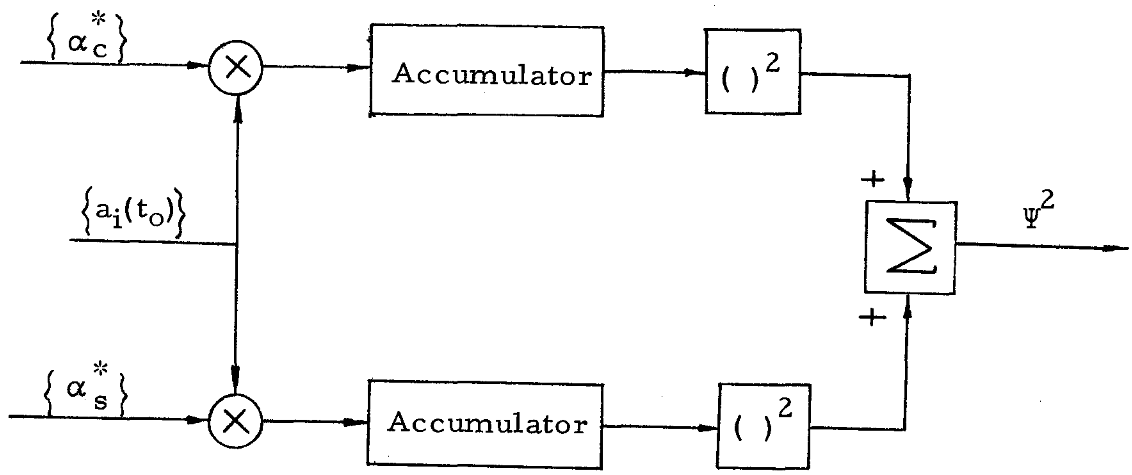


Figure 15b- Correlation Detector

## 6.5 Summary

The averaging operator, $E\{\cdot\}$, employed for the derivations in this Chapter yields a true average only in the limit when the time is infinite. However, if the random processes are very wide-band, $E\{\cdot\}$, will be approximately true even for a finite integration time. This may especially be true in the additive, white, gaussian noise case. In deriving a demodulation reference from the observable we accept a loss factor $\overline{A}(t) = E\left\{\frac{m^2(t)}{4}\right\}$. Since $\overline{A}(t)$ is computable under the assumptions made, it may be re-introduced for compensation further down in the receiver.

# CHAPTER VII

# IMPLEMENTATION, COMPUTER SIMULATION AND DISCUSSION OF RESULTS

Thus far we have presented in Chapter II through Chapter VI a theoretical design of an optimal echo ranging system to operate in a randomly fading environment. The system design is optimized with respect to both signal detection and estimation strategies. The system employs a pseudo-random binary code for signal encoding. The random variates in the propagation medium are modelled by either a Rayleigh or a Rician amplitude distribution. The former has an associated uniform phase distribution while the latter has an associated complex phase distribution. The joint amplitude and phase probability density functions for the Rayleigh and Rician processes are given respectively by equations (10) and (12). The receiver is a self-synchronized demodulator-estimator-correlator combination. A maximum a posteriori probability criterion has been used to derive the optimum estimator and correlator. The overall system can either be implemented or computer simulated. The procedure for system implementation are outlined in the next section. System performances are evaluated by digital computer simulation using the IBM 7040. A program listing of the overall computer simulation is given in Appendix

IV. The programming aspect and the level of subroutine calling are described there.

## 7.1 Implementation Procedures

The statistical averager employed in the design of zonal filter 2 and the estimator may be implemented by tapped-delay lines. A first order statistical averager, assuming x(t) is an Ergodic process, is given by the equation

$$E\left\{x(t)\right\} = \lim_{T\to\infty} \frac{1}{T}\int_{o}^{T} x(t)\,dt$$

$$= \lim_{M\to\infty} \frac{1}{M}\sum_{i=1}^{M} x_i \qquad (65)$$

Equation (65) can be implemented by a tapped-delay line as shown in Figure 16.

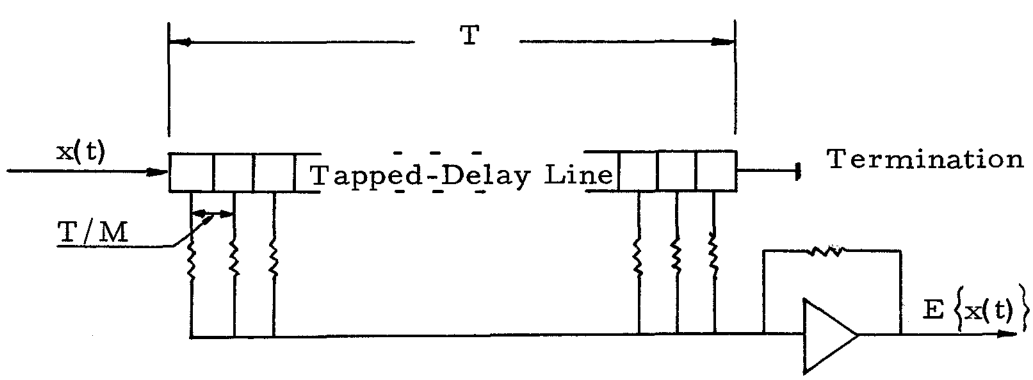


Figure 16 - Implementation for a First Order Statistical Averager

The first order statistical averager shown in Figure 16 can be utilized to implement the zonal filter of Figure 12 and the adaptive estimator of Figure 14. These are shown in Figures 17 and 18.

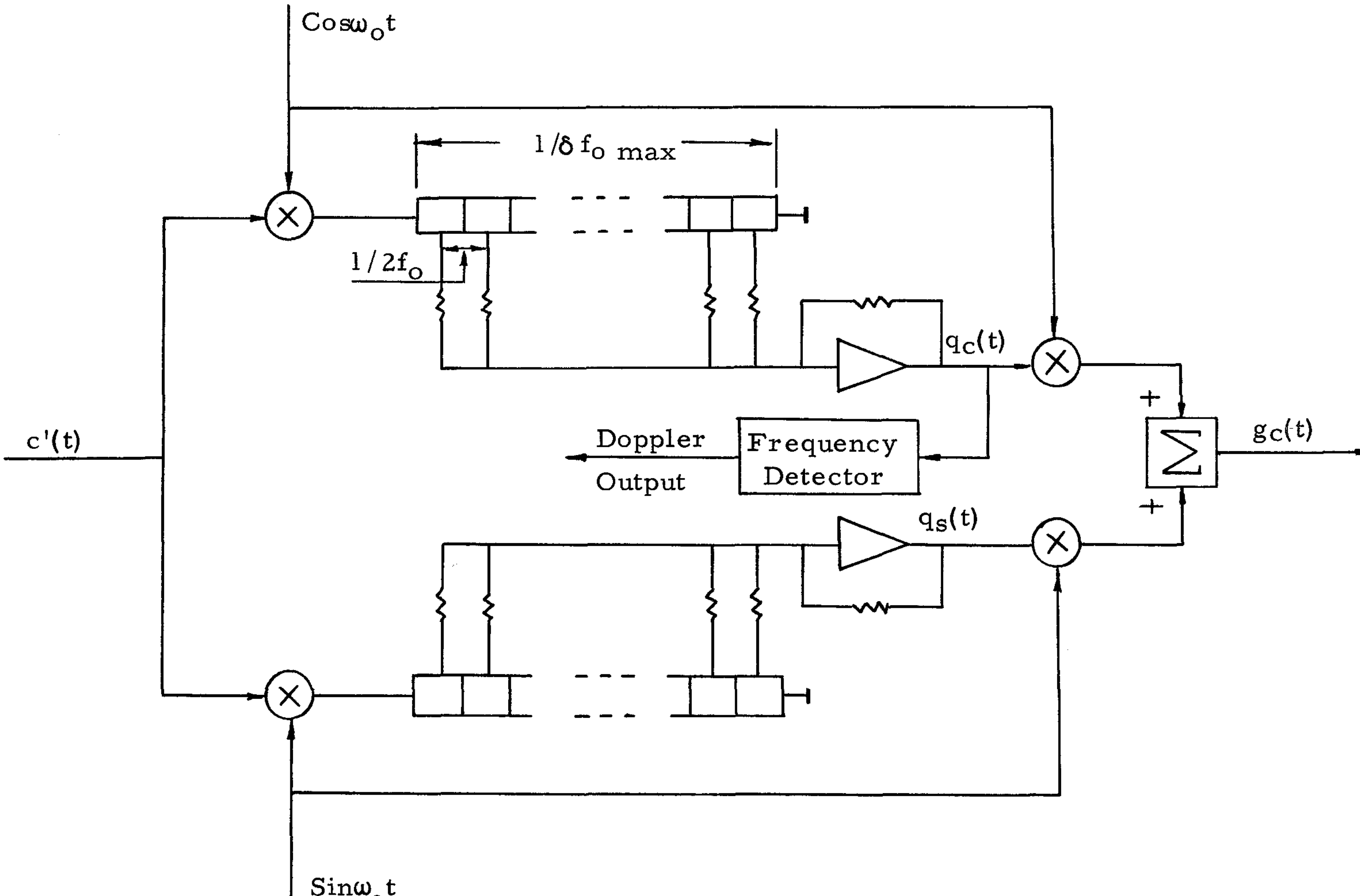


Figure 17 - Zonal Filter 2 Implementation

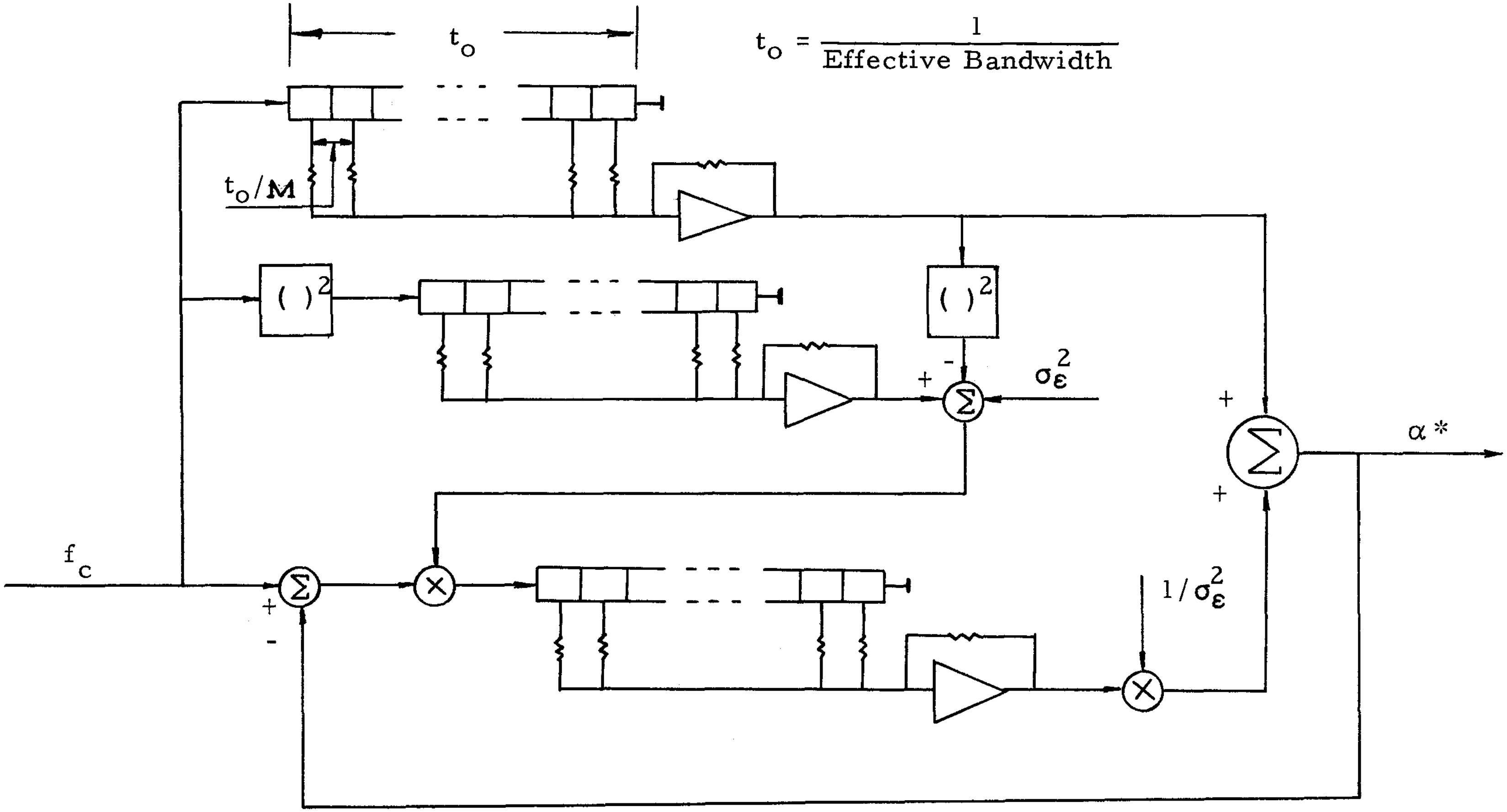


Figure 18 - Optimal Adaptive Estimator Implementation

## 7.2 Signal Encoding and Decoding By Computer Simulation

Since signal coding is an inexhaustible topic in itself, it is not a subject of this thesis. Nevertheless, a 105 digit binary convolution code discussed in Chapter III and Appendix I is utilized for signal encoding.

The computer simulation, a program listing of which is given in Appendix IV, encompasses the entirety of bandpass modulation, channel fading, self-synchronized demodulation and baseband estimation and correlation detection. The overall system functional block diagrams shown in Figures 2, 3, and 11 should be followed closely while reading the discussions in the remainder of this chapter. The waveforms presented in Figure 19 through Figure 33 are plotted by the Benson-Lehner digital X-Y plotter. Because of computer memory limitation, each carrier cycle of the bandpass signal is created by eight samples. The simulated system, therefore, unavoidably suffers a sampling error. All waveforms are plotted on a normalized amplitude basis.

Figure 19(a) is a 105 digit binary convolution code, where the digits have been simply joined by the X-Y plotter. A binary 1 has been mapped into a -1 amplitude level while a binary 0 has been mapped into a +1 amplitude level. Figure 19(b) shows a pure sinusoid, where a frequency drift with respect to the transmitter oscillator frequency has been injected. This particular sinusoid is used to effect the carrier regeneration process. The ripples shown are due to insufficient samples used in creating the carrier cycle. The frequency drift is designed to simulate a moving target situation. It is injected at this point for convenience; the frequency drift could equally well be injected during signal propagation. The transmitted waveform is shown in Figure 19(c). The propagation medium is made up of a multiplicative and an additive noise. The multiplicative noise is simulated by a sum of fixed and random components. The random component is a Rayleigh process with uniform phase distribution in the primary interval $(0, 2\pi)$. This is simulated by two orthogonal Gaussian processes. The additive noise is simulated by a Gaussian process. Since the Rayleigh process can be represented by two orthogonal Gaussian processes, the multiplicative noise and the additive noise differ only in spectrum or in rapidity of fluctuation with time. The target has been given a unity amplitude with an approximately 45 degree phase. The medium output is a perturbed signal shown in Figure 20(a). Figure 21(a) shows the frequency drift (Doppler shift frequency) extracted from operations on the received noisy signal. Figures 20(b) and 21(b) show,

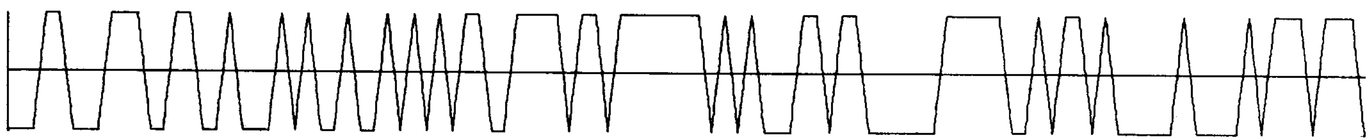

(a) 105 DIGIT CODE

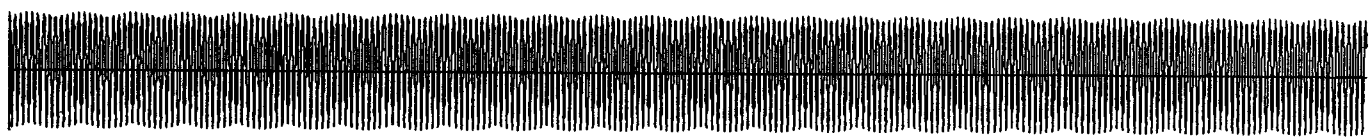

(b) SINUSOIDAL SIGNAL

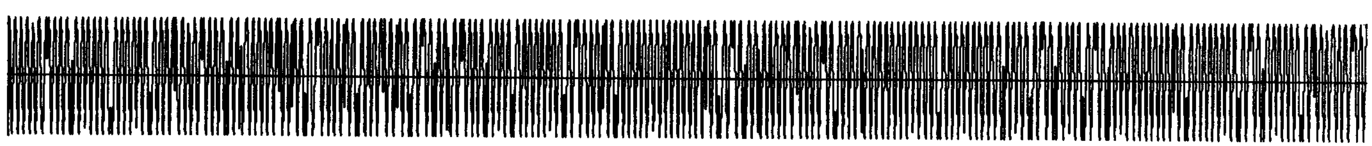

(c) ENCODED SIGNAL

Figure 19 - Waveforms Illustrating the Encoding Process

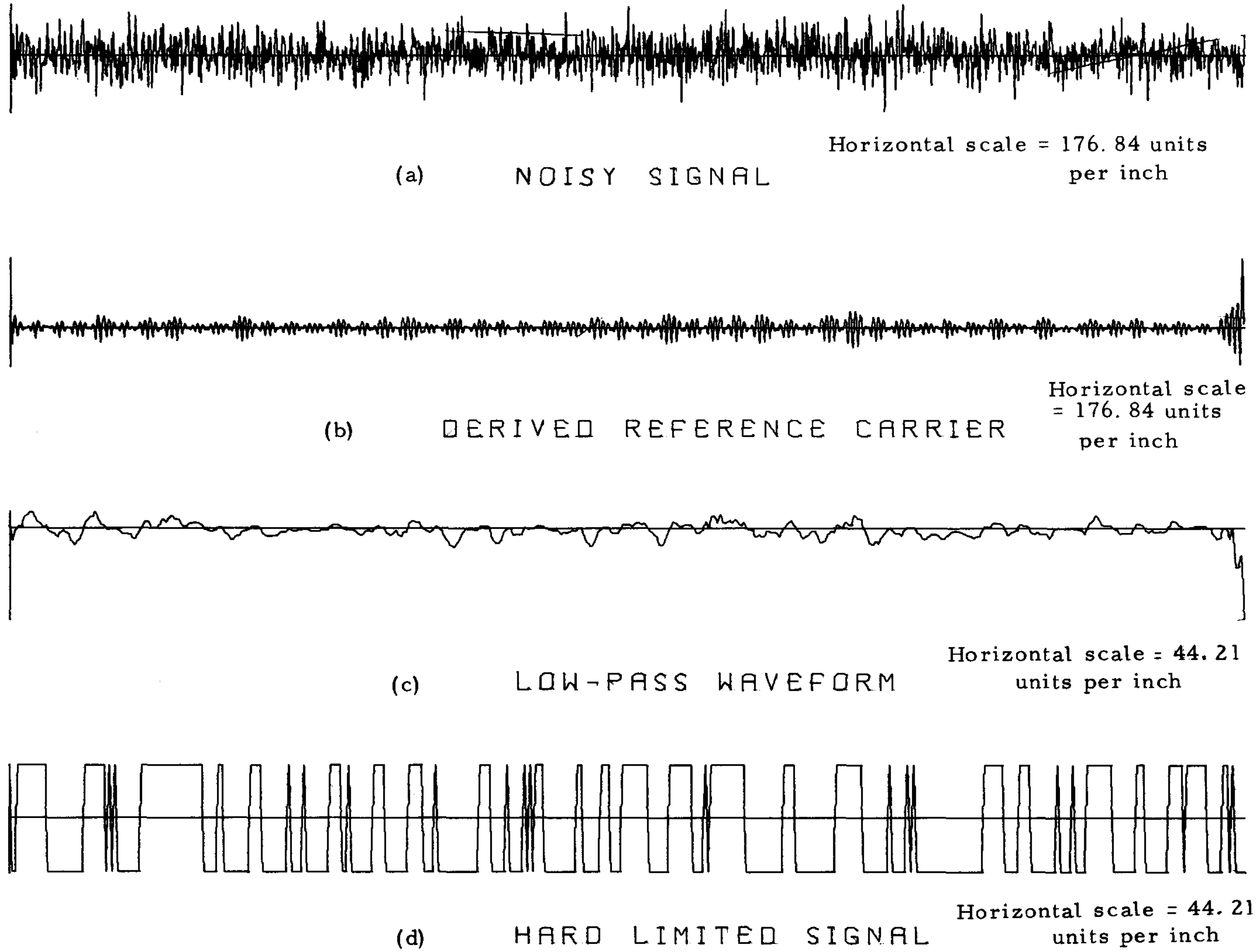


Figure 20 - Self-synchronized Demodulation Waveforms In Phase Channel

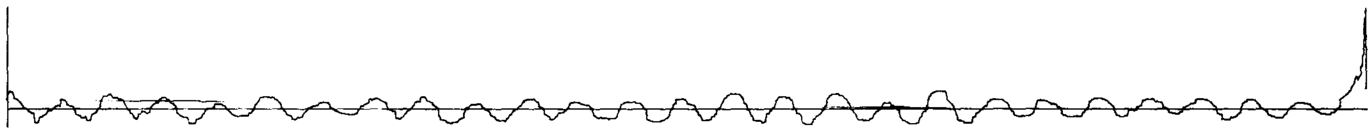

(a) FREQUENCY DRIFT

Horizontal scale = 176.84 units per inch

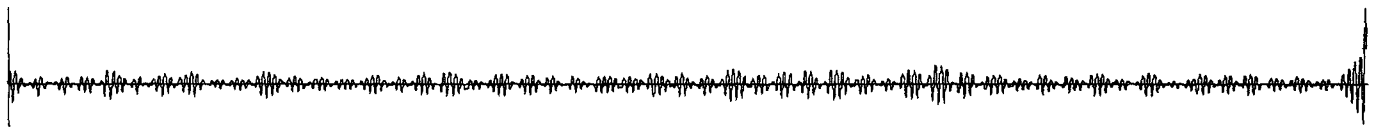

(b) DERIVED REFERENCE CARRIER

Horizontal scale = 176.84 units per inch

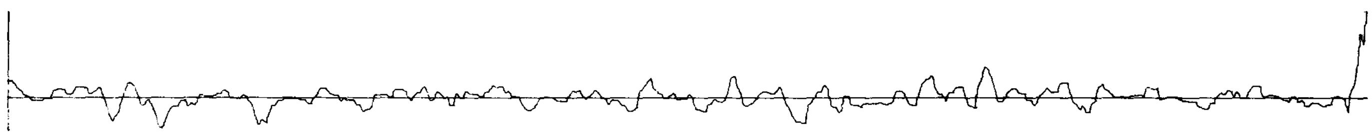

(c) LOW-PASS WAVEFORM

Horizontal scale = 44.21 units per inch

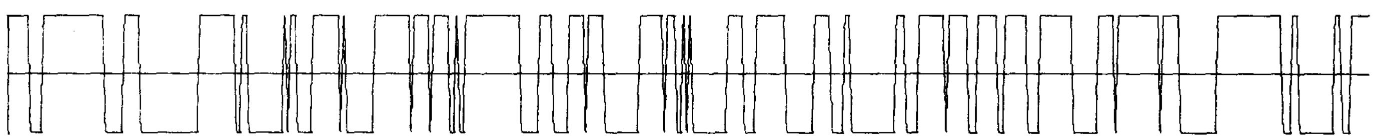

(d) HARD LIMITED SIGNAL

Horizontal scale = 44.21 units per inch

Figure 21 - Self-synchronized Demodulation Waveforms Quadrature Channel

respectively, the derived in-phase and quadrature reference carriers for self-synchronized demodulation. These waveforms together with the Doppler frequency signal of Figure 21(a) are the pertinent outputs from path 1 of Figure 11. The rippling phenomenon exhibited in the waveforms of Figures 20(b) and 21(b) is a direct result of finite averaging time employed in effecting Zonal Filter 2. That is, any noise component with periodicity greater than the averaging time will remain untouched. The demodulated baseband signals are shown in Figures 20(c) and 21(c); an infinitely clipped version of which is shown, respectively, in Figures 20(c), 20(d), 21(c) and 21(d) have been sampled at a rate of 5 samples per baud. In the absence of channel perturbation the baseband waveforms should be similar in shape before and after infinite clipping.

## 7.3 Computer Simulated Signal Estimation and Correlation Detection

As discussed in Chapter V the estimation process is designed to operate on random processes. If the input to the estimator is a noiseless deterministic function the estimator offers no enhancement. Moreover, anytime a decision is made one can expect to introduce error. Since an estimator makes a decision at the end of each estimation period, it introduces an error of its own, however small this error may be.

Figures 22 and 23 show the system final outputs for the cases without and with the estimator, respectively. In these cases the channel has been made noise free. Since, in the absence of channel perturbation, the time compressed waveforms are only limited by self-noise* , a comparison between Figures 22(c) and 23(c) does not shed much light on the adverse effect of the estimator. A comparison between the uncompressed waveforms of Figures 22(a) and 23(a), however, shows that the estimated waveform suffers from decision error. Fortunately, real channels are noisy; therefore, signal estimation is a necessary process in most signal processing analyses.

The carrier phase at the input to the receiver has been chosen to be approximately 45 degrees. The in-phase and the quadrature channels, therefore, have approximately equal signal captivity. It is sufficient, therefore, to show one of the two quadrature channel waveforms along with the combined output for visual observations. Similar presentation persists throughout figures 24 to 33 inclusive. The effects of quantization on noisy input signals are discussed in the next section.

* See Section 7. 5. 2

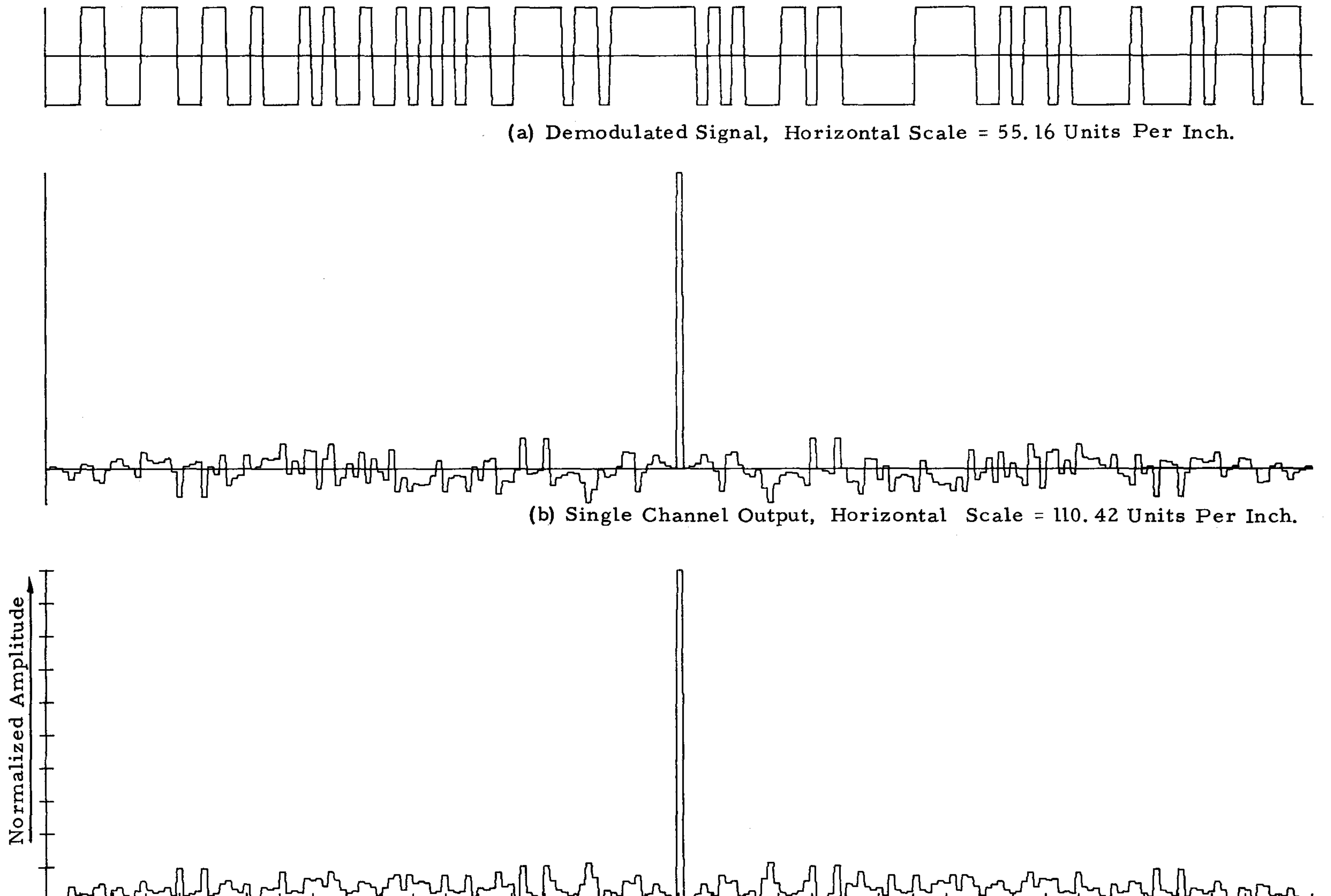


(a) Demodulated Signal, Horizontal Scale = 55.16 Units Per Inch.

(b) Single Channel Output, Horizontal Scale = 110.42 Units Per Inch.

(c) Combined Output, Horizontal Scale = 110.42 Units Per Inch.

Figure 22 - Output For System Without Estimator, Noiseless Case, Carrier Phase ≈ 45°.

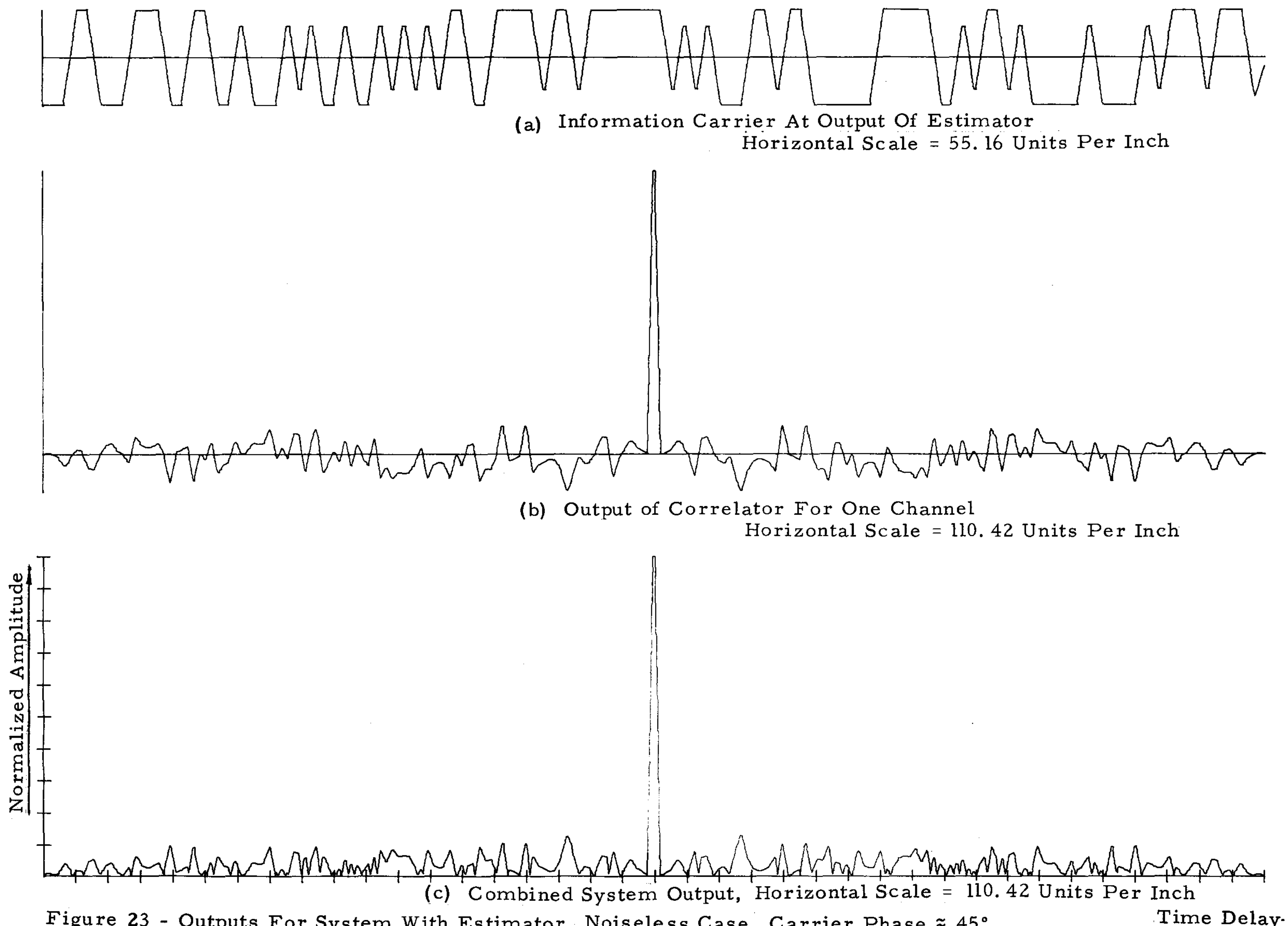


(a) Information Carrier At Output Of Estimator
Horizontal Scale = 55.16 Units Per Inch

(b) Output of Correlator For One Channel
Horizontal Scale = 110.42 Units Per Inch

(c) Combined System Output, Horizontal Scale = 110.42 Units Per Inch

Figure 23 - Outputs For System With Estimator, Noiseless Case, Carrier Phase ≈ 45°

## 7.4 Quantization

Signal quantization and sampling are two schemes commonly employed to simplify system implementation. Since both schemes introduce imperfections their utilization will have to be based on an optimum trade-off between degradation in system performance and simplification of system implementation. The sampling aspect for systems similar to the one under consideration has been described by Mark and Hicks [11] and will not be repeated here. No detailed quantization analysis will be presented here either. We note, however, that the extreme cases are (1) coarse or two level quantization and (2) fine or n (n large) level quantization. Coarse quantization results in an approximately 3 dB signal-to-noise ratio degradation [11]. The quantization noise resulting from fine quantization may be assumed to have a uniform distribution. In this case the quantization noise may be shown to be $\Delta^2/12$, where $\Delta$ is the quantization gap. To examine the effects of quantization on system performance a series of time compressed waveforms are presented in Figure 24 through Figure 33. These waveforms have been obtained with a -6.9 dB signal-to-noise ratio at the input to the receiver. The improvement offered by the estimator can be observed visually by comparing the output waveforms presented in Figures 24 to 33.

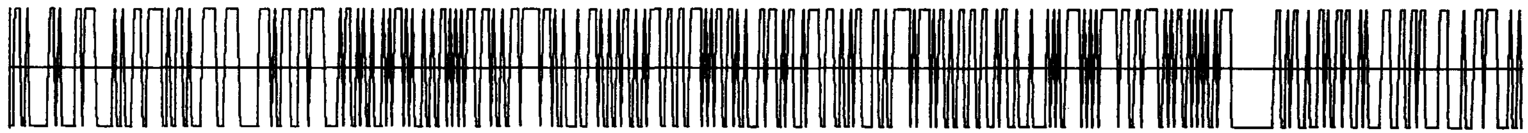

(a) Hard Limited Information Carrier, Horizontal Scale = 55. 16 Units Per Inch

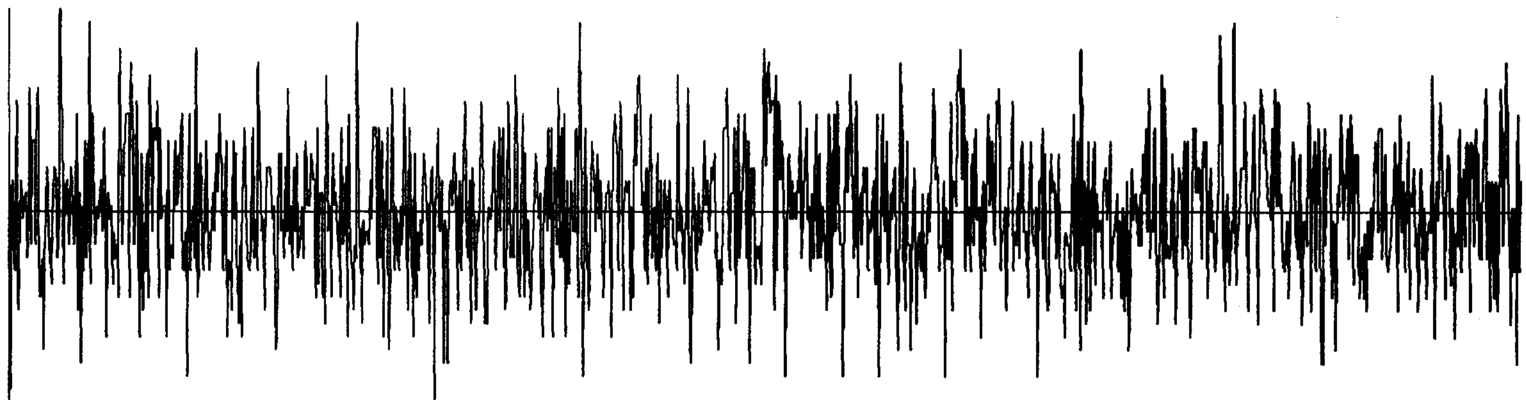

(b) Output From One Channel, Horizontal Scale = 110. 42 Units Per Inch

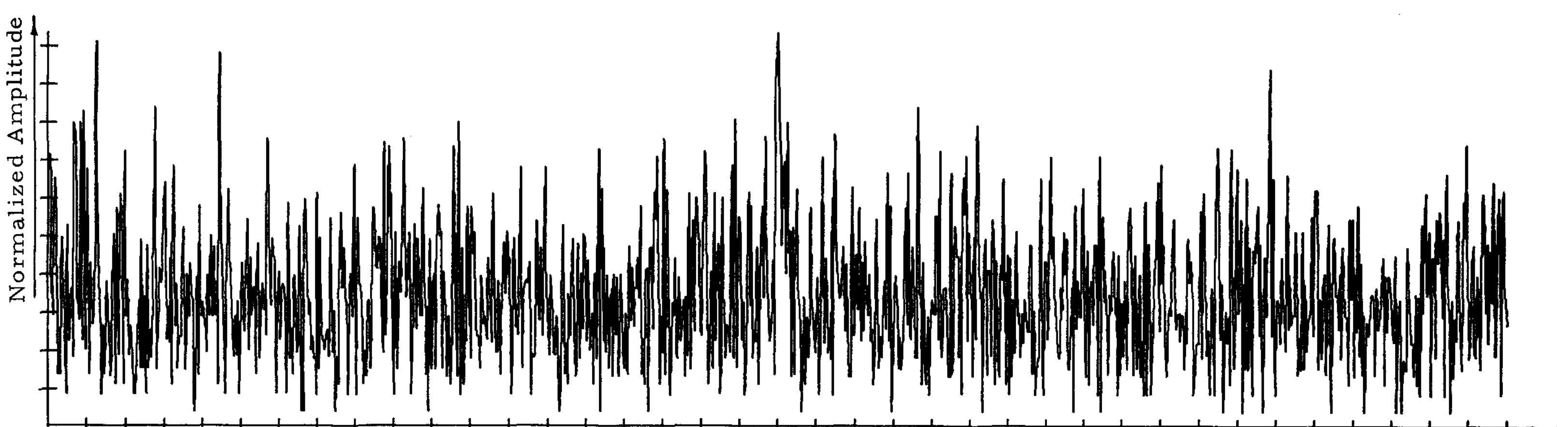


(c) Combined System Output, Horizontal Scale = 110. 42 Units Per Inch

Figure 24 - Hard Limited Detection Without Estimation, -6. 9 DB Input Signal-To-Noise Ratio, Carrier Phase ≈ 45°

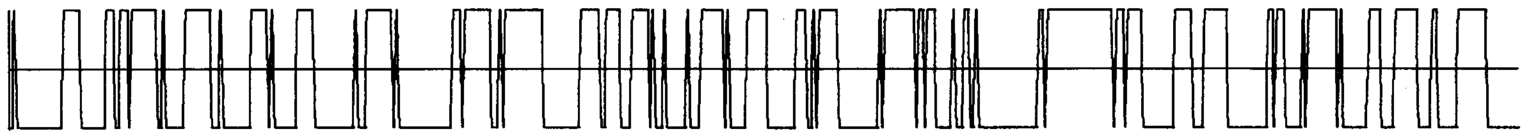

(a) Hard Limited Signal, Horizontal Scale = 55.16 Units Per Inch

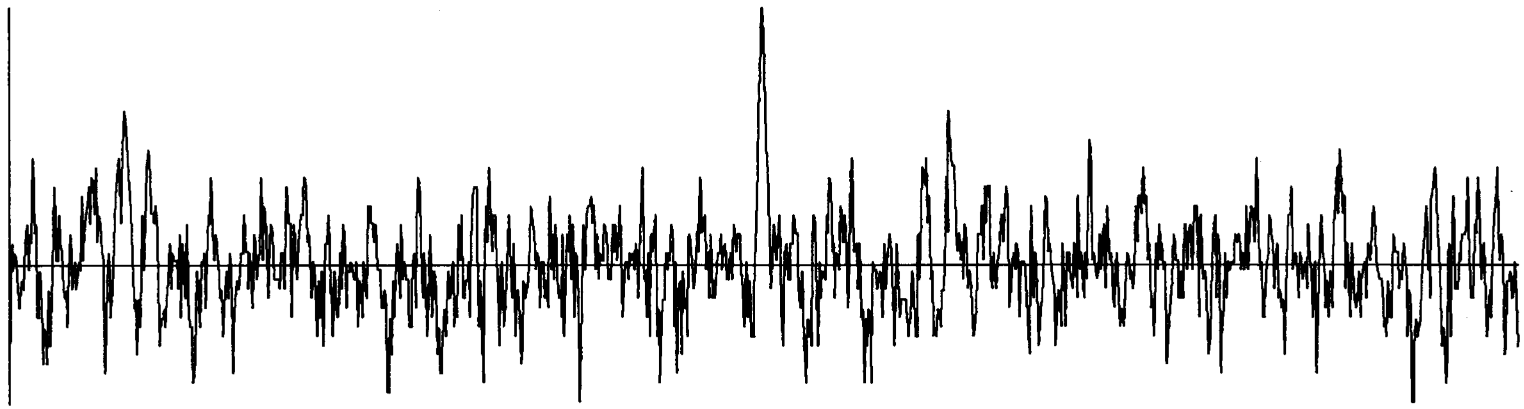

(b) Single Channel Output, Horizontal Scale = 110.42 Units Per Inch

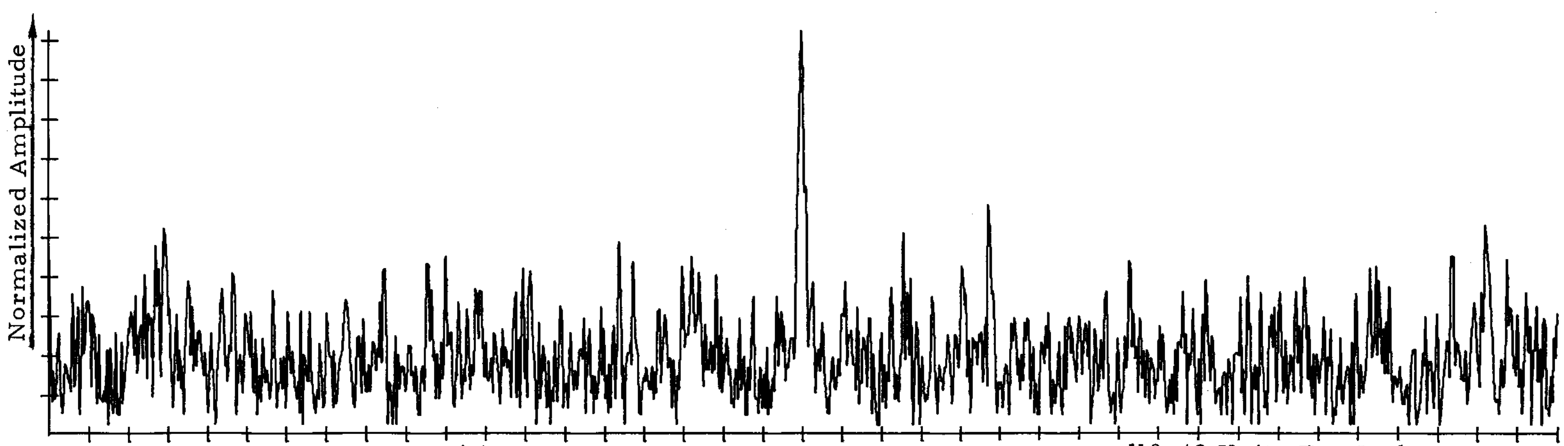


(c) Combined System Output, Horizontal Scale = 110.42 Units Per Inch

Figure 25 - Hard Limited Detection With Estimation, -6.9 DB Input SNR, Carrier Phase ≈ 45°

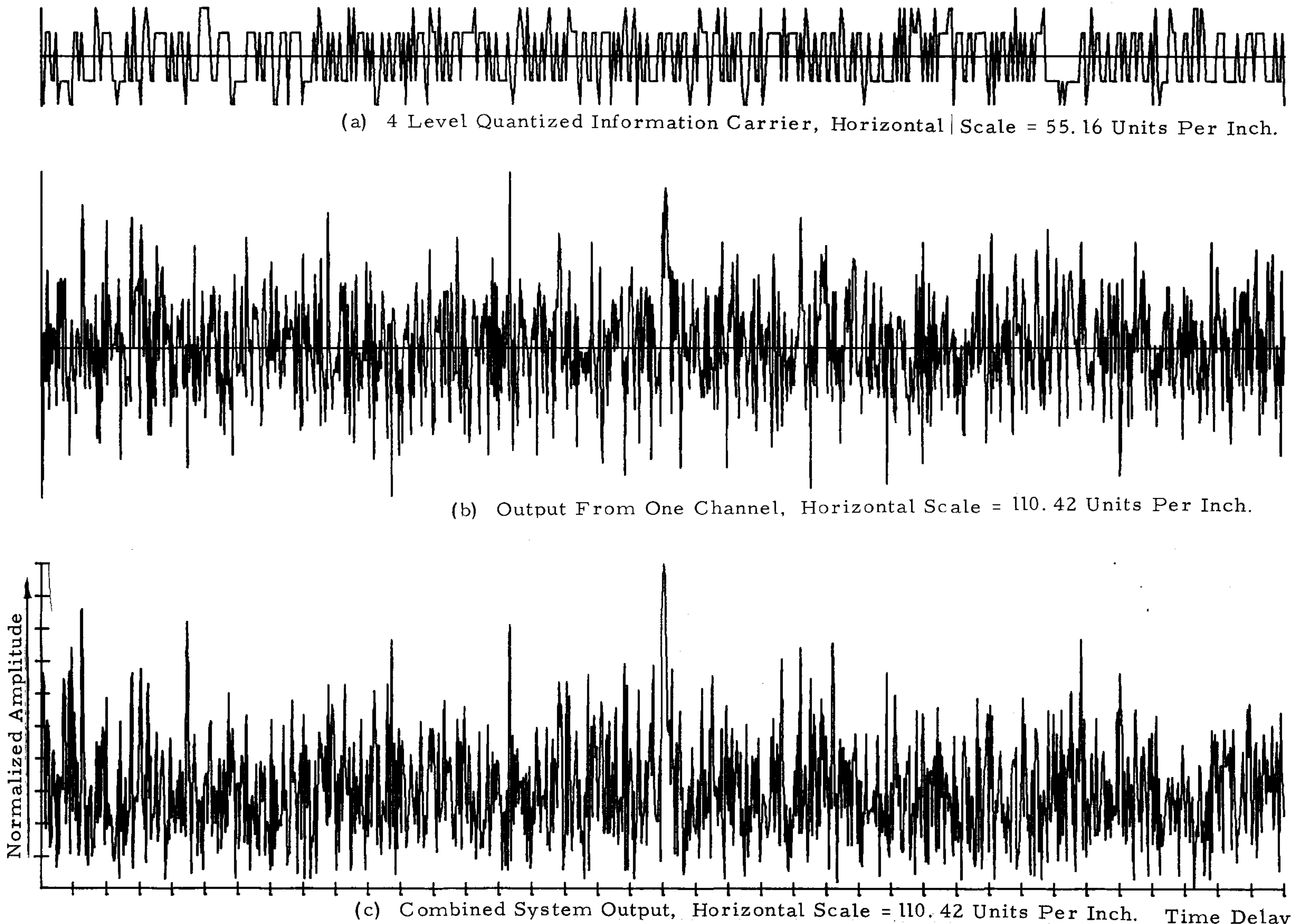


(a) 4 Level Quantized Information Carrier, Horizontal Scale = 55.16 Units Per Inch.

(b) Output From One Channel, Horizontal Scale = 110.42 Units Per Inch.

(c) Combined System Output, Horizontal Scale = 110.42 Units Per Inch.

Figure 26 - 4 Level Quantization Detection Without Estimation, -6.9 DB Input Signal-to-Noise Ratio, Carrier Phase ≈ 45°

(a) 4 Level Quantized Information Carrier, Horizontal Scale = 55.16 Units Per Inch.

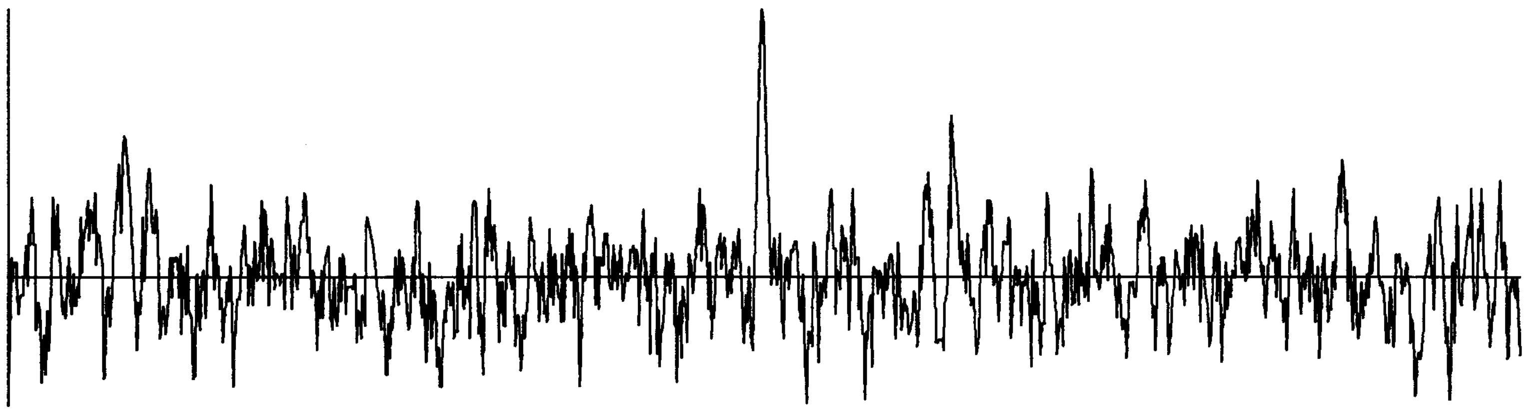

(b) Single Channel Output, Horizontal Scale = 110.42 Units Per Inch.

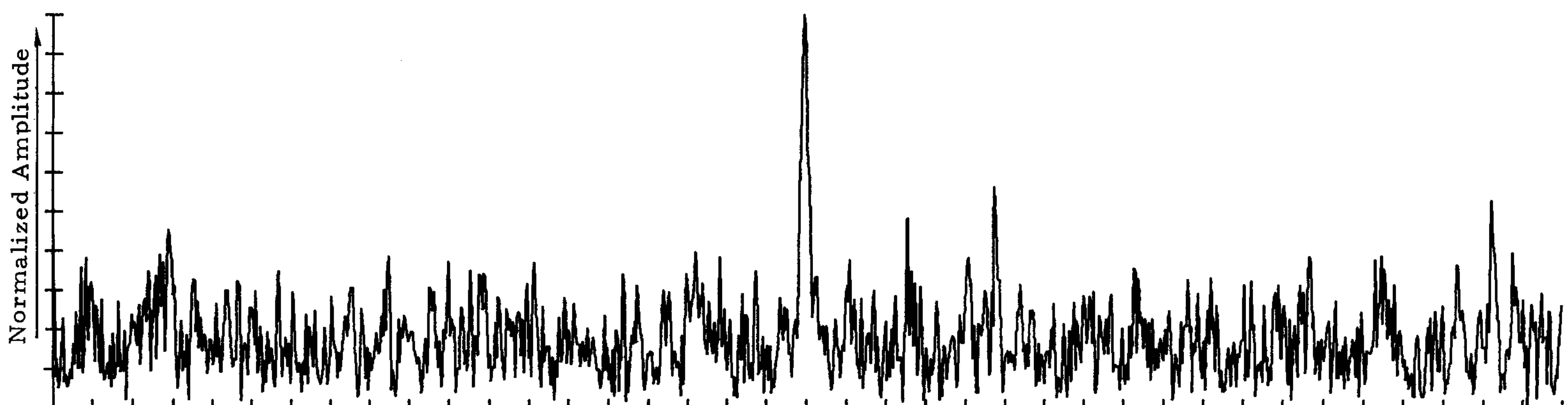


(c) Combined System Output, Horizontal Scale = 110.42 Units Per Inch.

Time Delay

Figure 27 - 4 Level Quantization Detection With Estimation, -6.9 DB Input SNR, Carrier Phase ≈ 45°

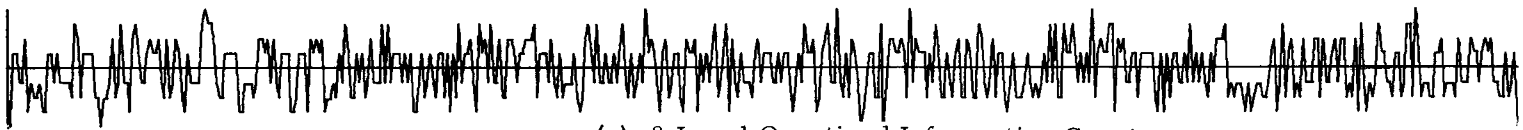

(a) 8 Level Quantized Information Carrier
Horizontal Scale = 55.16 Units Per Inch.

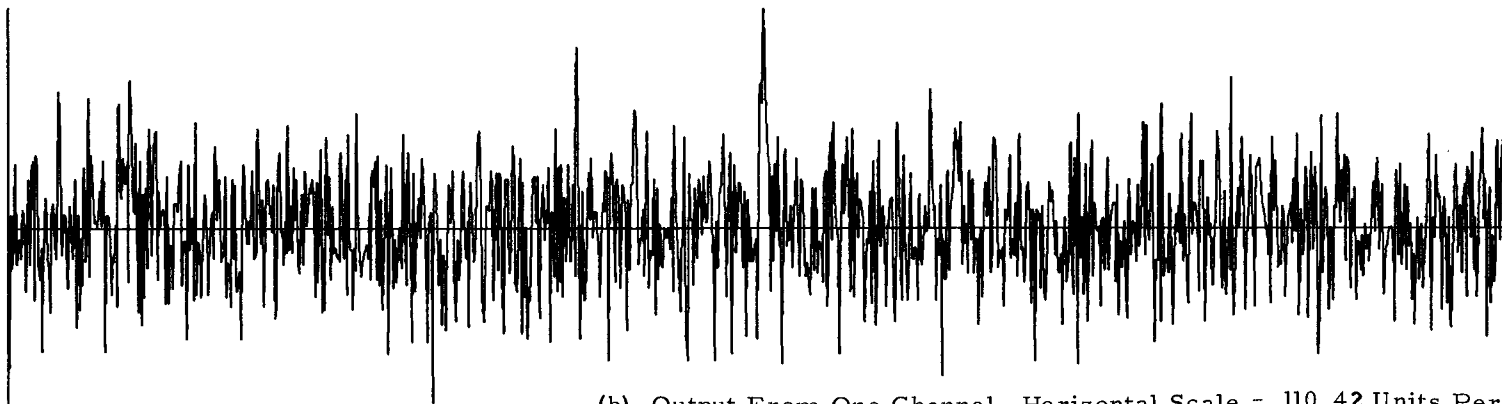

(b) Output From One Channel, Horizontal Scale = 110.42 Units Per Inch.

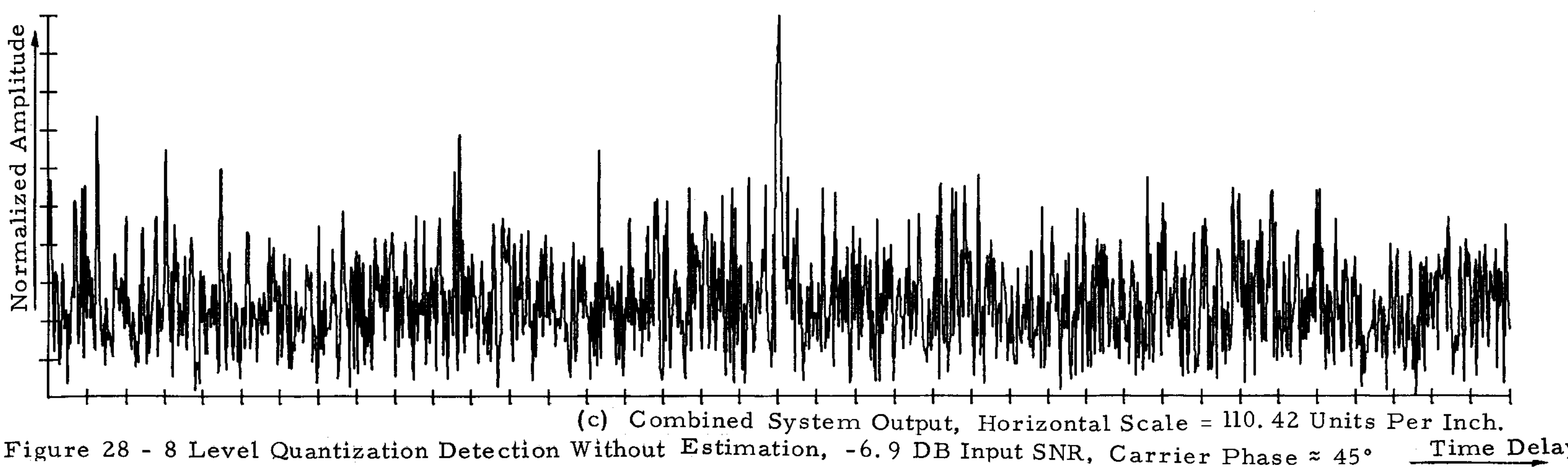


(c) Combined System Output, Horizontal Scale = 110.42 Units Per Inch.

Figure 28 - 8 Level Quantization Detection Without Estimation, -6.9 DB Input SNR, Carrier Phase ≈ 45°

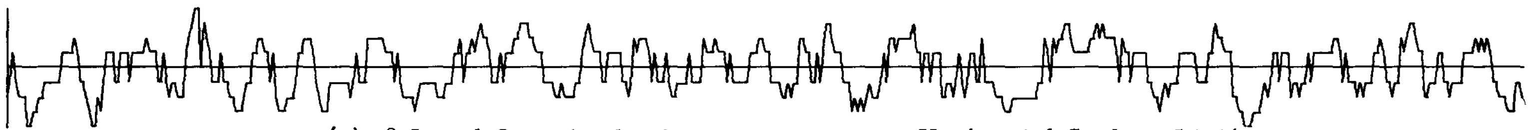

(a) 8 Level Quantized Information Carrier, Horizontal Scale = 55.16 Units Per Inch.

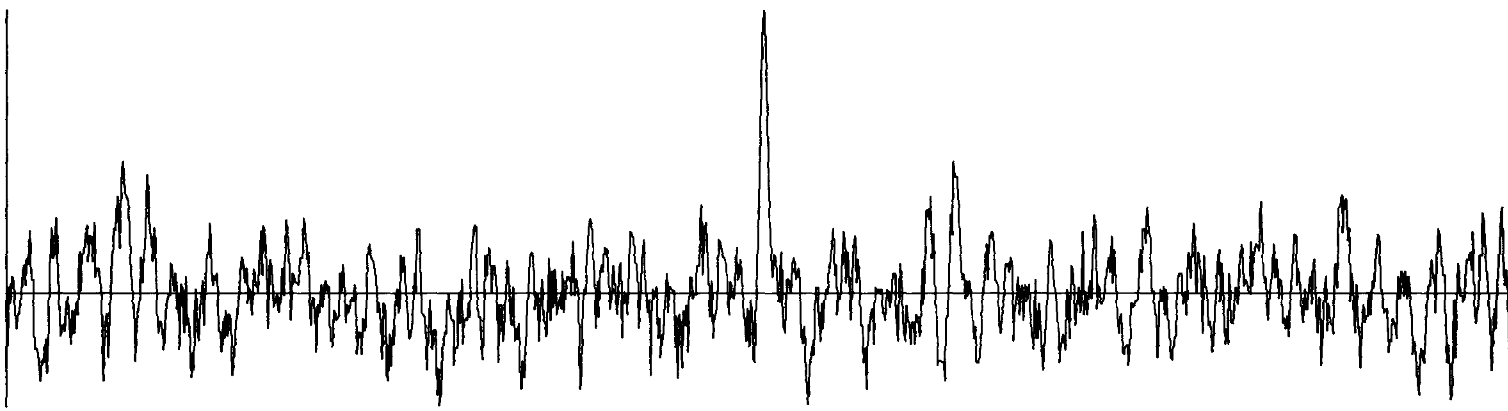

(b) Single Channel Output, Horizontal Scale = 110.42 Units Per Inch.

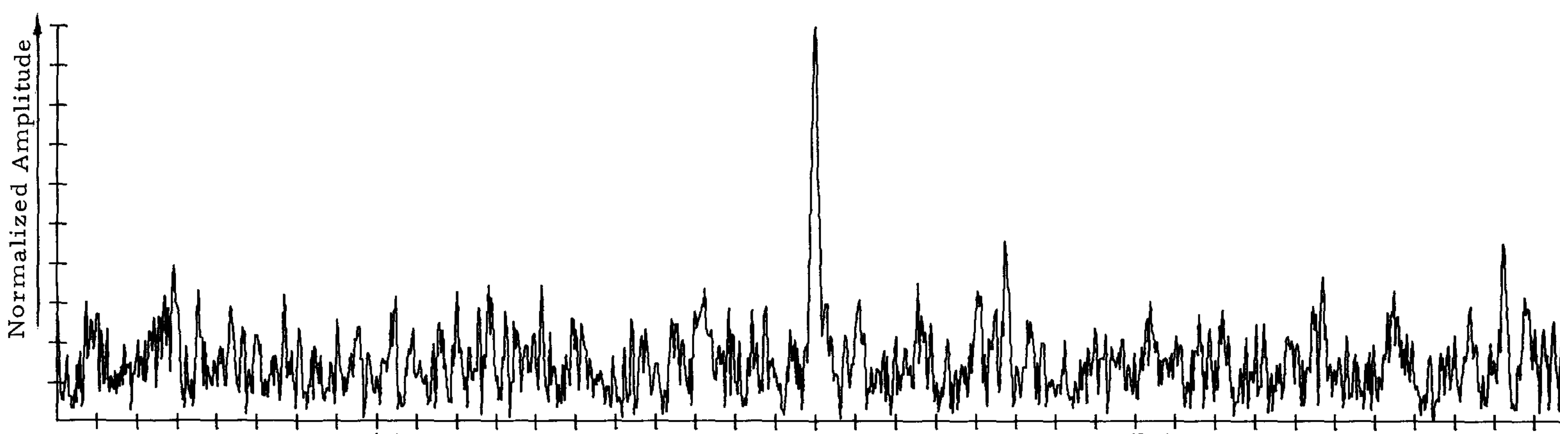


(c) Combined System Output, Horizontal Scale = 110.42 Units Per Inch.

Time Delay

Figure 29 - 8 Level Quantization Detection With Estimation, -6.9 DB Input SNR, Carrier Phase ≈ 45°

(a) 16 Level Quantized Information Carrier
Horizontal Scale = 55. 16 Units Per Inch

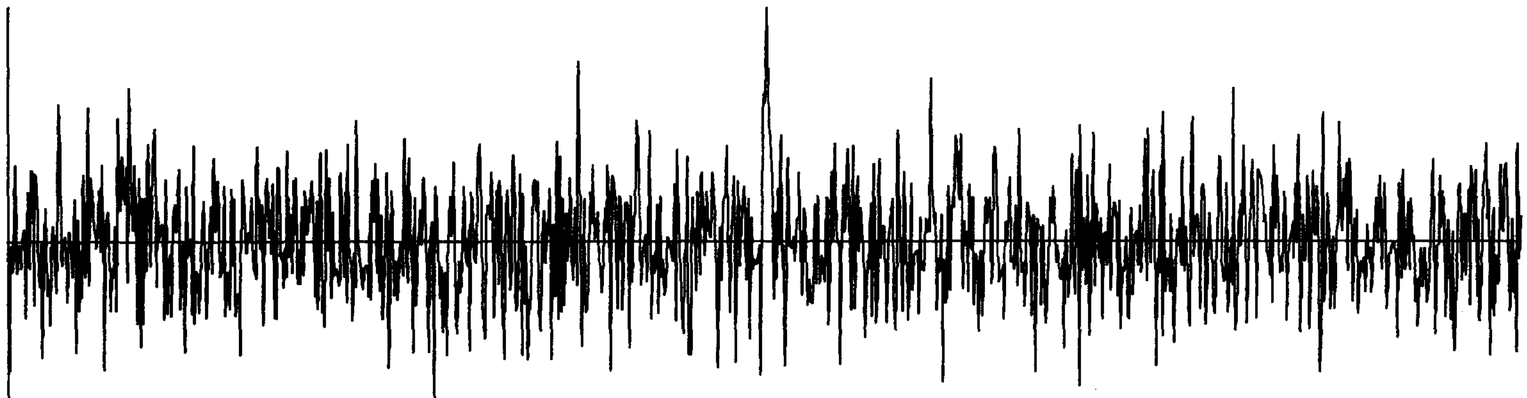

(b) Output From One Channel, Horizontal Scale = 110. 42 Units Per Inch

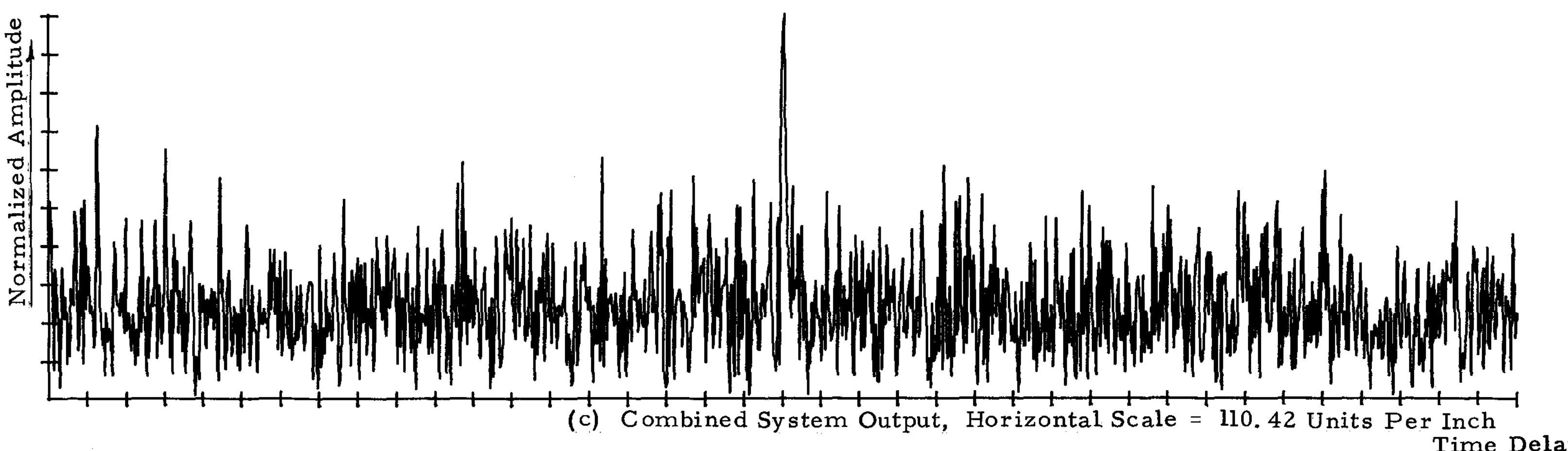


(c) Combined System Output, Horizontal Scale = 110. 42 Units Per Inch

Figure 30 - 16 Level Quantization Detection Without Estimation, -6. 9 DB Input SNR, Carrier Phase ≈ 45°

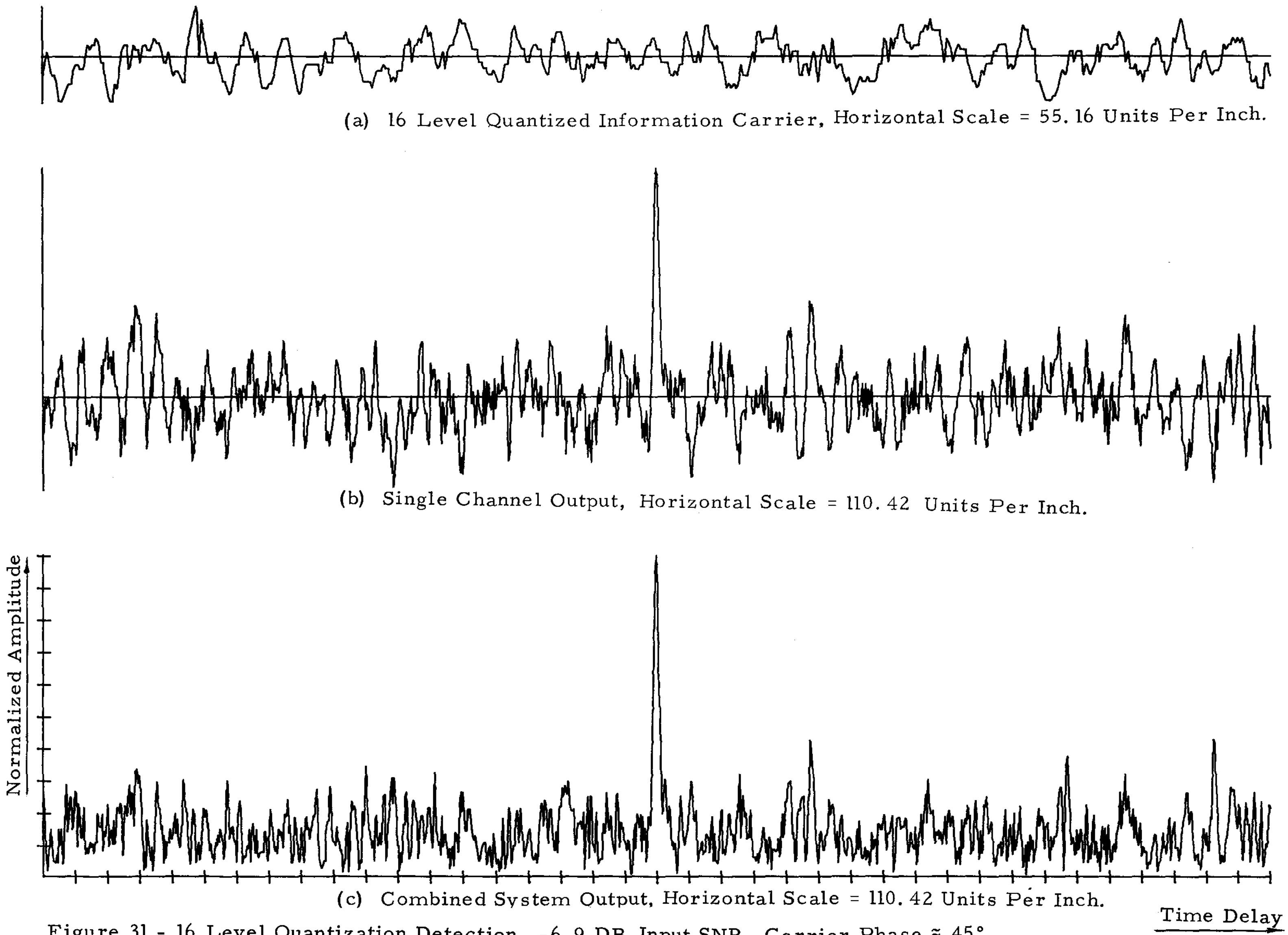


(a) 16 Level Quantized Information Carrier, Horizontal Scale = 55. 16 Units Per Inch.

(b) Single Channel Output, Horizontal Scale = 110. 42 Units Per Inch.

(c) Combined System Output, Horizontal Scale = 110. 42 Units Per Inch.

Figure 31 - 16 Level Quantization Detection, -6. 9 DB Input SNR, Carrier Phase ≈ 45°

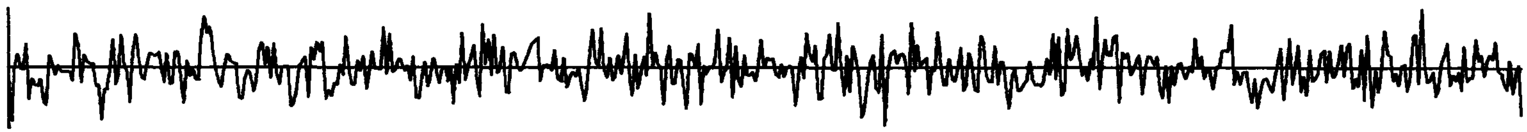

(a) Linear Low-Pass Waveform, Horizontal Scale = 55.16 Units Per Inch

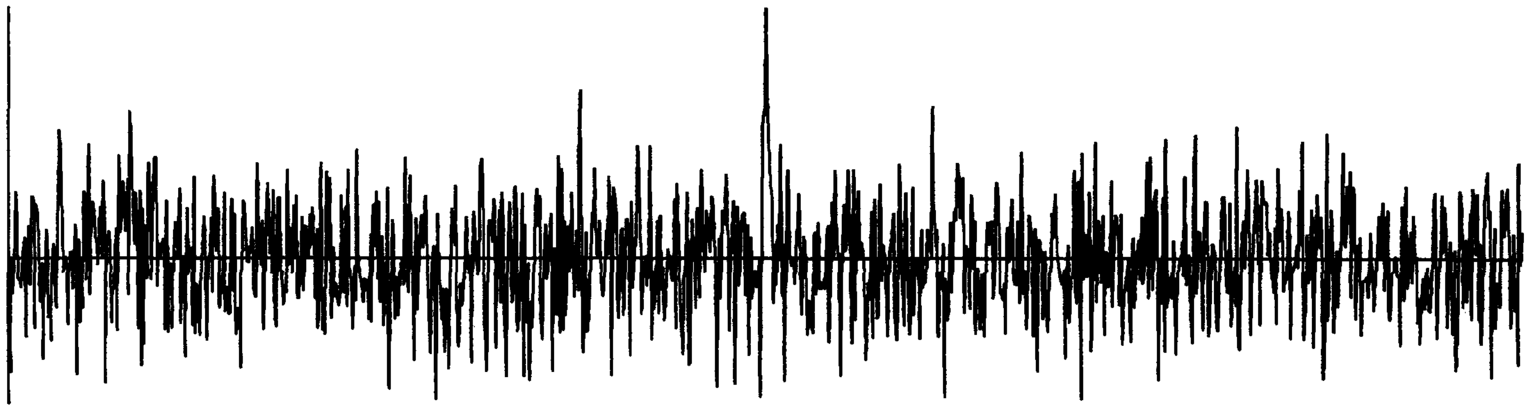

(b) Output From One Channel, Horizontal Scale = 110.42 Units Per Inch

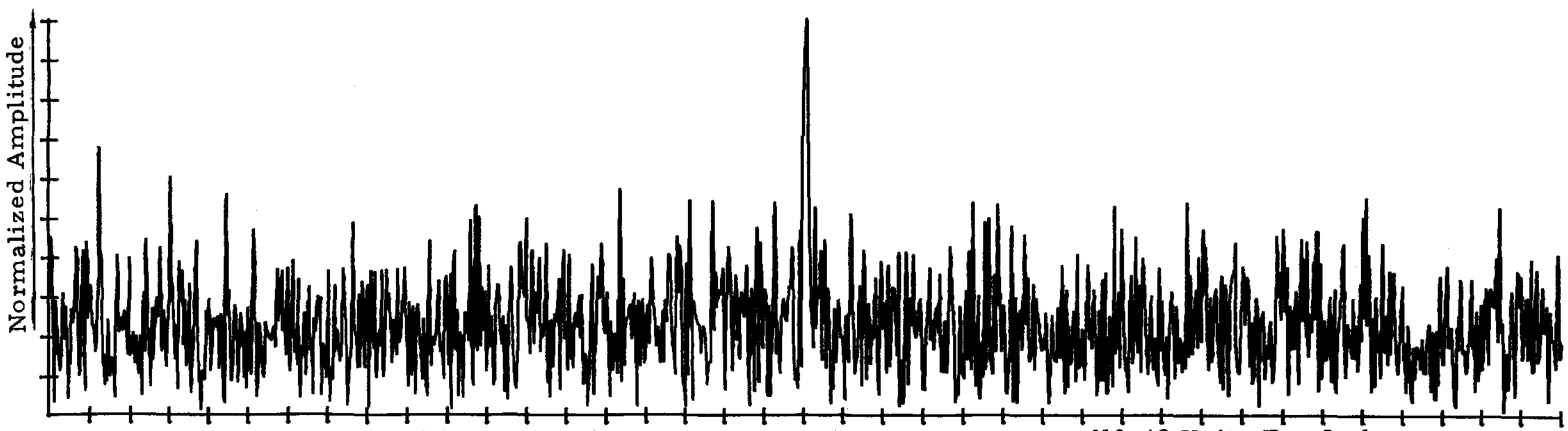


(c) Combined System Output, Horizontal Scale = 110.42 Units Per Inch

Figure 32 - Completely Linear Detection Without Estimation, -6.9 DB Input SNR, Carrier Phase ≈ 45°

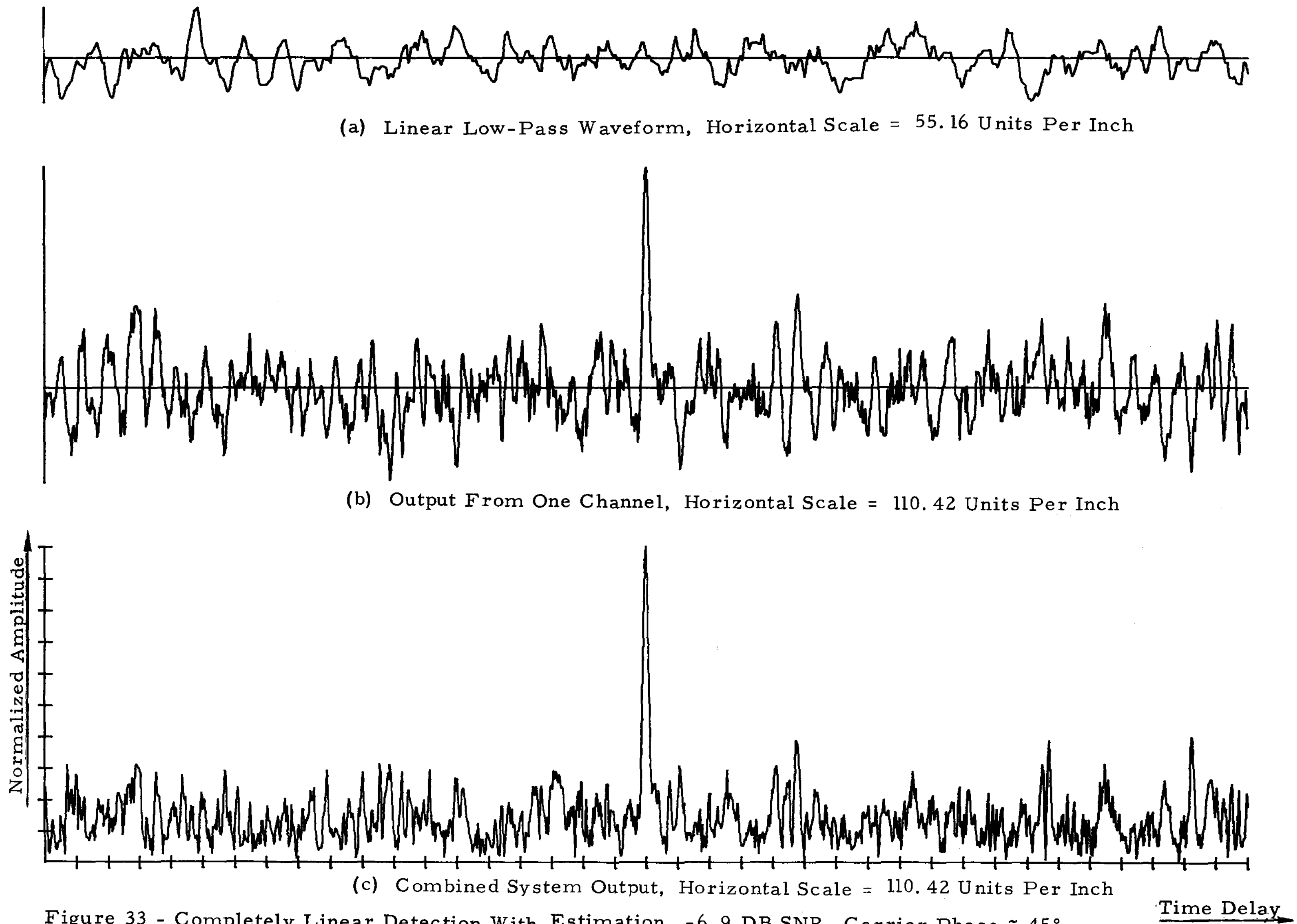


(a) Linear Low-Pass Waveform, Horizontal Scale = 55.16 Units Per Inch

(b) Output From One Channel, Horizontal Scale = 110.42 Units Per Inch

(c) Combined System Output, Horizontal Scale = 110.42 Units Per Inch

Figure 33 - Completely Linear Detection With Estimation, -6.9 DB SNR, Carrier Phase ≈ 45°

## 7.5 System Performance

### 7.5.1 Performance Criteria

As stated earlier our system performance criteria are signal processing gain and dynamic range together with a false alarm probability for a given threshold. Dynamic range, in our terminology, is measured by the peak-to-sidelobe ratio, i. e. the ratio of the central peak of the output waveform to the maximum off-centre lobe. The false alarm probability is obtained by counting the number of samples exceeding the threshold during an observation interval. The signal processing gain is defined as:-

$$G \triangleq \frac{(S/N)_o}{(S/N)_i} = \frac{r_o}{r_i}$$

where $(S/N)_o = r_o$ is the output signal-to-noise power ratio

$(S/N)_i = r_i$ is the input signal-to-noise power ratio

### 7.5.2 Signal-to-Noise Ratio Consideration

Consider the estimator-correlator combination of the overall receiver configuration of Figure 11, which is depicted in Figure 33a.

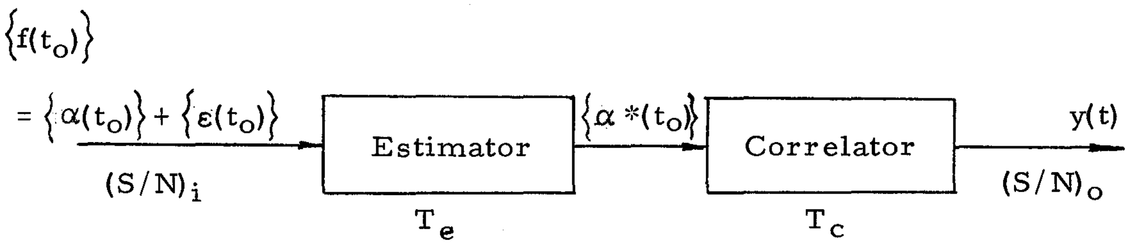


Figure 33a - Estimator-Correlator Combination

Our transmitted intelligence is $\left\{a(t_o)\right\}$ . Let the estimate be

$$\left\{\alpha^*(t_o)\right\} = \left\{a(t_o)\right\} + \left\{\eta\ (t_o)\right\}$$

that is, our estimate is not exactly the transmitted intelligence. At the input, $m(t_o)$ is the corrupted intelligence. We write

$$\alpha\ (t_o) = \left\{\xi\ (t_o)\ a(t_o)\right\}$$

to signify that the intelligence is perturbed by a multiplicative random noise. The variance of $\xi\ (t_o)$ is exactly the variance of the fading $\gamma(t_o)$. In the absence of the estimator the output is:-

$$y(t) = \sum_{i=1}^{N} \left[\ \xi(t_o)\ a(t_o) + \varepsilon(t_o)\ \right]_i\ a(t_o)_{i+k}\ , \quad k=0, \pm 1, \ldots, \pm N-1 \qquad \ldots . \quad (67)$$

where $\left\{a(t_o)\right\}_j$ is the reference signal.

Then, $y(t) = \sum_{i=1}^{N} [\xi(t_o)\ a(t_o)]_i\ a(t_o)_{i+k} + \sum_{i=1}^{N} \varepsilon_i(t_o)\ a_{i+k}(t_o)$

If $\xi(t_o)$ were a constant over the domain $(1, 2, \ldots, N)$ then, denoting this constant by K,

$$y(t) = K \sum_{i=1}^{N} a_i(t_o)\ a_{i+k}(t_o) + \sum_{i=1}^{N} \varepsilon_i(t_o)\ a_{i+k}(t_o)$$

$$= K\, R_{axa}(k) + R_{\varepsilon xa}(k) \tag{68}$$

It is thus intuitively satisfying to require, at least,

$$K = T_e\ [\xi(t_o)]\ ,$$

where $T_e$ is the estimation operator. Moreover, we expect the estimator to smooth the additive noise, $\varepsilon(t_o)$, so that the effect imposed by the additive noise component is minimized at the estimator output. If K is unity, our estimate is exact. In the normal situation $K < 1$. Moreover, K will not be the same throughout the domain $(1, 2, \ldots, N)$.

To evaluate output signal-to-noise ratio we ignore for the moment the multiplicative noise and derive the signal processing gain with the estimator absent. Equation (68) is then a correct representation of the correlator output. For simplicity, we let K = 1 and rewrite equation (68) as follows:

$$y(t) = \underbrace{R_{axa}(o)}_{\text{signal}} + \underbrace{R_{axa}(k)\,\big|\, k \neq o}_{\text{self-noise}} + \underbrace{R_{\varepsilon xa}(k)}_{\text{additive noise}}\ . \tag{69}$$

Since our intelligence is an equiprobable equal energy signal, the average power is given by

$$P_a = \overline{a^2(t_o)}.$$

The peak signal at the correlator output is then

$$R_{axa}(0) = N\,P_a$$

An estimate of the self-noise contribution is obtained by computing the variance for $k = 1, 2, \ldots, N-1$. Since N is odd, the number of self-noise samples to one side of the central peak in the correlation function is even. Assuming $\overline{R_{axa}(k)\,\big|_{k\neq 0}} = 0$, the variance of self-noise is given by

$$\sigma^2_{\text{self-noise}} = \overline{\left[R_{axa}(k)\,\big|_{k\neq 0}\right]^2}$$

An upper bound and a lower bound for the self-noise variance may be established by considering two cases of periodic binary sequences:

(i) Upper bound; the binary sequence $\{a_i\}$ is completely random (i. e., the $a_i$'s occur by chance).

$$\sigma^2_{\text{self-noise, periodic}} = \overline{\left[\sum_{i=1}^{N} a_i a_{i+k}\,\Big|_{k\neq 0}\right]^2}$$

$$= \sum_{i=1}^{N} \overline{a_i^2\, a_{i+k}^2} + \sum_{i\neq j}\sum \overline{a_i\, a_{i+k}\, a_j\, a_{j+k}}$$

$$= \sum_{i=1}^{N} P_a\, P_a + \sum_{i\neq j}\sum \overline{a_i}\; \overline{a_{i+k}}\; \overline{a_j}\; \overline{a_{j+k}}$$

$$= N\,P_a^2 + 0$$

(ii) Lower bound; the binary sequence $\{a_i\}$ is a pseudo-random (pn) code (the modulation code used in this thesis). A special property of the periodic pseudo-random sequence is that the off-centre lobes are all equal to -1. Thus

$$[\sum_{i=1}^{N} a_i]^2 = \sum_{i=1}^{N} a_i^2 + \sum_{k=1}^{N-1} \sum_{i=1}^{N} a_i a_{i+k}$$

$$= N P_a + \sum_{k=1}^{N-1} R_{axa}(k) \big|_{k \neq o}$$

$$= N P_a - (N-1) P_a$$

$$= P_a$$

Therefore

$$\sigma^2_{\text{self-noise periodic}} = \overline{[\sum_{i=1}^{N} R_{axa}(k) \big|_{k \neq o}]^2} = P_a^2$$

The variance of the aperiodic (or truncated) binary pseudo-random code lies in between these two bounds. That is,

$$\sigma^2_{\text{self-noise, periodic random}} > \sigma^2_{\text{self-noise, aperiodic pn}}$$

$$> \sigma^2_{\text{self-noise, periodic pn}}$$

or

$$N P_a^2 > \sigma^2_{\text{self-noise, aperiodic pn}} > P_a^2$$

The computed self-noise variance of the 105 digit binary convolution code is

$$\sigma^2_{\text{self-noise, 105 pn}} = 11.3\, P_a^{\,2}$$

The additive noise variance at the correlator output is

$$\sigma_o^2 = \overline{[R_{\varepsilon xa}(k)]^2}$$

$$= \sum_{i=1}^{N} \varepsilon_i^{\,2}(t_o)\, a_{i+k}^{\,2}(t_o) + \sum\sum_{i \neq j} \overline{\varepsilon_i(t_o) a_{i+k}(t_o)\, \varepsilon_j(t_o)\, \varepsilon_{j+k}(t_o)}$$

$$= N\sigma_\varepsilon^{\,2}\, P_a + 0$$

The output signal-to-noise power ratio is, by definition,

$$(S/N)_o = r_o = \frac{\text{peak signal squared}}{\text{total noise variances}}$$

$$= \frac{(\text{Peak})^2}{\sigma^2\,\text{self-noise} + \sigma^{\,2}}$$

$$\text{Then, } r_o = \frac{(N\, P_a)^2}{11.3 P_a^{\,2} + N\sigma_\varepsilon^{\,2}\, P_a}$$

$$= \frac{P_a}{\sigma_\varepsilon^{\,2}} \quad \frac{N^2}{11.3\,\frac{P_a}{\sigma_\varepsilon^{\,2}} + N}$$

$$= r_i \quad \frac{N^2}{11.3\, r_i + N} \tag{71}$$

where $r_i = \frac{P_a}{\sigma_\varepsilon^{\,2}}$ is the input signal-to-noise power ratio.

The signal processing gain is then given by

$$G = \frac{r_o}{r_i} = \frac{N^2}{11.3\, r_i + N} \tag{72}$$

For low input signal-to-noise ratio, i.e., $r_i \rightarrow 0$, $G \rightarrow N$.

For N = 105, the gain of the correlator is

$$10 \log_{10} 105 \doteq 20 \text{ dB} \tag{73}$$

In the absence of additive noise, i.e., $r_i \rightarrow \infty$, the output is limited by self-noise alone. The output signal-to-self-noise ratio is given by

$$r_o = \frac{N^2 P_a^2}{11.3\, P_a^2} = \frac{N^2}{11.3}$$

or $$10 \log_{10} r_o = 10 \log_{10} \frac{(105)^2}{11.3} \doteq 30 \text{ dB}$$

The presence of medium fading accentuates self-noise at the expense of the central peak. That is, the self-noise increases as the code deteriorates. In the absence of medium fading the signal processing gain of the correlator should fall to zero when the input signal-to-noise ratio is approximately 30 dB. The signal processing gain vs input signal-to-noise ratio graph, therefore, drops as $r_i$ increases.

Since explicit evaluation of the signal processing gain for the estimator is extremely difficult, if not impossible, its performance is measured by comparing overall system signal processing gains for the cases with and without the estimator.

### 7.5.3 Discussion of Results

The actual peak at the output of the correlator is

$$s_o = R_{axa}(o) + [\text{second moment of noise}]^{1/2}$$

Therefore, the power at the output is

$$P_o = s_o^2 = R_{axa}^2(o) + \text{second moment of noise}$$
$$+ 2\, R_{axa}(o)\, [\text{second moment of noise}]^{1/2} \qquad (74)$$

In computing the output signal-to-noise ratio and the signal processing gain presented in the graphs of Figures 34, 35, 37 and 39, $P_o$ rather than $R_{axa}^2(o)$ has been utilized. Since the actual output peak provides an indication of target presence, the method used imposes no loss in generality; we merely redefine output signal-to-noise ratio. For this reason the computed signal processing gains are higher than that indicated by equation (72) by an amount contributed by the last two terms in equation (74).

The graphs presented in Figures 34 to 40 are the results of an ensemble average of 12 sample curves, with Gaussian statistics obtained from different sections of the computer simulated Gaussian process*. These graphs, together

* Generated by the RANGAU subroutine, see Appendix IV.

with the false alarm probability curves of Figure 41 define signal detectability. The type of modulation, medium, sampling rate, and quantization level are indicated in the Figures. Figures 34 and 35 are alternate presentations of the system performance. The conjectured signal processing gain of the estimator is approximately 5 dB. Accompanying with this signal processing gain is an improvement in peak-to-sidelobe ratio of an approximately equal amount and a much smaller probability of false alarm. It is concluded then, that we have in the estimator an effective noise smoothing device. It is further conjectured that an 8 level quantized system is a best trade-off between degradation in performance and simplification in implementation. The false alarm probability curves shown in Figure 41 are obtained with the assumption of certainty of probability of detection. The thresholds are computed based on the peak amplitude at the output, the occurrence of which is known a priori.

The effects of medium fading are presented in Figures 37 and 38. For a given multiplicative noise variance, the fading effect is observable when the additive noise is comparable to or less than the multiplicative noise. Two different decisions functions used in combining the two quadrature channels of the overall receiver are as follows:

(i) $$d(X_1, X_2) = \left\{ R: X_1^2 + X_2^2 > R_o^2 \right\}$$

and (ii) $$d(X_1, X_2) = \left\{ Z: \text{Max}\,(X_1, X_2) > Z_o \right\} .$$

These aspects are discussed at length elsewhere [11]. Typical results of the present analysis are presented in Figures 39 and 40.

Because of the high resolution capability, the echo ranging system analyzed offers "good" discrimination in a multitarget situation. Three targets separated by distances less than the length are distinguishable as individual targets. This situation is presented in Figure 42.

## 7.6 Summary

The discrepancy between the theoretical output signal-to-noise ratios predicted by equation (72) and those computed by the simulation program is accounted for by a difference in definition. The definition used in computing the output signal-to-noise ratio is

$$(S/N)_o = \frac{(\text{peak signal + noise})^2}{\text{total noise variances}}$$

(cf. equation (70) )

The conjectured results from this Chapter are

(i) The estimator offers a gain of approximately 5 dB, a peak-to-sidelobe ratio improvement of approximately 5 dB and a much smaller false alarm probability.

(ii) The improvement offered by the estimator permits simplification in overall receiver implementation.

(iii) An 8 level (3 bit) quantized system is a best trade-off between degradation in system performance and simplification in system implementation.

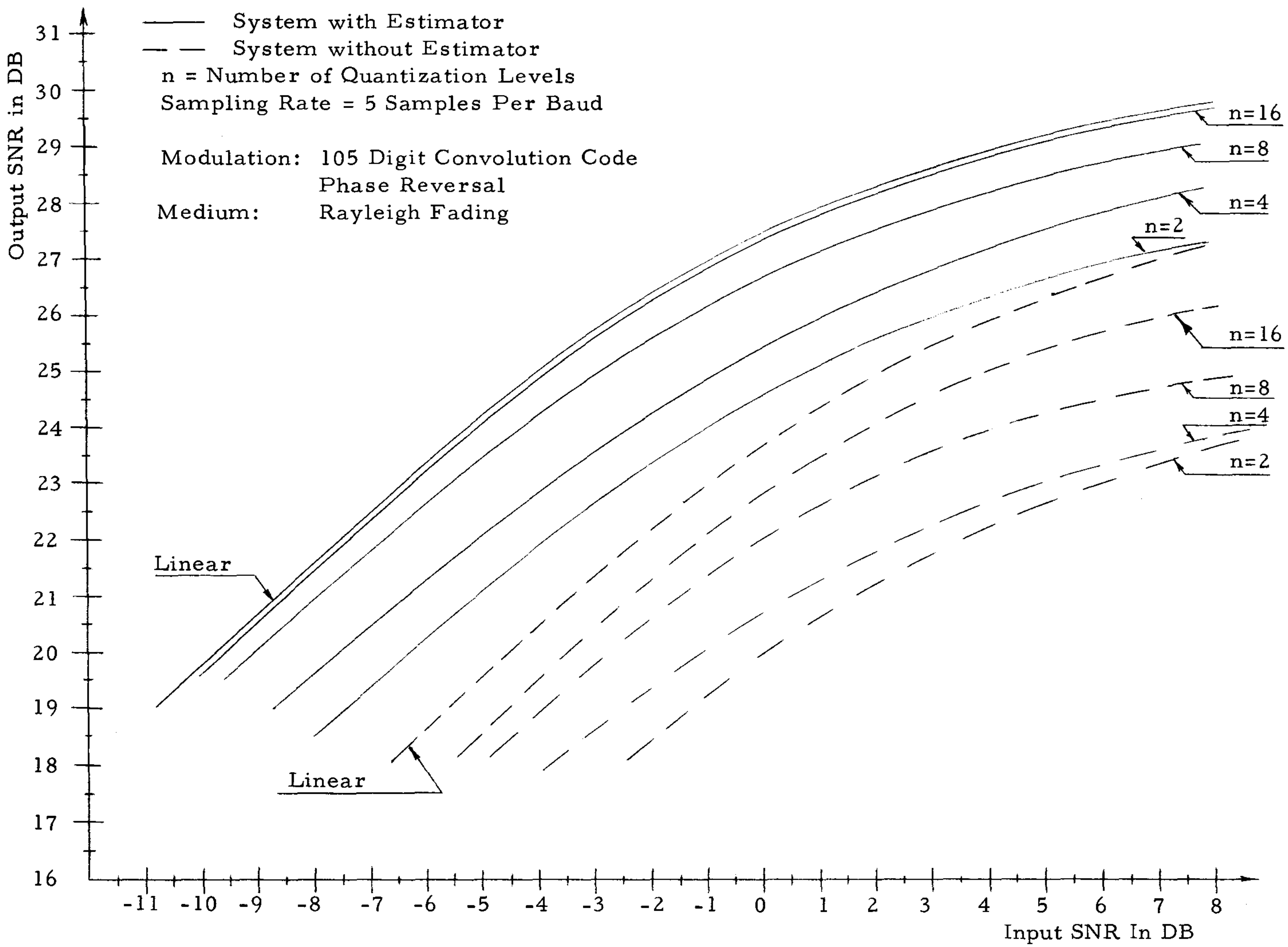


Figure 34 - Output Signal-to-Noise Ratio vs Input Signal-to-Noise Ratio Graphs

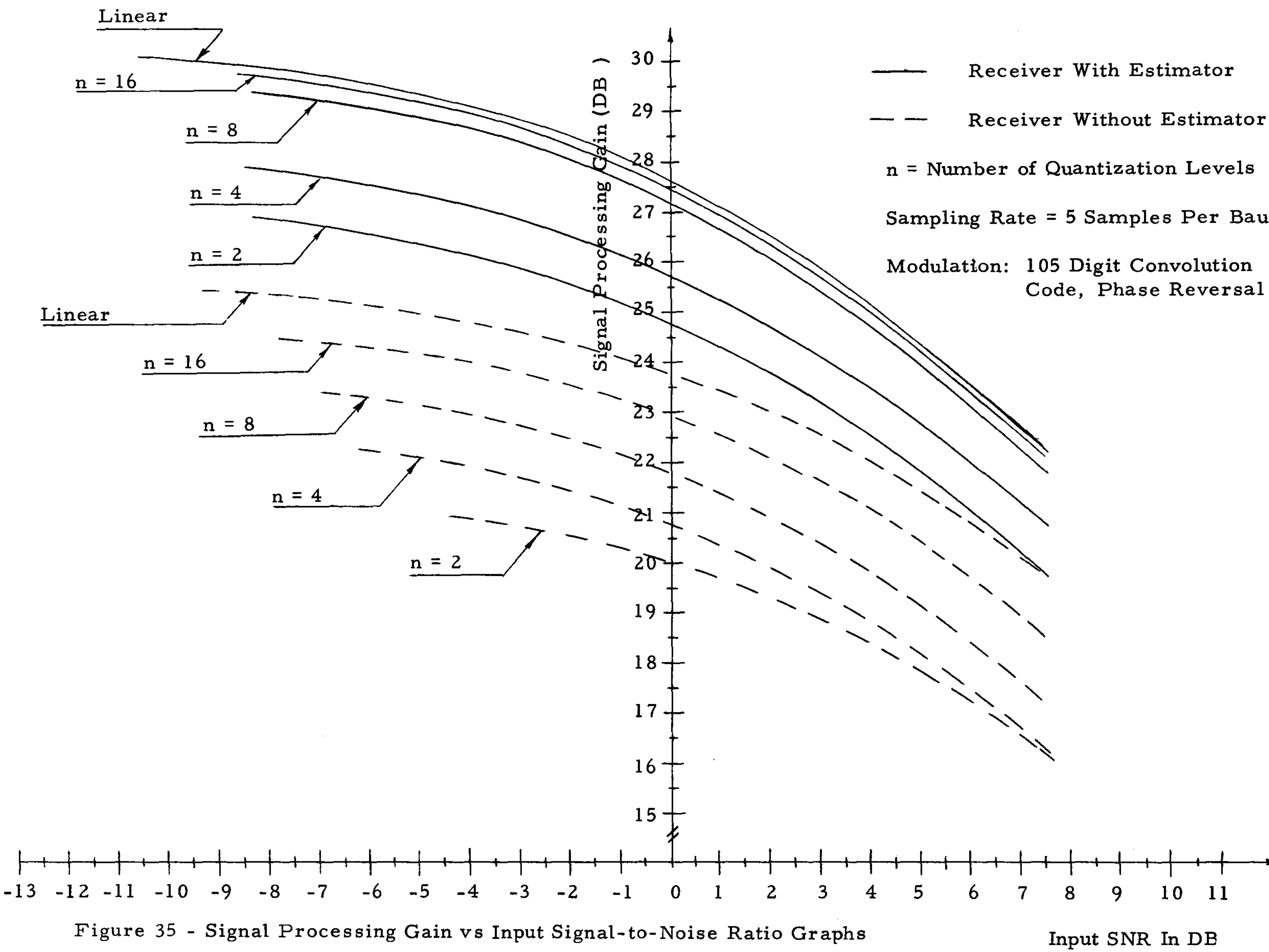


Figure 35 - Signal Processing Gain vs Input Signal-to-Noise Ratio Graphs

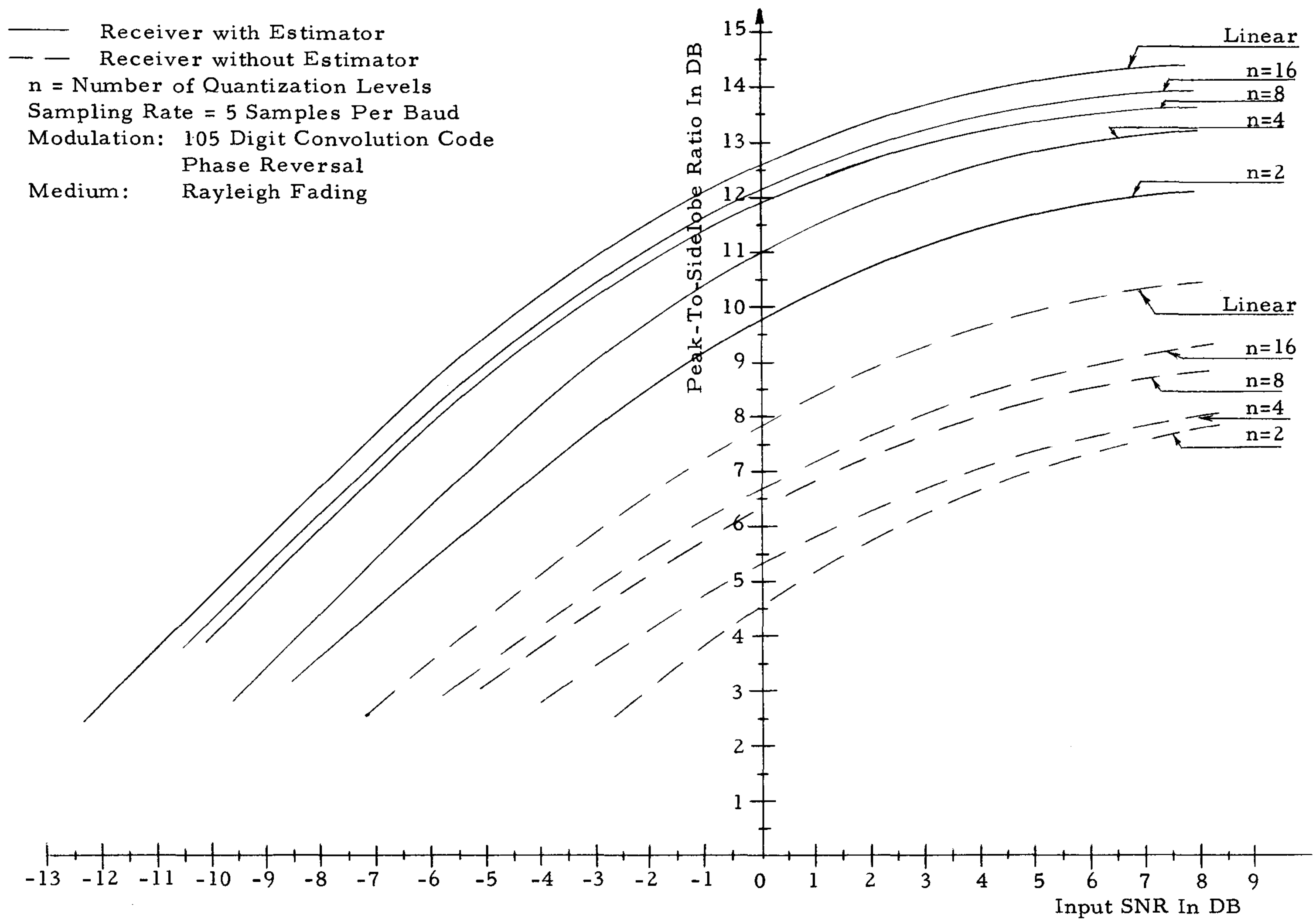


Figure 36 - Peak-to-Sidelobe Ratio vs Input Signal-to-Noise Ratio Graphs

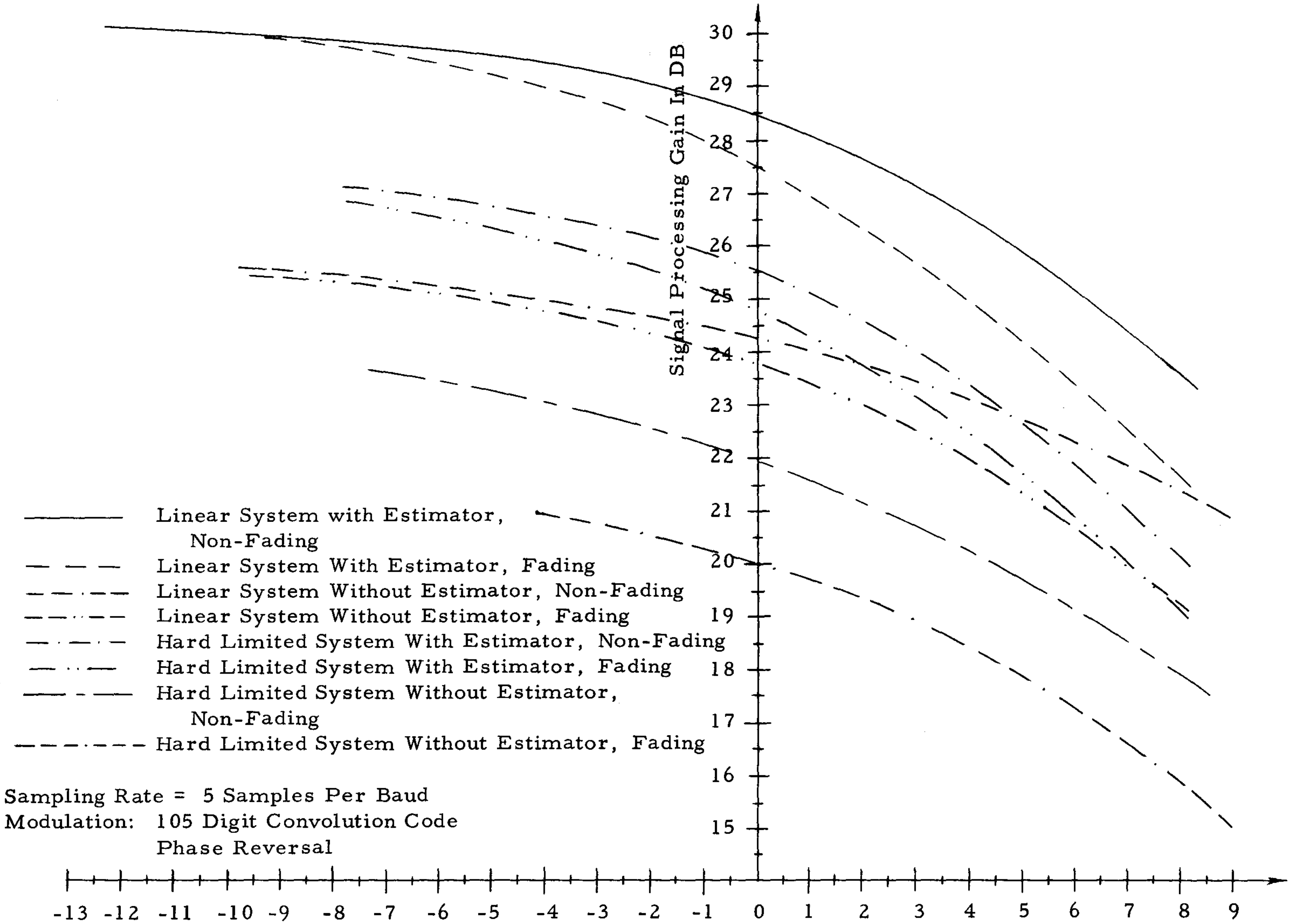


Figure 37 - Effects of Fading on Linear and Hard Limited Systems

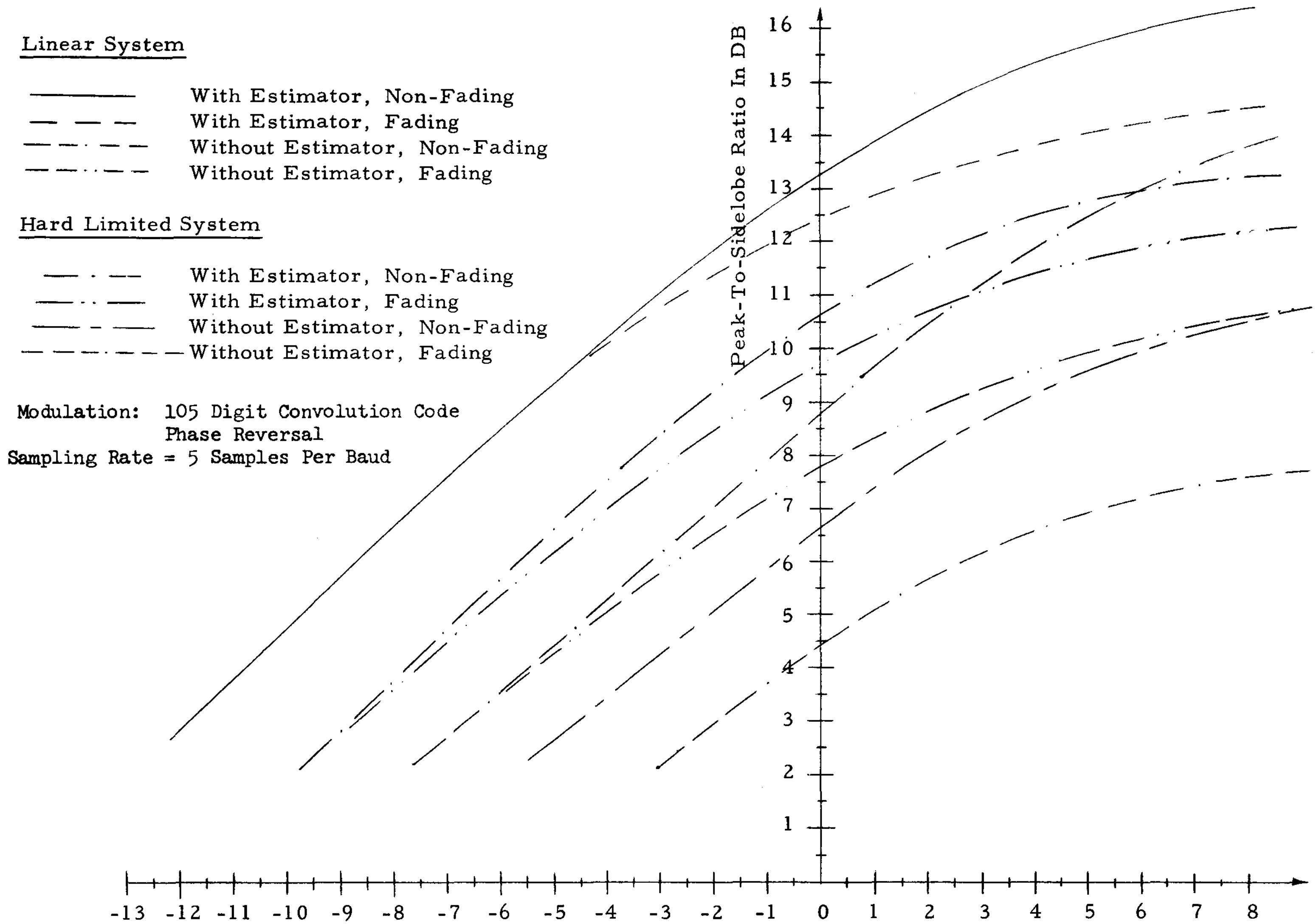


Figure 38 - Effects of Fading on Linear and Hard Limited Systems

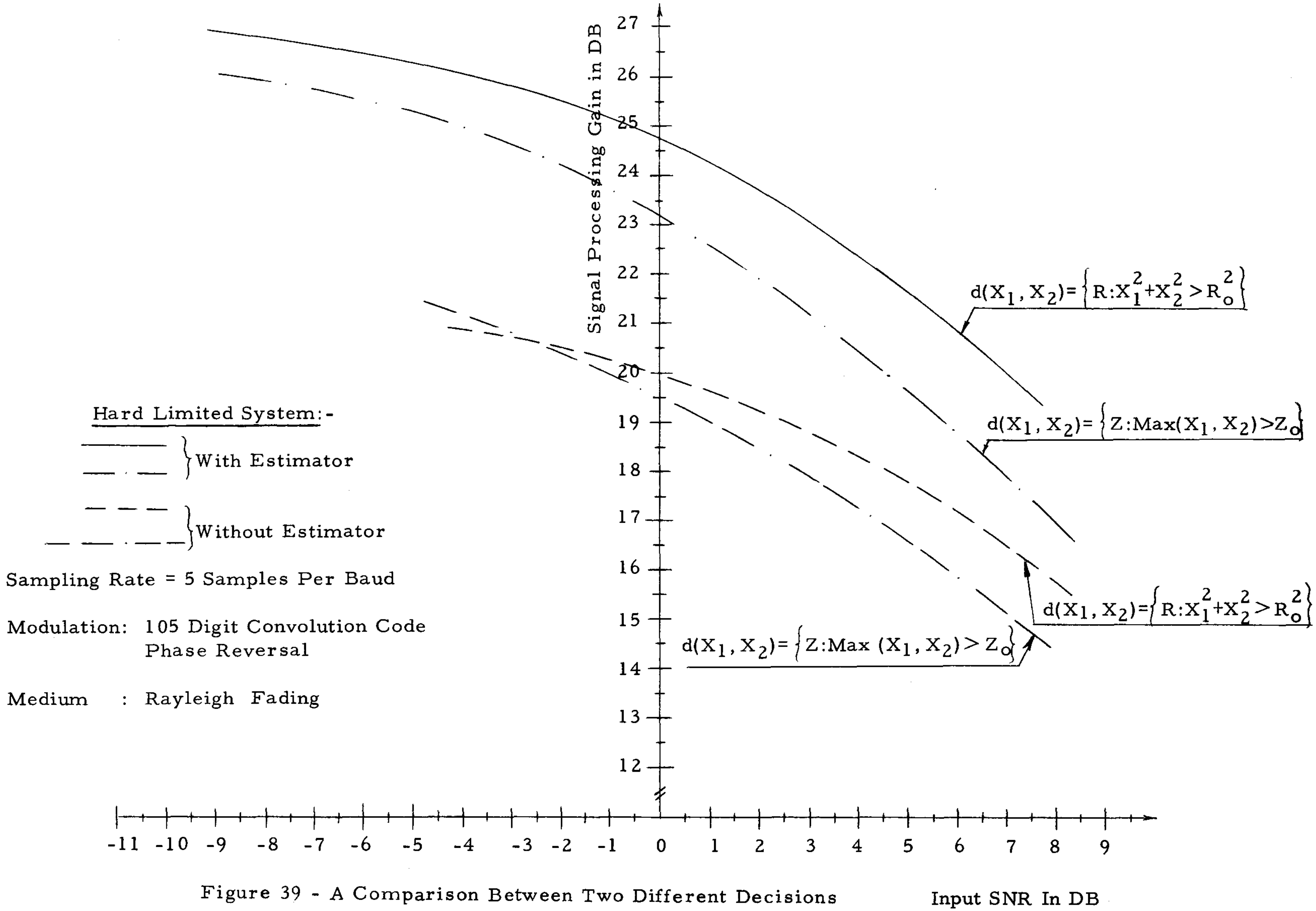


Figure 39 - A Comparison Between Two Different Decisions

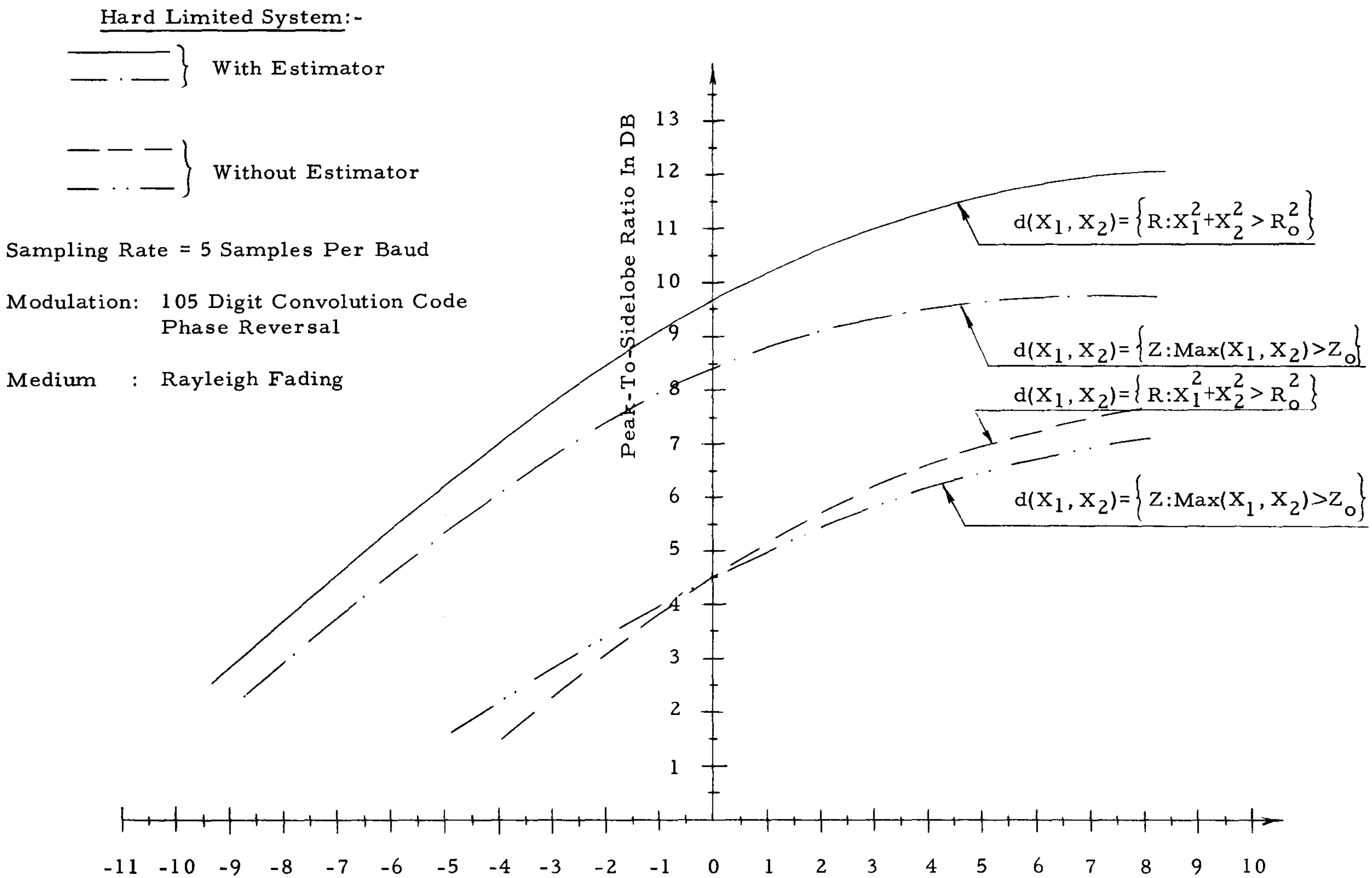


Figure 40 - A Comparison Between Two Different Decisions

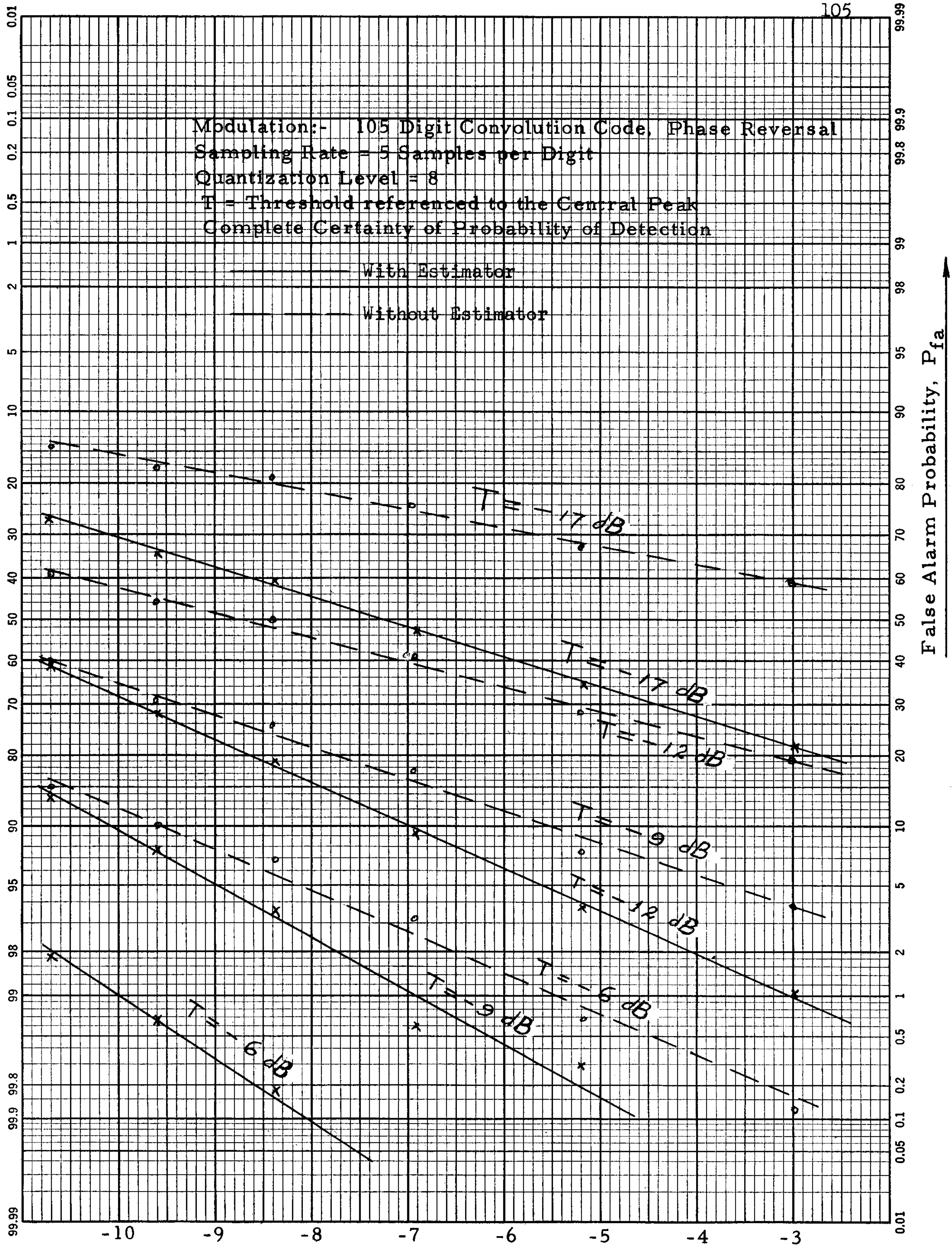


Figure 41 - False Alarm Probability vs SNR Ratio, with Threshold as Parameter

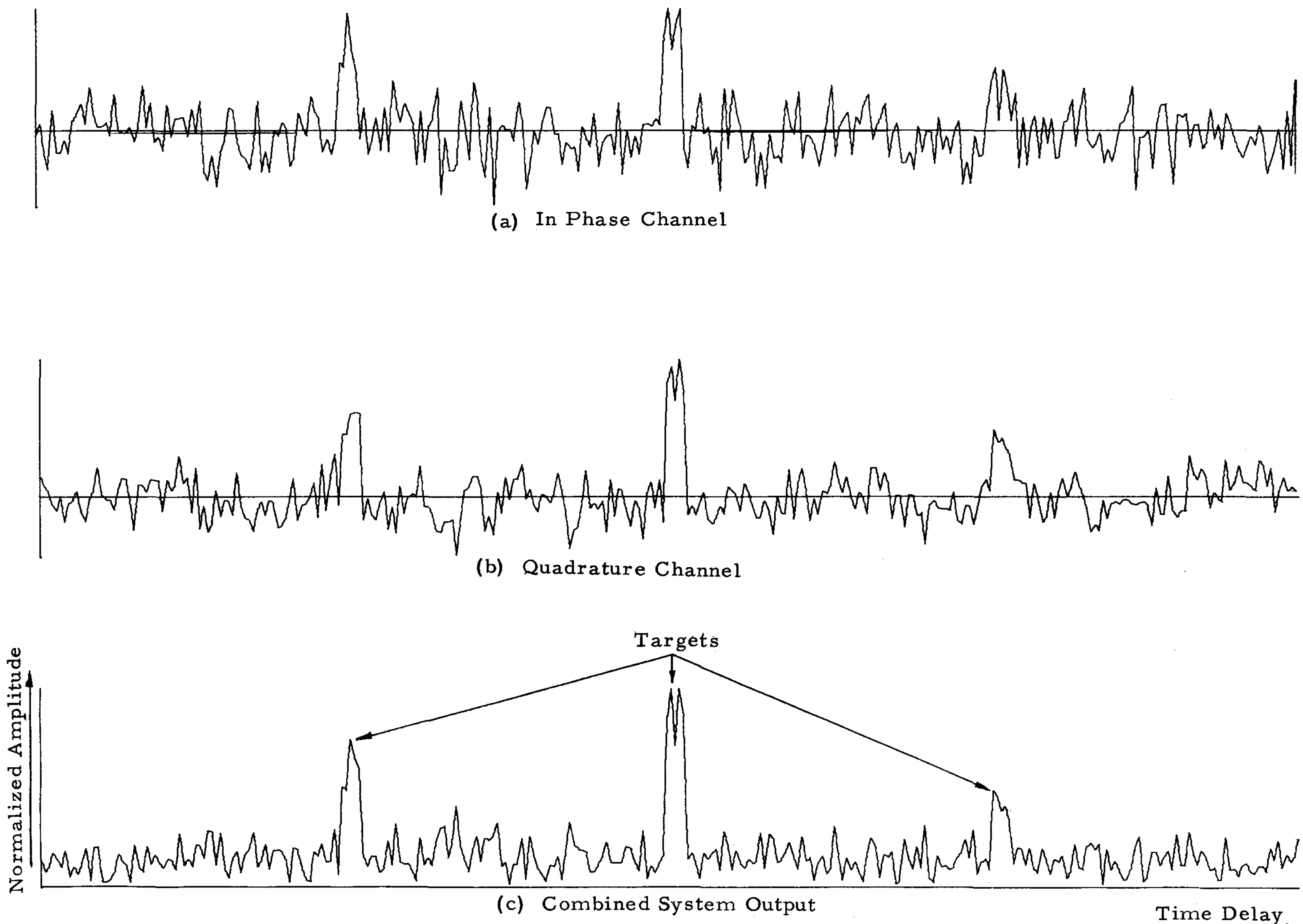


Figure 42 - Multiple Target Reception Using the 15 Digit Code, Horizontal Scale = 32.526 Units Per Inch

## CHAPTER VIII

## CONCLUSIONS AND FUTURE RECOMMENDATIONS

An optimum self-synchronized echo ranging system has been designed and simulated. The overall echo ranging system design has been categorized into three major parts, namely, the transmitter, the propagation medium, and the receiver. The receiver design carries more than 80% of the weight in this thesis.

Modern coding techniques together with Woodward's ambiguity function analysis have been employed as a basis for signal encoding at the transmitter end. The propagation medium has been modelled by a Rayleigh amplitude fading with or without a specular component. A maximum a posteriori probability criterion has been utilized to derive the estimator and a maximum likelihood criterion for the correlator in the receiver proper. In particular the estimator derived is a conditionally biased maximum a posteriori estimator. The estimator together with the correlator forms an optimum active detection receiver for the coding employed.

The orthogonal projection approach introduced by Kalman in 1960 was considered initially for the derivation of an optimal estimator [15]. However, the Kalman estimator involved too many iterations; it took too long to compute the iterative processes in the IBM 7040 computer. Moreover practical implementation difficulty was apparent. For this reason the Kalman approach was abandoned in the early part of this research.

The estimator provides approximately 5 to 6 db improvement in signal processing gain over and above the non-optimized system. From the results it has been conjectured that this improvement is more than sufficient to compensate for any loss due to hard limiting. It is concluded then that an optimized hard limited system yields better performance than a non-optimized linear system. The overall receiver implementation can thus be simplified by the introduction of the derived estimator. The gain offered by the estimator permits the system to operate further down in noise. It has been further conjectured from the simulation results that a 3 bit (8 level) quantized system is a good trade-off between system performance and system simplification.

Since optimum detection and estimation strategies depend on the characteristics of the signal and noise, the estimator derived in this thesis cannot be utilized in a passive detection receiver without modification. A similar approach can be used to derive an adaptive estimator for passive detection for whatever signal and noise characteristics known a priori. Frequency estimation can be introduced in the zonal filter 2 design in the overall receiver configuration (figure 11) to optimize carrier regeneration and Doppler determination.

# APPENDIX I

## BINARY CODES

This Appendix is a precis of a technical note by the author [14]. Other references are provided [12], [13].

Binary sequences (codes) are derived from the Finite Galois Field whose characteristics are 0 and 1. In Group Theory a cyclic group is generated from one element. Likewise a cyclic binary sequence may be generated from a primitive polynomial; the cyclic length is $2^n$. One of the $2^n$ elements in the cyclic sequence is an all-zero element. In terms of physical implementation the all-zero element is a trap element which must be excluded. Thus, the maximum length of a binary cyclic sequence (or binary periodic code) is $2^n-1$. These are invariably called binary M-sequences. The primitive polynomial (or generating function) has as coefficients the characteristics of the Finite Galois Field. That is, a primitive polynomial has the form

$$a_n x^n + \ldots + a_k x^k + \ldots + a_2 x^2 + a_1 x + 1$$

where $a_i = 0$ or $1$, $i = 1, \ldots, n$,

which may be implemented by the configuration shown in Figure I-1.

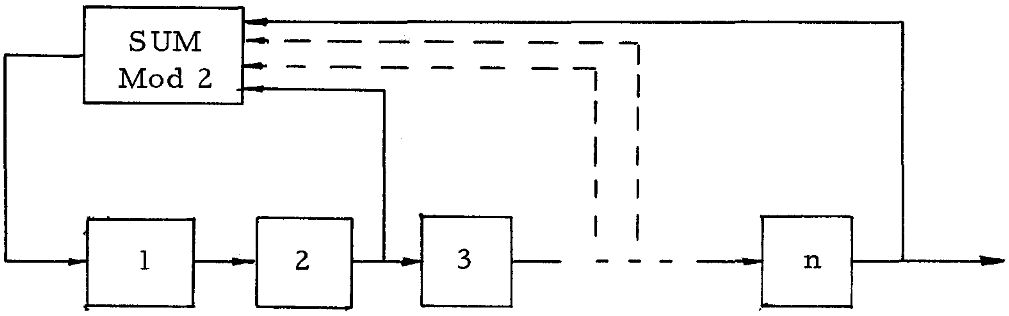


Figure I-1. M-Sequence Generator

Two binary sequences $\{u_i\}$ and $\{v_j\}$ have covariance function given by

$$R(u_i, v_j) = \sum_{i=1}^{N} \sum_{j=1}^{N} u_i v_j \tag{I-1}$$

$R(u_i, v_j) \underset{i \neq j}{=} 0$ if the sequences are orthogonal.

The autocovariance function of a sequence $\{u_i\}$ is given by

$$R_u(k) = \sum_{i=1}^{N} u_i \cdot u_{i+k}, \quad k = 0, \pm 1, \ldots, \pm(N-1) \tag{I-2}$$

Digit synchronization occurs when $k = 0$, that is,

$$R_u(0) = \sum_{i=1}^{N} u_i^2$$

The off-synchronization autocovariance shall be called the imbalance

$D_u$, that is,

$$D_u = R_u(k) = \sum_{i=1}^{N} u_i\, u_{i+k}\ , \quad k = \pm 1,\ \pm 2,\ \ldots,\ \pm(N-1)$$

The imbalance of a periodic binary sequence is $|D_u| \leqslant 1$ . $|D_u| = 0$ if the code is orthogonal; $|D_u| = 1$ if it is simplex. A truncated sequence would have imbalances of any magnitude less than $R_u(o)$. The criterion for choosing an optimum code is to minimize the maximum imbalance $|D_u|$. That is, the criterion is

$$\begin{array}{lll} \text{Min.} & \text{Max.} & R_u(k) \\ \text{Arg.} & k \neq o & \end{array}$$

Thus, to maximize the dynamic range is equivalent to maximizing the ratio

$$\frac{R_u(o)}{\max\limits_{k \neq o} R_u(k)}$$

## Convolution Code

Two or more short binary sequences may be convoluted to yield one long sequence. If two sequences $\{a\}$ and $\{b\}$ have periods p and q, respectively, the convoluted sequence $\{c\} = \{a\} \circ \{b\}$ will have period pq. The (unnormalized) correlation of $\{c\}$ is

$$R_c(k) = \sum_{n=o}^{pq-1} c_n \;\; c_{n+k}$$

$$R_c(k) = \sum_{n=o}^{pq-1} a_n \cdot a_{n+k} \cdot b_n \cdot b_{n+k}$$

Setting $n = i + jp$ and $o \leqslant i < p$, we have

$$R_c(k) = \sum_{i=o}^{p-1} \sum_{j=o}^{q-1} a_{i+jp} \cdot a_{i+jp+k} \cdot b_{i+jp} \cdot b_{i+jp+k}$$

Summing over i first and recognizing that $i + jp$ runs through all residues modulo q, we have

$$R_c(k) = \sum_{i=0}^{p-1} a_i \; a_{i+k} \cdot \sum_{i=0}^{q-1} b_i \cdot b_{i+k}$$

$$= R_a(k) \cdot R_b(k)$$

The autocorrelation function of the convolution code is thus given by the product of the autocorrelation functions of the individual codes. The convolution code is a term-wise combination. A 105 digit convolution code is obtained by convoluting a 7 digit M-sequence with a 15 digit M-sequence. The convolution code generator is shown in Figure I-2. The two primitive polynomials used are:

$$x^4 + x^3 + 1$$

and

$$x^3 + x + 1$$

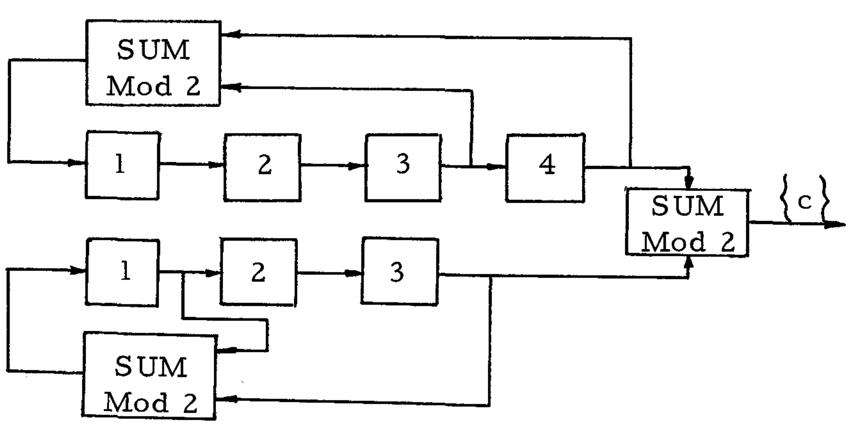


Figure I-2. 105 Digit Convolution Code Generator

## APPENDIX II

## MOVING TARGET REPRESENTATION

When a target is in motion there exists an uncertainty in range. Since time delay is proportional to range, a delay uncertainty is proportional to a range uncertainty. The delay uncertainty is an incremental change of time denoted by $\delta$. $\delta$ is called the delay rate.

The range may be represented by the equation

$$r(t) = r_o + \dot{r}t$$

$$= \text{nominal range} + \text{range uncertainty}$$

Equivalently the delay is given by

$$\tau(t) = \tau_o + \delta t$$

$$= \text{nominal delay} + \text{delay uncertainty}$$

For two way communications

$$\tau(t) = \frac{2\,r\,(t)}{(c + \dot{r})} \quad ,$$

where $c$ is velocity of propagation

$\dot{r}$ is target velocity

$$= \frac{2r_o/c}{1+\dot{r}/c} + \frac{2\dot{r}/c}{1+\dot{r}/c}\, t$$

Hence

$$\tau_o = \frac{2r_o/c}{1+\dot{r}/c}$$

$$\delta = \frac{2\dot{r}/c}{1+\dot{r}/c}$$

If $s(t) = \mathrm{Re}\left\{a(t)\, e^{j\omega_o t}\right\}$ is the transmitted signal, where a(t) is the intelligence and $\mathrm{Re}\left\{e^{j\omega_o t}\right\}$ is the energy carrier, the received signal, in the absence of fading, is given by

$$\begin{aligned} x(t) &= s(t - \tau(t)) \\ &= \mathrm{Re}\left\{a(t - \tau(t))\, e^{j\omega_o (t - \tau(t))}\right\} \end{aligned}$$

Since the nominal delay $\tau_o$ does not effect the signal, we may rewrite the above equation as

$$\begin{aligned} x(t) &= \mathrm{Re}\left\{a(t - \delta t)\, e^{j\omega_o(t - \delta t)}\right\} \\ &= \mathrm{Re}\left\{a(t - \delta t)\, e^{j(\omega_o - \delta\omega_o)t}\right\} \end{aligned}$$

The delay rate results in an epoch uncertainty on the envelope of the intelligence a(t) by an amount $\delta t$ and a frequency uncertainty on the carrier by an amount $\delta\omega_o$. The delay uncertainty $\delta t$ will be neglected in the system analysis in the main text while the frequency uncertainty will be taken to be a translation in carrier frequency.

## APPENDIX III

## THE BANDPASS SQUARER

The analysis of power-law devices has well been documented in the literature [5]. The bandpass squarer described in this Appendix is for the sake of completeness. The bandpass squarer analysis includes the zonal filter following it.

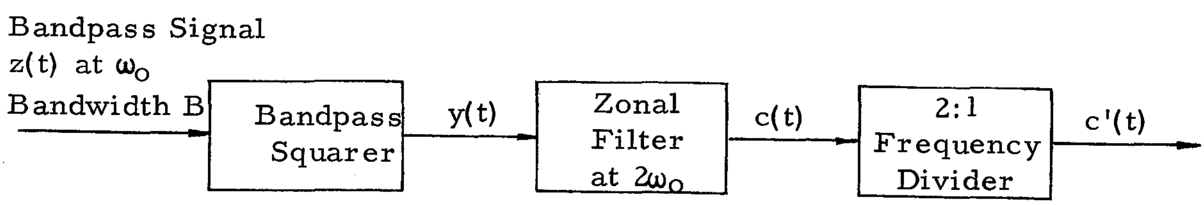


Figure III-1. Bandpass Squaring

As in the text we represent the observed waveform by

$z(t) = n(t)$ when signal is absent (III-1)

and $z(t) = x(t) + n(t)$ when signal is present (III-2)

where $x(t) = \gamma(t)\, b_t \left\{a(t_o)\right\} \operatorname{Cos} \omega_o(t - \delta t)$. The various components are as defined in section 5. 3. We analyze the cases with and without signal in the following:-

Case 1 - Signal Absent

When the signal is absent the observable is just the additive, white, Gaussian noise:-

$z(t) = n(t)$, with $E\left\{n(t)\right\} = 0$ and variance $\sigma_n^2$

The probability density function is given by:-

$$P(z) = \frac{1}{\sqrt{2\pi}\ \sigma_n} e^{-z^2/2\sigma_n^2} \tag{III-3}$$

Assuming the squarer to have unity again, the waveform at the output is given by

$$y(t) = z(t)^2 \tag{III-4}$$

The autocorrelation function of y(t) is

$$R_y(\tau) = \overline{y_1 y_2} = \overline{z_1^2 \cdot z_2^2} = 2\ R_2^2(\tau) + R_2^2(o) \tag{III-5}$$

since z(t) is a Gaussian process.

The power spectral density is given by the Fourier transform of $R_y(\tau)$. By Parseval's theorem

$$\int_{-\infty}^{\infty} R_1(\tau)\cdot R_2(\tau) \operatorname{Cos} \omega\tau d\tau = \int_{-\infty}^{\infty} G_1(\nu)\cdot G_2(f-\nu)\ d\nu$$

We then have

$$G_y(f) = \int_{-\infty}^{\infty} R_y(\tau) \operatorname{Cos} \omega\tau d\tau$$

$$= 2\int_{-\infty}^{\infty} R_z^2(\tau) \operatorname{Cos} \omega\tau d\tau + \int_{-\infty}^{\infty} R_z^2(o)\ \delta(\tau) \operatorname{Cos} \omega\tau d\tau$$

$$= 2\int_{-\infty}^{\infty} G_z(f)\cdot G_z(f-f^1)\ df^1 + \sigma_n^4\ \delta(f) \tag{III-6}$$

Let the bandwidth of the zonal filter be 2B. The signal spectral density at the output of the zonal filter is then

$$G_c(f) = 2 \int_{-2f_o-B}^{-2f_o+B} G_z(f^1) \cdot G_z(f-f^1)\, df^1$$

$$+ \int_{2f_o-B}^{2f_o+B} G_z(f^1) \cdot G_z(f-f^1)\, df^1 \qquad \text{(III-7)}$$

The low frequency components is removed by the zonal filter. For noise with constant spectral density across the bandwidth B, the spectrum of the signal c(t) may be illustrated as in Figure III-2.

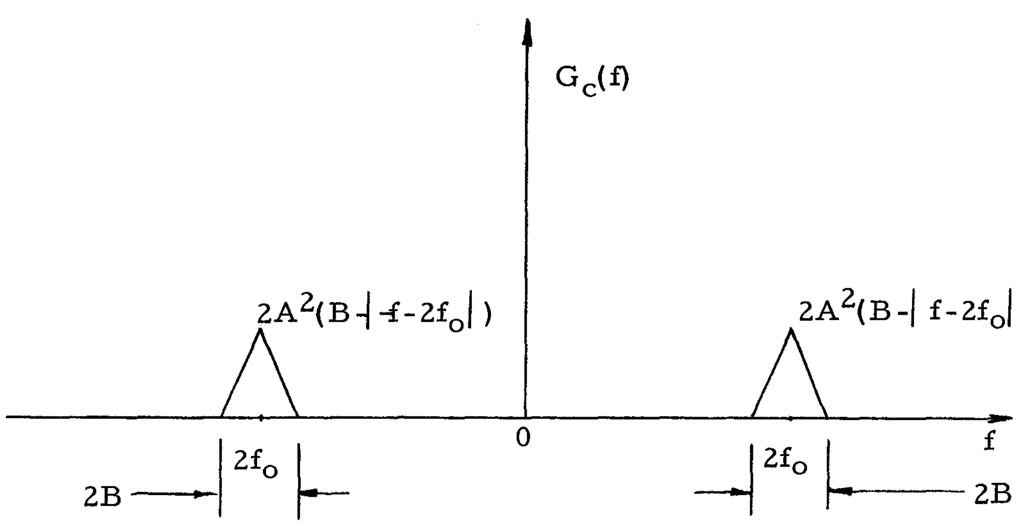


Figure III-2. Noise Spectrum At Output of Zonal Filter

Case 2 - Signal Present

$$z(t) = x(t) + n(t)$$

$$y(t) = z^2(t)$$

$$R_y(\tau) = \overline{(x_1 + n_1)^2 \cdot (x_2 + n_2)^2}$$

$$= \overline{x_1^2 \cdot x_2^2} + \overline{x_1^2 n_2^2} + 4\, \overline{x_1 x_2 n_1 n_2} + \overline{x_2^2 n_1^2} + \overline{n_1^2 n_2^2}$$

$$+ \overline{2x_1^2 \cdot x_2 \cdot n_2} + \overline{2x_1 \cdot x_2^2 \cdot n_1} + \overline{2x_1 n_1 n_2^2} + \overline{2x_2 n_1^2 n_2},$$

where $x_1 = x(t)$, $n_1 = n(t)$

$x_2 = x(t + \tau)$, $n_2 = n(t + \tau)$

Assumptions:- $\bar{n} = o$ and x & n are statistically independent.

Therefore $R_y(\tau) = \overline{x_1^2 x_2^2} + \overline{x_1^2 n_2^2} + 4\, \overline{x_1 x_2 n_1 n_2} + \overline{x_2^2 n_1^2} + \overline{n_1^2 n_2^2}$

..... (III-8)

or $R_y(\tau) = R_{xx}(\tau) + R_{xn}(\tau) + R_{nn}(\tau)$

where $R_{xx}(\tau) \triangleq \overline{x_1^2 x_2^2}$

$R_{xn}(\tau) \triangleq 4\, R_x(\tau) \cdot R_n(\tau) + 2\, R_x(o)\, R_n(o)$

$R_{nn}(\tau) \triangleq \overline{n_1^2\, n_2^2}$

$= 2R_n^2(\tau) + R_n^2(o)$

The corresponding power spectral density is

$$G_y(f) = G_{xx}(f) + G_{xn}(f) + G_{nn}(f)$$

The power spectral density of the squared function, y(t), thus consists of three components. The coherent part is the signal x signal term.

The incoherent part is made up of a noise x noise term and a signal x noise term, the latter being the additional noise as a result of the nonlinear operation of the squarer.

The noise x noise component is given by equation (III-6) repeated below:-

$$G_{nn}(f) = 2\int_{-\infty}^{\infty} G_n(f^1)\, G_n(f - f^1)\, df^1 + \sigma_n^4\, \delta(f) \qquad \text{(III-6)}$$

Since the signal, from equation (19a), is

$$x(t) = \gamma(t) \cdot b_t \left\{a(t_o)\right\} \operatorname{Cos} \omega_o(t - \delta t)$$

$$= m(t) \cdot \operatorname{Cos} \omega_o(t - \delta t),$$

we have

$$R_x(\tau) = 1/2\, [m(t)]^2 \operatorname{Cos} \omega_o (1 - \delta)\tau$$

Hence $G_x(f) = 1/4\, m^2(t)\, [\delta(f + f_o(1 - \delta)) + \delta(f - f_o(1 - \delta))]$* (III-9)

The signal x signal component:-

$$R_{xx}(\tau) = m^4(t)\, [1/4 + 1/8 \operatorname{Cos}[2\omega_o(1 - \delta)\tau]]$$

and

$$G_{xx}(f) = 1/4\, m^4(t)\, \delta f + 1/16\, m^4(t)\, [\delta(f + 2f_o(1 - \delta)) + \delta(f - 2f_o(1 - \delta))].$$

.... (III-10)

The signal x noise component:-

$$G_{xn}(f) = m^2(t)\, [G_n(f + 2f_o(1 - \delta)) + G_n(f - 2f_o(1 - \delta))]$$

$$+ m^2(t)\, \sigma_n^2\, \delta(f). \qquad \text{(III-11)}$$

* The symbol $\delta$ is used here to denote the Dirac Delta function as well as the delay rate. The respective meaning is clear in context.

The zonal filter removes the low-frequency components. The spectral density at the zonal filter output is then given by:-

$$G_c(f) = 1/16\ m^4(t)\ [\delta(f + 2f_o(1-\delta)) + \delta(f - 2f_o(1-\delta))]$$
$$+ m^2(t)[G_n(f + 2f_o(1-\delta)) + G_n(f - 2f_o(1-\delta))]$$
$$+ 2\left\{\int_{-2f_o-B}^{-2f_o+B} G_n(f^1)\cdot G_n(f-f^1)\,df^1 + \int_{+2f_o-B}^{+2f_o+B} G_n(f^1)\cdot G_n(f-f^1)\,df^1\right\}$$

.... (III-12)

With a constant input noise spectral density A over the narrow band B, we have

$$G_c(f) = \begin{cases} m^4(t)/16\ , & \text{for } |f| = 2f_o(1-\delta) \\ +m^2(t)A\ , & \text{for } 2f_o(1-\delta) - B/2 < |f| < 2f_o(1-\delta) + B/2 \\ +2A^2(B - \big||f| - 2f_o(1-\delta)\big|)\ , & \text{for } 2f_o(1-\delta) - B < |f| < 2f_o(1-\delta) + B \end{cases}$$

.... (III-13)

Equation (III-13) is illustrated graphically in Figure III-3.

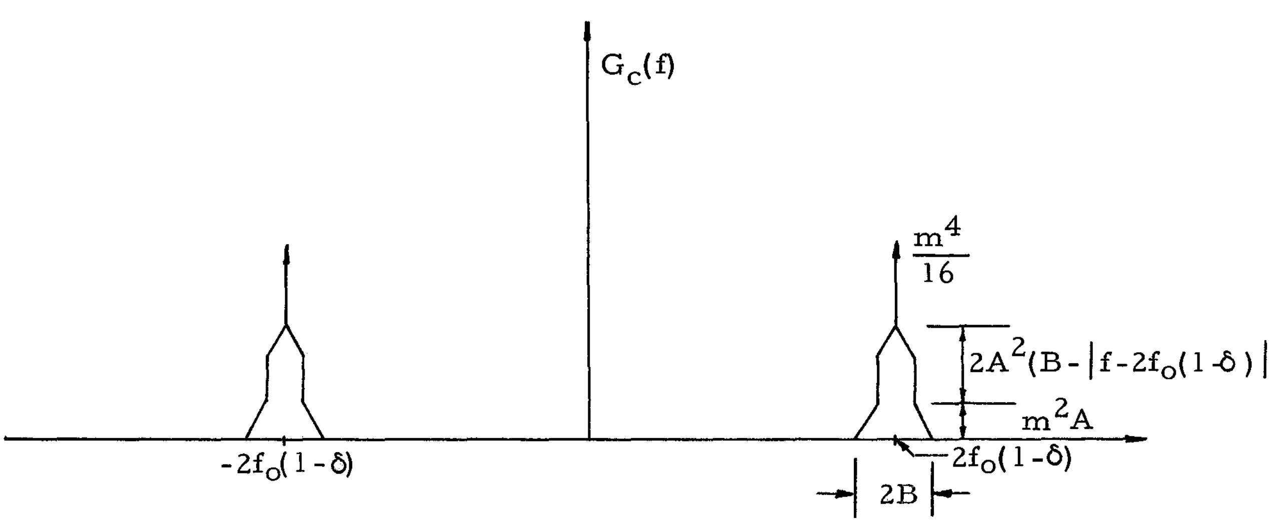


Figure III-3. Spectral Density At Output of Zonal Filter

The coherent power = $2(m^4/16) = m^4/8$

The incoherent or fluctuation power = $2(2A^2B^2+m^2AB)$

$$= 2AB(2AB + m^2)$$

Now, the signal power at the input to the squarer = $m^2/2$

and the noise power at the input = $2AB$

The input signal-to-noise ratio is $r_i = \frac{m^2}{2} \;/\; 2AB = \frac{m^2}{4AB}$

The output signal-to-noise ratio is:-

$$r_o = \frac{m^4/B}{2AB(2AB + m^2)} = \frac{m^4/16A^2B}{2+ m^2/AB} = \frac{r_i^{\,2}}{2(1+2r_i)}$$

We note that, as $r_i \rightarrow o$ , $r_o \, \alpha \, r_i^2$

as $r_i \rightarrow \infty$, $r_o \, \alpha \, r_i$

A plot of $r_o$ vs $r_i$ for the bandpass squarer is shown in Figure III-4. Equation (III-13) is the power spectral density of the signal c(t). The signal c(t) may be derived in the following manner:-

$$z(t) = x(t) + n(t)$$

$$= m(t) \operatorname{Cos} \omega_o(1 - \delta)t + v_c(t) \operatorname{Cos} \omega_o(1 - \delta)t - v_s(t) \operatorname{Sin} \omega_o(1 - \delta)t,$$

where we have represented the narrow band gaussian noise by two random functions at quadrature:

$$v_c(t) = n(t) \operatorname{Cos} \phi_n(t)$$

$$v_s(t) = n(t) \operatorname{Sin} \phi_n(t)$$

Hence $\phi_n(t) = \tan^{-1} \frac{v_s(t)}{v_c(t)}$

and $n(t) = [\, v_c{}^2(t) + v_s{}^2(t) \,]^{1/2}$

In the above representation we have $E\left\{v_c(t)\right\} = E\left\{v_s(t)\right\} = o$

Also $\sigma_{v_c}^2 = \sigma_{v_s}^2 = \sigma_n^2$

Then $y(t) = z^2(t)$

$$= m^2(t)\,\mathrm{Cos}^2\,\omega_o(1-\delta)t + 2m(t)\,\mathrm{Cos}\,\omega_o(1-\delta)t$$

$$\cdot\left[v_c(t)\,\mathrm{Cos}\,\omega_o(1-\delta)t - v_s(t)\,\mathrm{Sin}\,\omega_o(1-\delta)t\right]$$

$$+\left[v_c(t)\,\mathrm{Cos}\,\omega_o(1-\delta)t - v_s(t)\,\mathrm{Sin}\,\omega_o(1-\delta)t\right]^2$$

and

$$c(t) = 1/2\,m^2(t)\,\mathrm{Cos}\left[2\omega_o(1-\delta)t\right]$$

$$+ m(t)\,v_c(t)\,\mathrm{Cos}\left[2\omega_o(1-\delta)t\right]$$

$$- m(t)\,v_s(t)\,\mathrm{Sin}\left[2\omega_o(1-\delta)t\right]$$

$$+ \frac{v_c^2(t) - v_s^2(t)}{2}\,\mathrm{Cos}\,2\omega_o(1-\delta)t$$

$$- v_c(t)\,v_s(t)\,\mathrm{Sin}\,2\omega_o(1-\delta)t$$

After frequency division we have

$$c'(t) = 1/2\,m^2(t)\,\mathrm{Cos}\,\omega_o(1-\delta)t \qquad \text{coherent component}$$

$$\left.\begin{aligned} &+ m(t)\,v_c(t)\,\mathrm{Cos}\,\omega_o(1-\delta)t \\ &- m(t)\,v_s(t)\,\mathrm{Sin}\,\omega_o(1-\delta)t \\ &+ 1/2\left(v_c^2(t) - v_s^2(t)\right)\mathrm{Cos}\,\omega_o(1-\delta)t \\ &- v_c(t)\cdot v_s(t)\cdot\mathrm{Sin}\,\omega_o(1-\delta)t \end{aligned}\right\}\ \text{incoherent component} \qquad \text{(III-14)}$$

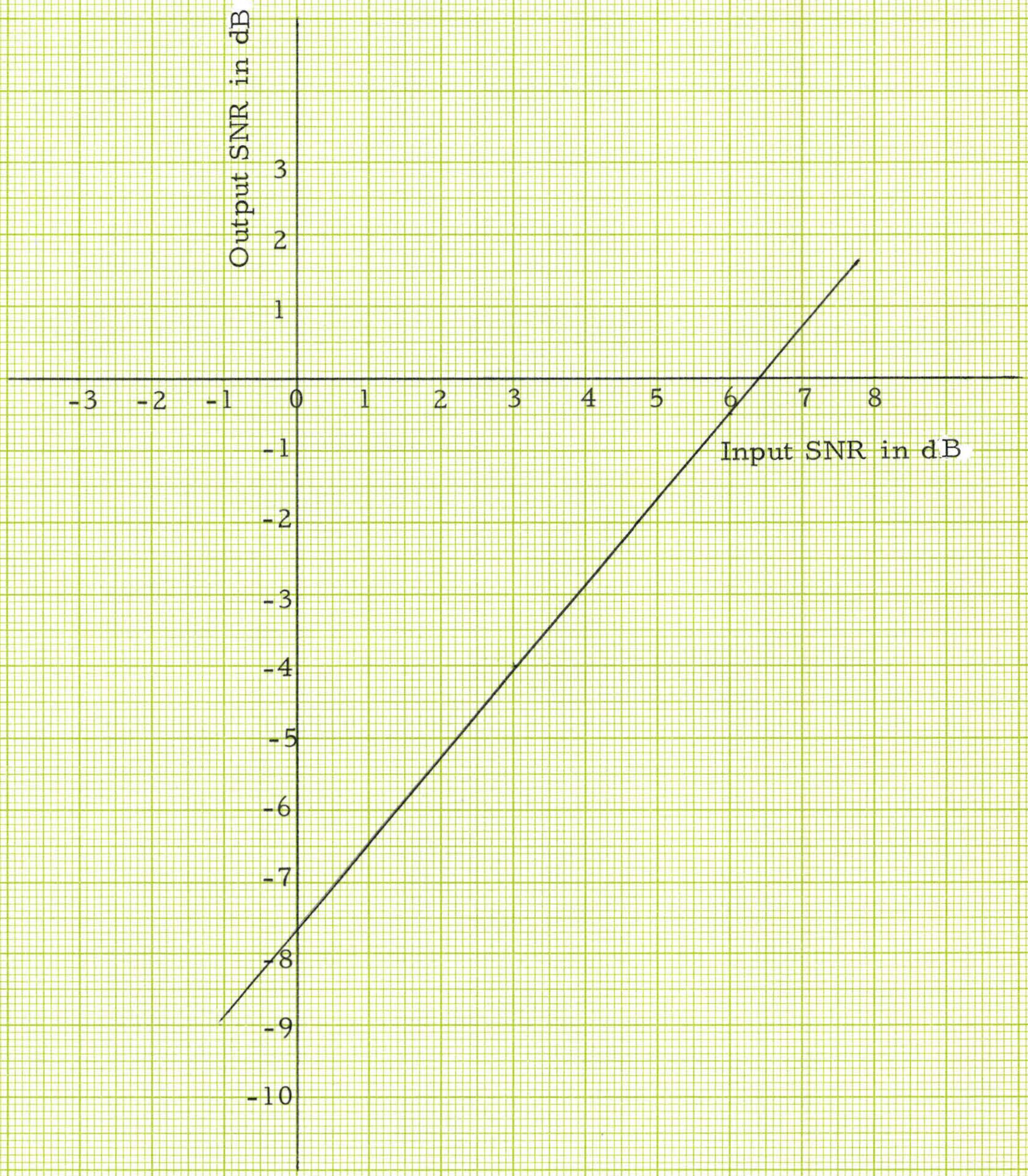


Figure III - 4 Bandpass Squarer Characteristic

## APPENDIX IV

## COMPUTER SIMULATION PROGRAMS

The overall computer simulation for the echo ranging system described in the main text is briefly described in this Appendix. A listing of the computer simulation programs used for system evaluation is given at the end of this Appendix. The components which make up the overall echo ranging system are simulated in subroutine forms. A main routine called ADAPT monitors the signal flow of the overall system by calling upon the subroutines to perform their functions at appropriate points.

All routines are written in FORTRAN IV for the IBM 7040 computer. All waveforms presented in Chapter VII are plotted by a Benson-Lehner digital X-Y plotter. Except for a subroutine called RANGAU, which is a McMaster Computer Centre Gaussian noise generator, all other subroutines are system component simulation programs written by the author. All subroutines communicate with the main routine ADAPT in the manner depicted in Figure IV-1. Detailed flow charts, which would amount to a minimum of 1 to 2 pages per subroutine, are not included, since the central theme of this thesis is not an exposition on computer programming. However, an exposition on computer programming with detailed flow charts for problems of similar complexity can be found in reference [16]. A list of the various subroutines accompanied by a short description is given below:

| Subroutine Name | Description |
|---|---|
| CCGEN | A convolution code generator; this subroutine calls on another subroutine, CGEN, to generate the component M-sequence. |
| CGEN | A binary M-sequence generator. |
| BPSIG | A pure sinusoidal signal generator and/or bandpass signal encoder. |
| FADING | A channel fading model, simulated by a sum of fixed and random components. |
| RANGAU | A Gaussian noise generator (McMaster Library program). |
| BPSQFT | A bandpass squarer, tuner and frequency divider. |
| BPFTR | A bandpass zonal filter which regenerates the carrier and extracts the Doppler shift frequency. |
| MIXER | A quadrature demodulator. |
| VARCE | A subroutine to compute the mean and variance of any random process. |
| INSNR | A subroutine to compute input signal-to-noise ratio when the observable is signal+noise. This subroutine calls INVAR. |

| Subroutine Name | Description |
|---|---|
| INVAR | Computes the variance of noise, excluding the signal occupancy. |
| ESTMR | A baseband signal estimator. |
| QUANTR | An n level quantizer, n even. |
| RECVR | A cross-correlator which yields a time compressed output waveform at each of the quadrature channels and the combined channel. |
| FMAX | Locates the peak value of the compressed waveform and identifies its location. |
| SNR | Computes the output signal-to-noise ratio and/or the peak-to-sidelobe ratio. |
| PROBAN | Computes the false alarm rate. |
| C GRAPH | Sets up the plot parameters and calls GRAPH to do the actual plotting. |
| GRAPH | Plots data on the Benson-Lehner digital X-Y plotter. |

The level of subroutine calling by the main routine ADAPT is typified in the gross flow chart of Figure IV-2.

A second main routine called ADAPT2 simulates a multiple target situation. The main routine ADAPT2 calls upon the appropriate subroutines listed above and the following additional subroutines.

| Subroutine Name | Description |
| --- | --- |
| MULTGT | A subroutine to simulate multiple targets and/ or reverberation. |
| M NOISE | A subroutine to simulate multiplicative noise at complex low-pass. |

A gross flow chart for the multiple target simulation is shown in Figure IV-3.

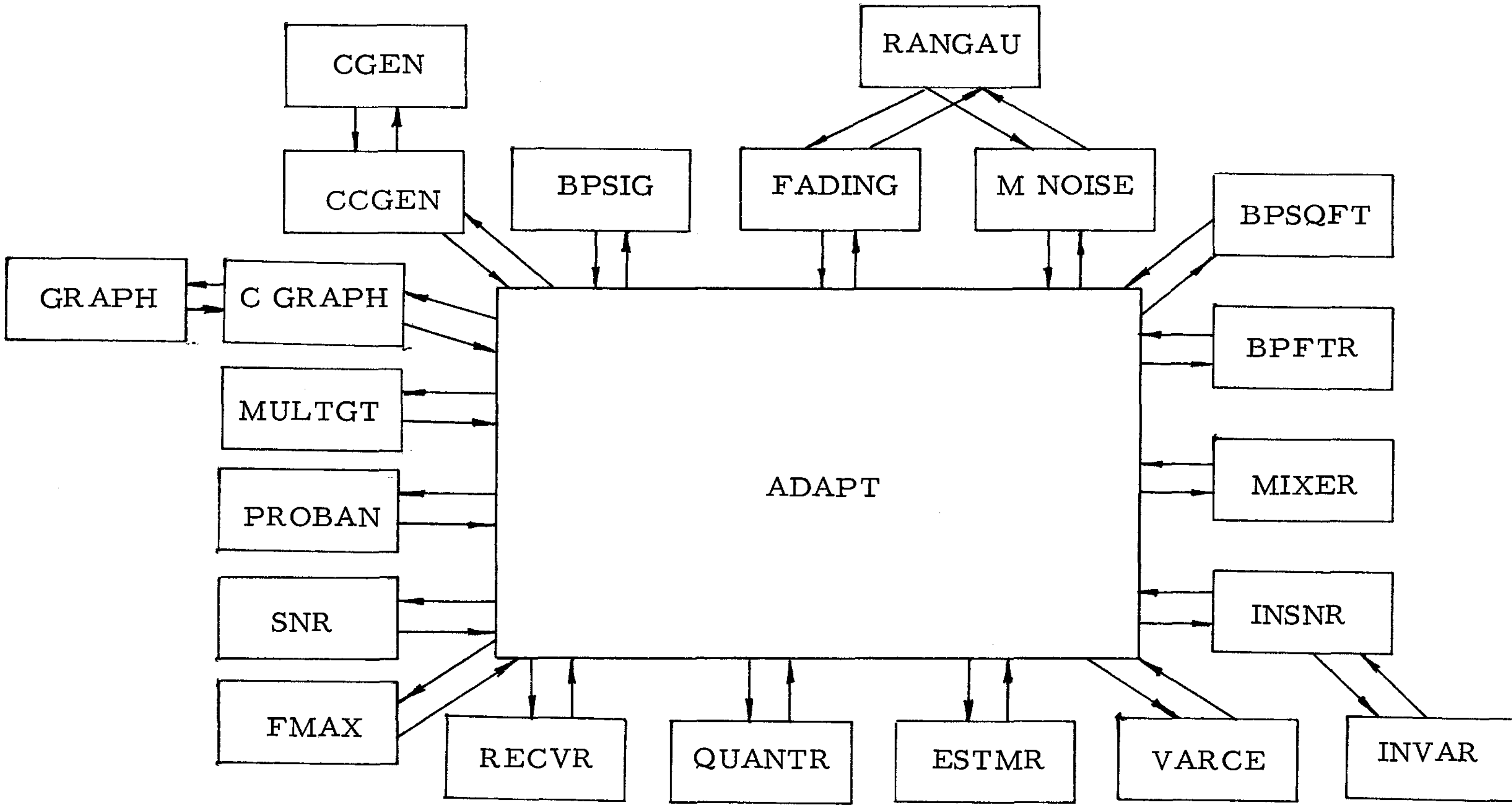


Figure IV-1. Hierarchy of Subroutines for System Simulation


Figure IV-2. Sequence of Subroutine Calling by ADAPT

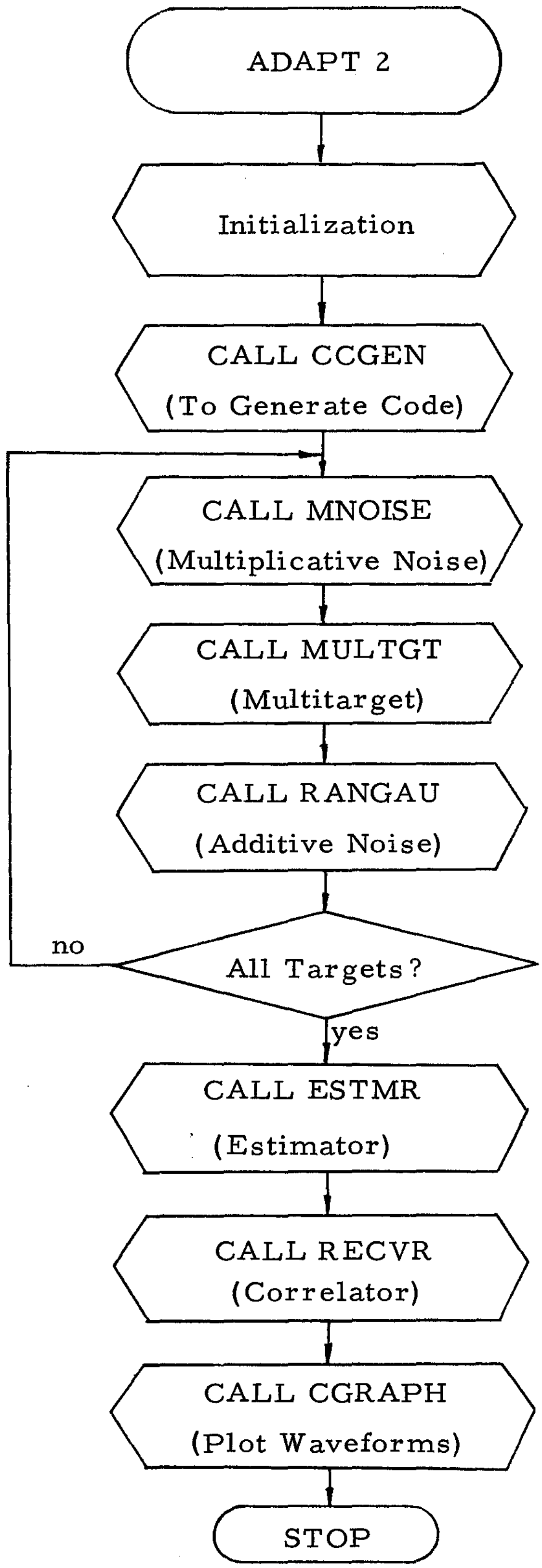


Figure IV-3. Sequence of Subroutine Calling for Multitarget Simulation

```
$JOB              003506 JWMARK              100   010   030
$PAUSE PLEASE MOUNT 300 FT MINI REEL ON TC2 FOR B-L PLOTTER.       130
$IBJOB            DECK
$IBFTC ADAPT      NODECK
C     SELF-SYNCHRONYZED ADAPTIVE DETECTION SYSTEM
      DIMENSION SHRG(4),ATAPS(3),TAPS(4),SIG1(15),SIG2(7),BUFF1(105),BUF
     1F2(105),BUFF4(420)
      DIMENSION AVC(1681),AUTOP(1681),AUTOQ(1681),PSIG(1681),QSIG(1681),
     1SIGP(1681),SIGQ(1681),AVCLG(1681)
      DIMENSION AVC1(1681),AUTOP1(1681),AUTOQ1(1681),AVCLG1(1681)
      DIMENSION X(1681),Y(420),Z(1681)
      DIMENSION PNSG(420),QNSG(420),CSIG(1681),SSIG(1681),CRSIG(1681),
     1SRSIG(1681),CTSIG(1681),STSIG(1681)
      EQUIVALENCE (PSIG,CRSIG),(QSIG,SRSIG),(SIGP,CTSIG),(SIGQ,STSIG,Z),
     1(BUFF4,PNSG),(Y,QNSG)
      EQUIVALENCE (AUTOP1,AUTOP,CSIG),(AUTOQ1,AUTOQ,SSIG),(AVC1,AVC,AVCL
     1G1,AVCLG,X)
      DIMENSION  PLVL(1),ANLVL(1)
      DIMENSION T(5)
      DATA T/-0.85,-0.30,-0.45,-0.60,-0.75/
      DATA LBTWO/4/,L/1/,PMAX/0.0/
      DATA TAPS/0.0,0.0,1.0,1.0/
      DATA ATAPS/1.0,0.0,1.0/
      DATA ICDLTH,MCDLTH,LL,ML/7,15,3,4/
      DATA STR,SD/0.0,0.001/
      DATA STN/0.0/
      DATA FCTR,THETA,ISAMP/1.0,0.8,4/
      DATA STA,STQ,STD/11500.0,0.0,1.75/
      DATA ISWCH,JSWCH,MSWCH/1,0,1/
      MM=MCDLTH*ICDLTH
      MN=ISAMP*MM
      DATA ICYCLE,NDIVR/2,4/
      DATA PHIR/0.0/
      PI=3.1415926
      PHIC=PI/3.0
      KM=4*NDIVR*ICYCLE
      ILENTH=ICYCLE*MM
      NN=2*NDIVR*ICYCLE*MM+1
      DRIF=PI/32.0
      ACYCLE=ICYCLE
      ACDLTH=MM
      DIVR=NDIVR
      DOPPLR=(DRIF *ACYCLE*ACDLTH*DIVR)/PI
      WRITE(6,7)DOPPLR
    7 FORMAT(1H0,42HDOPPLER SHIFT FOR ONE CODE LENGTH IN CPS =,F12.6)
      CALL CCGEN(SIG1,SIG2,MCDLTH,ICDLTH,BUFF1,BUFF2,MM,ISWCH,JSWCH,BUFF
     14,MN,FCTR,TAPS,ML,ATAPS,LL,SHRG,ISAMP)
      CALL BPSIG(CSIG,STSIG,NN,NDIVR,ICYCLE,PHIC,PHIR,BUFF1,MM,0,0,DRIF)
      CALL LETTER(24,5,90,0.0,1.0,24HJ.W. MARK/105 DIGIT CODE)
      CALL PLOT(3.0,1.0,-3)
      YDISP=0.0
      XDISP=0.0
      XINCH=9.0
      YINCH=1.25
      CALL CGRAPH(NN,CSIG,X,XDISP,YDISP,XINCH,YINCH,1)
      YDISP=2.0
      CALL CGRAPH(NN,STSIG,X,XDISP,YDISP,XINCH,YINCH,1)
      CALL CGRAPH(MM,BUFF1,X,XDISP,YDISP,XINCH,YINCH,1)
      CALL LETTER(14,2,0,4.0,00.0,14H105 DIGIT CODE)
```

```
      CALL LETTER(17,2,0,4.0,-2.0,17HSINUSOIDAL SIGNAL)
      CALL LETTER(14,2,0,4.0,-4.0,14HENCODED SIGNAL)
      CALL PLOT(13.0,-4.0,-3)
      PHIR=PHIR+PI/2.0
      CALL BPSIG(CSIG,STSIG,NN,NDIVR,ICYCLE,PHIC,PHIR,BUFF1,MM,1,0,DRIF)
      DATA MMRY/10/,SLOW/0.0/
      DATA PMEAN/0.0/,VAR/0.0/,PHI/0.0/,DPHI/0.001/
      CALL FADING(X,NN,MMRY,STR,SD,PMEAN,VAR,PHI,DPHI,SLOW)
      DO 11 I=1,NN
   11 CSIG(I)=CSIG(I)*X(I)
      CALL RANGAU(X,NN,STN,STD)
      DO 12 I=1,NN
   12 CSIG(I)=CSIG(I)+X(I)
      CALL BPSQFT(CSIG,CRSIG,SRSIG,NN,NDIVR,ILENTH,PHIC)
      CALL BPFTR(NN,CRSIG,SRSIG,CTSIG,STSIG,KM,NDIVR,SSIG)
      CALL MIXER(CSIG,CRSIG,SRSIG,CTSIG,STSIG,NN,PNSG,QNSG,ISAMP,NDIVR,
     1ICYCLE,MN)
      CALL LETTER(19,3,90,0.0,1.0,19HQCHANNEL STATISTICS)
      CALL PLOT(3.0,0.0,-3)
      YDISP=0.0
      CALL CGRAPH(MN,QNSG, X,XDISP,YDISP,XINCH,YINCH,1)
      YDISP=2.0
      CALL CGRAPH(NN,SRSIG,X,XDISP,YDISP,XINCH,YINCH,1)
      CALL CGRAPH(NN,CSIG,X,XDISP,YDISP,XINCH,YINCH,1)
      CALL LETTER(12,2,0,4.0, 0.0,12HNOISY SIGNAL)
      CALL LETTER(25,2,0,3.5,-2.00,25HDERIVED REFERENCE CARRIER)
      CALL LETTER(17,2,0,4.0,-4.00,17HLOW-PASS WAVEFORM)
      CALL PLOT(13.0,-4.00,-3)
      CALL LETTER(19,3,90,0.0,1.0,19HPCHANNEL STATISTICS)
      CALL PLOT(3.0,0.0,-3)
      YDISP=0.0
      CALL CGRAPH(MN,PNSG, X,XDISP,YDISP,XINCH,YINCH,1)
      YDISP=2.0
      CALL CGRAPH(NN,CRSIG,X,XDISP,YDISP,XINCH,YINCH,1)
      CALL CGRAPH(NN,SSIG,X,XDISP,YDISP,XINCH,YINCH,1)
      CALL LETTER(15,2,0,4.0, 0.0,15HFREQUENCY DRIFT)
      CALL LETTER(25,3,0,3.5,-2.0,25HDERIVED REFERENCE CARRIER)
      CALL LETTER(17,3,0,4.0,-4.0,17HLOW-PASS WAVEFORM)
      CALL PLOT(13.0,-4.0,-3)
      DATA ANOP,ANOQ,PVAR,QVAR/0.0,0.0,0.0,0.0/
      DATA AMEAN,AVAR/0.0,0.0/
      INTL=MN
      IFNL=2*MN-1
      IDMM=3*MN
      IDMN=IDMM-ISAMP
      CALL RANGAU(PSIG,IDMM,STA,STD)
      CALL RANGAU(QSIG,IDMM,STQ,STD)
      CALL AVRG(PSIG,IDMM,PSIG,IDMN,ISAMP)
      CALL AVRG(QSIG,IDMM,QSIG,IDMN,ISAMP)
      CALL VARCE(PSIG,IDMM,ANOP,PVAR,1)
      CALL VARCE(QSIG,IDMM,ANOQ,QVAR,1)
      PSNR=10.0*ALOG10(PMEAN**2/PVAR)
      WRITE(6,9)PSNR
    9 FORMAT(1H0,21H  INPUT  SNR IN DBS =,E15.10)
      DO 8 I=INTL,IFNL
      J=I-INTL+1
      QSIG(I)=0.0
      PSIG(I)=0.0
```

```
      QSIG(I)=QSIG(I)+QNSG(J)
    8 PSIG(I)=PSIG(I)+PNSG(J)
      LM=2*MN
      CALL ESTMR(PSIG,IDMM,SIGP,IDMN,ISAMP,PVAR)
      CALL ESTMR(QSIG,IDMM,SIGQ,IDMN,ISAMP,QVAR)
      CALL QUANTR(PSIG,IDMM,PLVL,ANLVL,LBTWO,CMAX,L)
      CALL QUANTR(QSIG,IDMM,PLVL,ANLVL,LBTWO,SMAX,L)
      CALL QUANTR(SIGP,IDMN,PLVL,ANLVL,LBTWO,CMAX,L)
      CALL QUANTR(SIGQ,IDMN,PLVL,ANLVL,LBTWO,SMAX,L)
      DATA FARATE,IOBNT/0.0,5/
      WRITE(6,108)
  108 FORMAT(1H-,64HTHE FOLLOWING ARE OUTPUT STATISTICS FOR SYSTEM WITHO
     1UT ESTIMATOR)
      DATA PEAK,IPOSN,TRNG,SNR1,SNR2,VAR,SW,NNT,ICNTL,ISIDE/0.0,0,0.0,0.
     10,0.0,0.0,1.0,420,10,10/
      CALL RECVR(AVC,AUTOP,AUTOQ,BUFF1,IDMN,MM,SIGP,SIGQ,ISAMP,LM,MSWCH,
     1AVCLG)
      CALL FMAX(AVC,MM,PEAK,IPOSN)
      CALL SNR(AVC ,MM,SNR1,SNR2,PEAK,IPOSN,VAR,SW,NNT,ICNTL,ISIDE,IFLAG
     1)
      DO 20 JL=1,4
      THOLD=PEAK*10.0**T(JL)
      WRITE(6,22)LBTWO,THOLD
   22 FORMAT(1H ,25HHALF QUANTIZATION LEVEL =,I3,11HTHRESHOLD =,F12.5)
      CALL PROBAN(AVC,MM,THOLD,PEAK,FARATE,IOBNT,IPOSN)
   20 CONTINUE
      DO 10 I=INTL,IFNL
      J=I-INTL+1
   10 Y(J)=SIGP(I)
      CALL LETTER(14,5,90,0.0,1.0,14HSYSTEM OUTPUTS)
      CALL PLOT(3.0,0.0,-3)
      XDISP=0.0
      XINCH=10.0
      YINCH=3.0
      YDISP=0.0
C       IF DIVISION MARKS ARE REQUIRED PUT NDIV = 0
      CALL CGRAPH(LM,AVC, Z,XDISP,YDISP,XINCH,YINCH,0)
      YDISP=3.0
      CALL CGRAPH(LM,AUTOP, Z,XDISP,YDISP,XINCH,YINCH,1)
      YINCH=1.25
      CALL CGRAPH(MN,Y,     Z,XDISP,YDISP,XINCH,YINCH,1)
      WRITE(6,107)
  107 FORMAT(1H-,61HTHE FOLLOWING ARE OUTPUT STATISTICS FOR SYSTEM WITH
     1ESTIMATOR)
      CALL RECVR(AVC1,AUTOP1,AUTOQ1,BUFF1,IDMM,MM,PSIG,QSIG,ISAMP,LM,MSW
     1CH,AVCLG1)
      CALL FMAX(AVC1,MM,PEAK,IPOSN)
      CALL SNR(AVC1,MM,SNR1,SNR2,PEAK,IPOSN,VAR,SW,NNT,ICNTL,ISIDE,IFLAG
     1)
      DO 25 JH=1,4
      THOLD=PEAK*10.0**T(JH)
      WRITE(6,22)LBTWO,THOLD
      CALL PROBAN(AVC,MM,THOLD,PEAK,FARATE,IOBNT,IPOSN)
   25 CONTINUE
      DO 19 I=INTL,IFNL
      J=I-INTL+1
   19 Y(J)=PSIG(I)
      CALL PLOT(13.0,-6.0,-3)
```

```
      YINCH=3.0
      YDISP=0.0
      CALL CGRAPH(LM,AVC1,Z,XDISP,YDISP,XINCH,YINCH,0)
      YDISP=3.0
      CALL CGRAPH(LM,AUTOP1,Z,XDISP,YDISP,XINCH,YINCH,1)
      YINCH=1.25
      CALL CGRAPH(MN,Y,     Z,XDISP,YDISP,XINCH,YINCH,1)
      CALL PLOT(13.0,-6.0,-3)
      CALL LETTER(17,5,90,0.0,1.0,17HFINISHED PLOTTING)
      CALL PLOT(0.0,0.0,999)
      STOP
      END
$IBFTC CCGEN   DECK
C     IF ISWCH=0,ONLY M-SEQUENCE IS GENERATED
C     IF JSWCH=0, SIGNAL IS TO BE SAMPLED ONCE
      SUBROUTINE CCGEN(SIG1,SIG2,MCDLTH,ICDLTH,BUFF1,BUFF2,NN,ISWCH,JSWC
     1H,BUFF4,MN,FCTR,TAPS,ML,ATAPS,LL,SHRG,ISAMP)
      DIMENSION SIG1(MCDLTH),SIG2(ICDLTH),BUFF1(NN),BUFF2(NN),BUFF4(MN),
     1TAPS(ML),SHRG(ML),ATAPS(LL)
      CALL CGEN(SIG1,MCDLTH,TAPS,ML,SHRG)
      IF(ISWCH.EQ.0)GO TO 81
      CALL CGEN(SIG2,ICDLTH,ATAPS,LL,SHRG)
      M=0
    1 DO 4 I=1,MCDLTH
      J=I+M
    4 BUFF1(J)=SIG1(I)
      M=M+MCDLTH
      IF(M.LT.NN)GO TO 1
      M=0
    2 DO 5 I=1,ICDLTH
      J=I+M
    5 BUFF2(J)=SIG2(I)
      M=M+ICDLTH
      IF(M.LT.NN)GO TO 2
      DO 6 I=1,NN
      SUM=BUFF1(I)+BUFF2(I)
    6 BUFF1(I)=AMOD(SUM,2.0)
    8 DO 7 J=1,NN
      IF(BUFF1(J).EQ.0.0)BUFF1(J)=-1.0
    7 CONTINUE
      WRITE(6,17)(BUFF1(I),I=1,NN)
   17 FORMAT(1H0,17HCOMBINATION CODE.,/(1H ,25F5.1))
      IF(JSWCH.EQ.0)GO TO 9
      M=1
      K=ISAMP
      DO 31 I=1,NN
      DO 32 J=M,K
   32 BUFF4(J)=BUFF1(I)*FCTR
      M=M+ISAMP
      K=K+ISAMP
   31 CONTINUE
    9 RETURN
   81 DO 82 I=1,MCDLTH
   82 BUFF1(I)=SIG1(I)
      GO TO 8
      END
$IBFTC CGEN    DECK
C     GENERAL CODE GENERATOR, INCLUDING SINGLE PULSE
```

```
C     CMSEQ = M-SEQUENCE, ICDLTH = LENGTH OF M-SEQUENCE
C      ATAPS = FEEDBACK TAPS, LL = NO. OF SHIFT REGISTER STAGES
       SUBROUTINE CGEN(CMSEQ,ICDLTH,ATAPS,LL,SHRG)
       DIMENSION CMSEQ(ICDLTH),ATAPS(LL),SHRG(LL)
       SUM = 0.0
       DO 1 I=1,LL
     1 SHRG(I)=1.0
       NN = LL-1
       DO 2 J=1,ICDLTH
       CMSEQ(J)=SHRG(LL)
       SUM = 0.0
       DO 4 I = 1,LL
     4 SUM=SUM+SHRG(I)*ATAPS(I)
       DO 3 I =1,NN
       K=LL-I
       N=K+1
     3 SHRG(N)=SHRG(K)
     2 SHRG(1)=AMOD(SUM,2.0)
       WRITE(6,17)(CMSEQ(I),I=1,ICDLTH)
    17 FORMAT(1H0,15HREFERENCE CODE.,/(1H ,25F5.1))
       RETURN
       END
$IBFTC BPSIG   DECK
       SUBROUTINE BPSIG(CSIG,RSIG,NN,NDIVR,ICYCLE,PHIC,PHIR,CODE,ICDLTH,I
      1SW,JSW,DRIFT)
C      THIS SUBROUTINE GENERATES A BINARY CODED SIGNAL AND/OR A PURE
C      SINUSOIDAL WAVEFORM
C     IF ISW = 0,BINARY ENCODED SIGNAL IS REQUIRED
C      IF JSW = 0,PURE SINUSOIDAL SIGNAL IS REQUIRED
C      ICYCLE=NUMBER OF CYCLES PER BAUD
C      NDIVR=NUMBER OF SAMPLES PER HALF CYCLE OF CARRIER FREQUENCY
C      KM=NUMBER OF SAMPLES PER BAUD
C         =2*NDIVR*ICYCLE
C      NN=KM*ICDLTH+1
C      CSIG = CODED SIGNAL ARRAY
C      RSIG = SINUSOIDAL CARRIER
C      CODE = MODULATION CODE
       DIMENSION CSIG(NN),RSIG(NN),CODE(ICDLTH)
       PI=3.1415926
       DIVR=NDIVR
       DTHETA=PI/DIVR
       KM=2*NDIVR*ICYCLE
       KCT=1
       K=1
       KK=KM
       IF(ISW.NE.0)GO TO 6
       THETA=0.0
     3 DO 2 J=K,KK
       CSIG(J)=SIN(PHIC+THETA)
     2 THETA=THETA+DTHETA
       KCT=KCT+1
       IF(KCT.GT.ICDLTH)GO TO 5
       KK=KK+KM
       K=K+KM
       IF(CODE(KCT).EQ.CODE(KCT-1))GO TO 4
       THETA=THETA+DTHETA+PI
       GO TO 3
     4 THETA=THETA+DTHETA
```

```
      GO TO 3
    5 THETA=THETA+DTHETA
      CSIG(NN)=SIN(PHIC+THETA)
      IF(JSW.NE.0)GO TO 7
    6 THETA=0.0
      DTHETA=DTHETA+DRIFT
      DO 1 I=1,NN
      RSIG(I)=SIN(PHIR+THETA)
    1 THETA=THETA+DTHETA
    7 RETURN
      END
$IBFTC BPFTR   DECK
      SUBROUTINE BPFTR(NN,CRSIG,SRSIG,CTSIG,STSIG,KM,NDIVR,FDSIG)
C     THIS SUBROUTINE PERFORMS BANDPASS FILTERING FOR BANDWIDTHS
C     SPECIFIED BY  'KM' ,WHERE KM IS THE FILTER MEMORY
C     IF THE BANDWIDTH IS THE SAME AS THE SIGNAL BANDWIDTH,THEN
C     KM=2*NDIVR*ICYCLE
      DIMENSION CTSIG(NN),STSIG(NN),CRSIG(NN),SRSIG(NN),FDSIG(NN)
      MM=NN-KM+1
C     MULTIPLY THE TWO SIGNALS
      DO 1 I=1,NN
      CRSIG(I)=CRSIG(I)*CTSIG(I)
    1 SRSIG(I)=SRSIG(I)*STSIG(I)
C     PERFORM STATISTICAL AVERAGING
      DO 2 I=1,NN
      AKM=KM
      TEMPC=0.0
      TEMPS=0.0
      IFNL=I+KM-1
      DO 3 J=I,IFNL
      TEMPC=TEMPC+CRSIG(J)
    3 TEMPS=TEMPS+SRSIG(J)
      IF(I.LT.MM)GO TO 5
      KM=KM-1
    5 CRSIG(I)=TEMPC/AKM
      SRSIG(I)=TEMPS/AKM
      FDSIG(I)=SRSIG(I)
    2 CONTINUE
C     PERFORM MODULATION AND SUM THE TWO CHANNELS ALGEBRIACALLY TO YIELD
C     A BANDPASS SIGNAL
      DO 4 J=1,NN
      CRSIG(J)=CRSIG(J)*CTSIG(J)
      SRSIG(J)=SRSIG(J)*STSIG(J)
    4 CRSIG(J)=CRSIG(J)+SRSIG(J)
C     SHIFT THE SIGNAL BY 90 DEGREES
      ISHIFT=NDIVR/2
      IEND=NN-ISHIFT
      DO 8 I=1,ISHIFT
      J=IEND+I
    8 SRSIG(J)=CRSIG(I)
      IGBN=ISHIFT+1
      DO 6 I=IBGN,NN
      J=I-ISHIFT
    6 SRSIG(J)=CRSIG(I)
      RETURN
      END
$IBFTC BPSQFT  DECK
      SUBROUTINE BPSQFT(SIGIN,CRSIG,SRSIG,NN,NDIVR,ILENIH,PHIC)
```

```
C     THIS SUBROUTINE PERFORMS SQUARING + RETUNING OF A BANDPASS SIGNAL
      DIMENSION SIGIN(NN),CRSIG(NN),SRSIG(NN)
      PI=3.1415926
      DIVR=NDIVR
      DTHETA=PI/DIVR
      DO 1 I=1,NN
    1 CRSIG(I)=SIGIN(I)**2
      ANUM=PHIC/DTHETA
      NUM=ANUM
      K=2*NDIVR
      IF(ANUM.GT.1.0)GO TO 5
      INTL=NDIVR+1
      IFNL=K
      KCT=1
    3 DO 2 I=INTL,IFNL
    2 CRSIG(I)=-CRSIG(I)
      KCT=KCT+1
      IF(KCT.GT.ILENTH)GO TO 4
      INTL=INTL+K
      IFNL=IFNL+K
      GO TO 3
    5 INTL=NDIVR+1-NUM
      IFNL=K-NUM
      KCT=1
      GO TO 3
    4 ISHIFT=NDIVR/2
      IEND=NN-ISHIFT
      DO 8 I=1,ISHIFT
      J=IEND+I
    8 SRSIG(J)=CRSIG(I)
      IBGN=ISHIFT+1
      DO 6 I=IBGN,NN
      J=I-ISHIFT
    6 SRSIG(J)=CRSIG(I)
      RETURN
      END
$IBFTC MIXER   DECK
      SUBROUTINE MIXER(SIGIN,CRSIG,SRSIG,CTSIG,STSIG,NN,PSIG,QSIG,ISAMP,
     1NDIVR,ICYCLE,MN)
C     THIS SUBROUTINE PERFORMS DEMODULATION AT QUADRATURES
C     THE SIGNALS IN ARRAYS PSIG AND QSIG ARE LOW-PASS WAVEFORMS SAMPLED
C     AT A RATE OF ISAMP SAMPLES PER BAUD
C     ALL SIGNALS INPUT TO THE SUBROUTINE ARE PRESERVED
      DIMENSION CRSIG(NN),SRSIG(NN),SIGIN(NN),PSIG(MN),QSIG(MN)
      DIMENSION CTSIG(NN),STSIG(NN)
      DO 1 I=1,NN
      CTSIG(I)=SIGIN(I)*CRSIG(I)
    1 STSIG(I)=SIGIN(I)*SRSIG(I)
      KM=NDIVR*2*ICYCLE
      KN=KM
      MM=NN-KM +1
      DO 2 I=1,NN
      AKM=KM
      TEMPC=0.0
      TEMPS=0.0
      IFNL=I+KM-1
      DO 3 J=I,IFNL
      TEMPC=TEMPC+CTSIG(J)
```

```
    3 TEMPS=TEMPS+STSIG(J)
      IF(I.LT.MM)GO TO 5
      KM=KM-1
    5 CTSIG(I)=TEMPC/AKM
      STSIG(I)=TEMPS/AKM
    2 CONTINUE
      NJ=NN-1
      IRATE=KN/ISAMP
      DO 4 I=1,NJ,IRATE
      J=(I+IRATE-1)/IRATE
      PSIG(J)=CTSIG(I)
    4 QSIG(J)=STSIG(I)
      RETURN
      END
$IBFTC FADE    DECK
      SUBROUTINE FADING(ALPHA,MN,MMRY,STR,SD,PMEAN,VAR,PHI,DPHI,SLOW)
      DIMENSION ALPHA(MN)
      MM=MN-MMRY
      CALL RANGAU(ALPHA,MN,STR,SD)
      DO 12 I=1,MN
      PHI=PHI+DPHI
   12 ALPHA(I)=SQRT(ALPHA(I)**2)
      IF(SLOW.NE.0.0)GO TO 5
      AMRY=MMRY
      DO 1 I=1,MN
      KK=I+MMRY-1
      SUM=0.0
      DO 2 J=I,KK
      SUM=SUM+ALPHA(J)
    2 ALPHA(I)=SUM/AMRY
      IF(I.LT.MM)GO TO 1
      MMRY=MMRY-1
      AMRY=MMRY
    1 CONTINUE
    5 CALL VARCE(ALPHA,MN,PMEAN,VAR,1)
      IF(PMEAN.LT.1.0)GO TO 14
      DCSH=0.0
      GO TO 13
   14 DCSH=1.0-PMEAN
   13 DO 3 I=1,MN
    3 ALPHA(I)=DCSH+ALPHA(I)
      CALL VARCE(ALPHA,MN,PMEAN,VAR,1)
      WRITE(6,95)PMEAN,VAR
   95 FORMAT(1H0,40HMEAN VALUE OF RANDOMLY FADING VARIATES =,E15.8/38HVA
     1RIANCE OF RANDOMLY FADING VARIATES =, E15.8)
      RETURN
      END
$IBFTC INSNR   DECK
      SUBROUTINE INSNR(SIGP,IDMN,INTL,IFNL)
      DIMENSION SIGP(IDMN)
      DATA PMEAN,PSMT,PVAR,PWR,ANSNR/0.0,0.0,0.0,0.0,0.0/
      CALL INVAR(SIGP,IDMN,INTL,IFNL,PMEAN,PSMT,PVAR)
      SSQ=0.0
      ANORM=IFNL-INTL
      DO 1 I=INTL,IFNL
    1 SSQ=SSQ+SIGP(I)**2
      PWR=SSQ/ANORM-PSMT
      ANSNR=10.0*ALOG10(PWR/PVAR)
```

```
      WRITE(6,8)PWR,ANSNR
    8 FORMAT(1H0,37HSIGNAL POWER AT OUTPUT OF ESTIMATOR =,E15.10/1H0,53H
     1SIGNAL-TO-NOISE RATIO AT OUTPUT OF ESTIMATOR IN DBS =,E15.10)
      RETURN
      END
$IBFTC INVAR   DECK
      SUBROUTINE INVAR(SIGP,IDMN,INTL,IFNL,PMEAN,PSMT,PVAR)
      DIMENSION SIGP(IDMN)
      SUM=0.0
      SSQ=0.0
      ANORM=IDMN-IFNL+INTL
      IFNLP=IFNL+1
      DO 1 I=1,INTL
      SUM=SUM+SIGP(I)
    1 SSQ=SSQ+SIGP(I)**2
      DO 2 I=IFNLP,IDMN
      SUM=SUM+SIGP(I)
    2 SSQ=SSQ+SIGP(I)**2
      PMEAN=SUM/ANORM
      PSMT=SSQ/ANORM
      PVAR=PSMT-PMEAN**2
      WRITE(6,9)PMEAN,PVAR
    9 FORMAT(1H0,44HMEAN VALUE OF NOISE AT OUTPUT OF ESTIMAIOR =,E15.10/
     11H0,39HNOISE VARIANCE AT OUTPUT OF ESTIMATOR =,E15.10)
      RETURN
      END
$IBFTC VARCE   DECK
C      SUBROUTINE TO COMPUTE MEAN AND VARIANCE OF RANDOM PROCESSES
C      IF ONLY THE MEAN VALUE IS DESIRED SET ISWCH=0.  FOR ISWCH EQUAL
C      TO ANY OTHER VALUE BOTH MEAN AND VARIANCE WILL BE COMPUTED.
C      ARAY = BUFFER FOR RANDOM PROCESS TO BE ANALYSED
C      ISS = SAMPLE SIZE OF THE RANDOM PROCESS
C      AMEAN = MEAN OF RANDOM PROCESS
C      VAR = VARIANCE OF RANDOM PROCESS
      SUBROUTINE VARCE(ARAY,ISS,AMEAN,VAR,ISWCH)
      DIMENSION ARAY(ISS)
      AMEAN = 0.0
      SMONT = 0.0
      DO 2 I=1,ISS
    2 AMEAN=AMEAN+ARAY(I)
      SS=ISS
      AMEAN=AMEAN/SS
      WRITE(6,10)AMEAN
   10 FORMAT(1H-,28HTHE MEAN VALUE OF THE DATA =,E14.9)
      IF(ISWCH.EQ.0)GO TO 5
      DO 3 I=1,ISS
    3 SMONT = SMONT+ARAY(I)**2
      SMONT = SMONT/SS
      VAR = SMONT - AMEAN**2
      WRITE(6,11)VAR
   11 FORMAT(1H0,26HTHE VARIANCE OF THE DATA =,E14.9)
    5 RETURN
      END
$IBFTC ESTMR   DECK
      SUBROUTINE ESTMR(PSIG,IDMM,SIGP,IDMN,ISAMP,VARN)
      DIMENSION PSIG(IDMM),SIGP(IDMN)
      SAMP=ISAMP
      K=2
```

```
    2 SUM1=0.0
      SQ=0.0
      IFNL=ISAMP+K
      DO 1 I=K,IFNL
      SUM1=SUM1+PSIG(I)
    1 SQ=SQ+PSIG(I)**2
      SUM1=SUM1/SAMP
      COVF=SQ/SAMP-SUM1**2-VARN
      DIFF=PSIG(K)-SIGP(K-1)
      UPDATE=DIFF*COVF/VARN
      SIGP(K)=SUM1+UPDATE
      IF(K.EQ.IDMN) GO TO 3
      GO TO 2
    3 RETURN
      END
$IBFTC QUANTR  DECK
      SUBROUTINE QUANTR(ARRAY,IDMN,PLVL,ANLVL,LBTWO,PMAX,L)
      DIMENSION ARRAY(IDMN),PLVL(LBTWO),ANLVL(LBTWO)
      AN=LBTWO
      IF(L.EQ.0)GO TO 2
      PMAX=0.0
      PMIN=0.0
      DO 1 I=1,IDMN
      PMAX=AMAX1(PMAX,ARRAY(I))
    1 PMIN=AMIN1(PMIN,ARRAY(I))
      IF(ABS(PMAX).GE.ABS(PMIN))GO TO 2
      AINCR=ABS(PMIN)/AN
      GO TO 3
    2 AINCR=ABS(PMAX)/AN
    3 PLVL(1)=AINCR
      ANLVL(1)=-AINCR
      IF(LBTWO.LE.1)GO TO 5
      DO 4 I=2,LBTWO
      PLVL(I)=PLVL(I-1)+AINCR
    4 ANLVL(I)=ANLVL(I-1)-AINCR
    5 DO 6 I=1,IDMN
      IF(ARRAY(I).LE.0.0)GO TO 7
      DO 8 J=1,LBTWO
      DIFF=ARRAY(I)-PLVL(J)
      IF(DIFF.LE.0.0)GO TO 9
    8 CONTINUE
    9 ARRAY(I)=PLVL(J)
      GO TO 6
    7 DO 10 J=1,LBTWO
      DIFF=ARRAY(I)-ANLVL(J)
      IF(DIFF.GE.0.0)GO TO 11
   10 CONTINUE
   11 ARRAY(I)=ANLVL(J)
    6 CONTINUE
      RETURN
      END
$IBFTC RECVR   DECK
      SUBROUTINE RECVR(AVC,AUTOP,AUTOQ,CMSEQ,ISS,ICDLTH,PSIG,QSIG,ISAMP,
     1MM)
C     GENERAL RECEIVER SUBROUTINE
C     AVC = AUTOCOVARIANCE COMBINED OUTPUT (MAGNITUDE ONLY)
C     AUTOP = PCHANNEL AUTOCORRELATION FUNCTION (MAGNITUDE AND SIGN)
C     AUTOQ = QCHANNEL AUTOCORRELATION FUNCTION (MAGNITUDE AND SIGN)
```

```
C   'CMSEQ' = THE REFERENCE SEQUENCE.
C       ISS = SAMPLE SIZE (= 'IQBY2')
C       ICDLTH = CODE LENGTH
C       PSIG = PCHANNEL SIGNAL TO BE CORRELATED
C       QSIG = QCHANNEL SIGNAL TO BE CORRELATED
        DIMENSION AVC(MM ),AUTOP(MM ),AUTOQ(MM ),CMSEQ(ICDLTH),PSIG(ISS),Q
       1SIG(ISS)
        DO 2 K=1,MM
        AUTOP(K) = 0.0
        AUTOQ(K) = 0.0
        JJ=ISAMP*(ICDLTH-1)+K
        DO 2 I=K,JJ,ISAMP
        L = (I+ISAMP-K)/ISAMP
        AUTOP(K)=AUTOP(K)+CMSEQ(L)*PSIG(I)
      2 AUTOQ(K)=AUTOQ(K)+CMSEQ(L)*QSIG(I)
        DO 3 I=1,MM
      3 AVC(I) = SQRT(AUTOP(I) **2 + AUTOQ(I) **2)
        RETURN
        END
$IBFTC FMAX    DECK
C       A SUBROUTINE TO FIND MAXIMUM VALUE AND TO IDENTIFY LOCATION
        SUBROUTINE FMAX(AUTO,IDMM,PEAK,IPOSN)
        DIMENSION AUTO(IDMM)
        PEAK=0.0
        DO 2 I=1,IDMM
      2 PEAK=AMAX1(PEAK,ABS(AUTO(I)))
        DO 3 I=1,IDMM
      3 IF(PEAK.EQ.ABS(AUTO(I)))GO TO 4
      4 IPOSN=I
        WRITE(6,16)PEAK,IPOSN
     16 FORMAT(1H0,6HPEAK =,F10.4,/1H0,10HLOCATION =,I4)
        RETURN
        END
$IBFTC SNR     DECK
        SUBROUTINE SNR(AUTO,MM,SNR1,SNR2,PEAK,IPOSN,VAR,SW,NNT,ICNTL,ISIDE
       1,IFLAG)
C       SUBROUTINE TO COMPUTE SIGNAL-TO-NOISE RATIO
C       AUTO = AUTOCORRELATION FUNCTION, MM = SIZE OF AUTOCORRELATION
C       FUNCTION (=ISS-ICDLTH)  SNR1 = PEAK SIGNAL-TO-SIDELOBE
C       RATIO IN DB  SNR2 = PEAK SIGNAL POWER-TO-AVERAGE NOISE
C       POWER RATIO IN DB   VAR = VARIANCE OF COMPRESSED
C       WAVEFORM, EXCLUDING THE PEAK  NNT = INTERVAL ON
C       EITHER SIDE OF CENTRAL PEAK IN THE AUTOCORRELATION
C       FUNCTION FOR WHICH THE VARIANCE OF CORRELATION NOISE
C       IS TO BE COMPUTED.
C       ISIDE = NO. OF SAMPLE ON EITHER SIDE OF CENTRAL PEAK THAT ARE
C       EXCLUDED FOR PURPOSE OF OUTPUT MEAN SQUARE NOISE CALCULATION.
C       ICNTL = DISTANCE AWAY FROM CENTRAL PEAK AT WHICH SEARCH FOR
C       MAXIMUM OFF-CENTRE PEAK STARTS.
C       IPOSN = LOCATION OF CENTRAL PEAK RELATIVE TO THE 1ST SAMPLE OF THE
C       'AUTO' ARRAY
C       SW = SWITCH TO SIGNIFY WHETHER PEAK-TO-SIDELOBE RATIO IS
C       DESIRED.
C       SW = 0 SIGNIFIES THAT PEAK-TO-SIDELOBE RATIO IS NOT
C       DESIRED  ANYTHING ELSE WOULD INDICATE A YES ANSWER
        DIMENSION AUTO(MM)
        IF (SW.EQ.0.0) GO TO 8
        IF(IPOSN.LE.NNT)GO TO 6
```

```
      NN = IPOSN-NNT
      GO TO 4
    6 NN = 1
    4 NM = IPOSN+NNT
      IF(NM.GT.MM) NM = MM
      ILEAD = IPOSN-ICNTL
      IF(ILEAD.LE.0)GO TO 21
      SMAX = 0.0
      DO 5 I=NN,ILEAD
    5 SMAX = AMAX1(SMAX,ABS(AUTO(I)))
      ITRAIL = IPOSN+ICNTL
      IF(ITRAIL.GE.NM)GO TO 21
      DO 7 I=ITRAIL,NM
    7 SMAX = AMAX1(SMAX,ABS(AUTO(I)))
      WRITE(6,30)SMAX
   30 FORMAT(1H-,18HMAXIMUM SIDELOBE =,E15.8)
      SNR1=10.0*ALOG10((PEAK/SMAX)**2)
      WRITE(6,28)SNR1
   28 FORMAT(1H ,31HPEAK-TO-SIDELOBE RATIO IN DBS =,E15.8)
    8 SUM = 0.0
      SSQRT = 0.0
      ILEAD = IPOSN-ISIDE
      IF(ILEAD.LE.0)GO TO 21
      ITRAIL = IPOSN+ISIDE
      IF(IPOSN.GT.NNT)GO TO 9
      K = 1
      NM = IPOSN+NNT
      IF(NM.GT.MM)NM=MM
      IF(ITRAIL.GE.NM)GO TO 21
      IRANGE = NM-(2*ISIDE-1)
      GO TO 11
    9 K = IPOSN - NNT
      NM = IPOSN + NNT
      IF(NM.GT.MM)NM=MM
      IRANGE = NM-K-2*(ISIDE-1)
   11 DO 10 I=K,ILEAD
      SUM=SUM+AUTO(I)
   10 SSQRT = SSQRT+AUTO(I)**2
      DO 12 I=ITRAIL,NM
      SUM = SUM+AUTO(I)
   12 SSQRT = SSQRT+AUTO(I)**2
      RANGE = IRANGE
      SUM = SUM/RANGE
      SSQRT = SSQRT/RANGE
      SQRTM = SUM**2
      VAR = SSQRT - SQRTM
      WRITE(6,27)VAR
   27 FORMAT(1H0,22HOUTPUT NOISE VARIANCE=,E15.8)
      SNR2 = 10.0*ALOG10(PEAK**2/VAR)
      WRITE(6,29)SNR2
   29 FORMAT(1H ,59HPEAK SIGNAL POWER-TO-MEAN SQUARE NOISE POWER RATIO I
     1N DBS =,E15.8)
   23 RETURN
   21 IFLAG=1
      WRITE(6,22)
   22 FORMAT(1H0,57H*****INVALID TARGET LOCATION, FALSE ALARM DECLARED B
     1Y SNR)
      GO TO 23
```

```
      END
$IBFTC PROBAN  DECK
      SUBROUTINE PROBAN(OUTP,MM,THOLD,PEAK,FARATE,IOBNT,IPOSN)
C     SUBROUTINE TO COMPUTE FALSE ALARM RATE
C     OUTP = COMPRESSED WAVEFORM, MM = DIMENSION OF COMPRESSED
C     WAVEFORM
C     THOLD = THRESHOLD, A PRIOR KNOWLEDGE OF EXPECTED PEAK VALUE
C     OF CORRELATION FUNCTION ASSUMED. PEAK = MAXIMUM VALUE
C     OF COMPRESSED WAVEFORM. FARATE = FALSE ALARM RATE ON
C     A THOUSAND BASIS.
C  IPOSN = THE POSITION IN ARRAY OUTP WHERE THE PEAK OCCURS.
C     IOBNT=OBSERVATION INTERVAL ON EITHER SIDE OF THE CENTRAL PEAK
C     OUTSIDE OF WHICH FALSE ALARMS ARE SEARCHED FOR.
      DIMENSION OUTP(MM)
      ILEAD=IPOSN-IOBNT
      ITRAIL=IPOSN+IOBNT
      FALSE = 0.0
    1 IF( PEAK.LE.THOLD) GO TO    4
      DO 3 I=1,ILEAD
      IF(ABS(OUTP(I)).LE.THOLD)GO TO 3
      FALSE = FALSE + 1.0
    3 CONTINUE
      DO 5 I=ITRAIL,MM
      IF(ABS(OUTP(I)).LE.THOLD)GO TO 5
      FALSE=FALSE+1.0
    5 CONTINUE
      AMM=MM-2*IOBNT
      FARATE = (FALSE/AMM)*1000.0
      WRITE(6,17)THOLD,FARATE
   17 FORMAT(1H-,11HTHRESHOLD =,F8.4,/1H ,28HFALSE ALARM RATE IN 1000TH
     1=,E15.5)
      RETURN
    4 WRITE(6,9)
      CALL EXIT
    9 FORMAT(1H0,53HPEAK VALUE IS SMALLER THAN THRESHOLD, EXIT IS CALLED
     1.)
      END
$IBFTC MULTGT  DECK
      SUBROUTINE MULTGT(PFMEM,QFMEM,PSIG,QSIG,NN,MI,IDLAY,TGT)
      DIMENSION PFMEM(MI),QFMEM(MI),PSIG(NN),QSIG(NN)
      DO 3 I=1,NN
      J=IDLAY+I
      PFMEM(J)=PFMEM(J)+PSIG(I)*TGT
    3 QFMEM(J)=QFMEM(J)+QSIG(I)*TGT
      RETURN
      END
$IBFTC MNOISE  DECK
      SUBROUTINE MNOISE(ALPHA,PCHAN,QCHAN,MN,STR,SD,PMEAN,QMEAN,VARP,VAR
     1Q,IFIRST,THETA,TGT)
      DIMENSION ALPHA(MN),PCHAN(MN),QCHAN(MN)
      AMEAN=0.0
      AVAR=0.0
      IF(IFIRST.NE.1)GO TO 13
      CALL RANGAU(ALPHA,MN,STR,SD)
      DO 12 I=1,MN
   12 ALPHA(I)=ALPHA(I)**2
      CALL VARCE(ALPHA,MN,AMEAN,AVAR,1)
      DCSH=1.0-AMEAN
```

```
      IF(AMEAN.GE.1.0)GO TO 13
      DO 4 I=1,MN
    4 ALPHA(I)=DCSH+ALPHA(I)
   13 PFACE=COS(THETA)*TGT
      QFACE=SIN(THETA)*TGT
      DO 3 I=1,MN
      PCHAN(I)=ALPHA(I)*PFACE
    3 QCHAN(I)=ALPHA(I)*QFACE
      WRITE(6,95)
   95 FORMAT(1H0,27HPCHANNEL M-NOISE STATISTICS)
      CALL VARCE(PCHAN,MN,PMEAN,VARP,1)
      WRITE(6,94)
   94 FORMAT(1H0,27HQCHANNEL M-NOISE STATISTICS)
      CALL VARCE(QCHAN,MN,QMEAN,VARQ,1)
      RETURN
      END
$IBFTC CGRAPH  DECK
C       IF DIVISION MARKS ARE REQUIRED PUT NDIV = 0
      SUBROUTINE CGRAPH(NN,Y,X,XDISP,YDISP,XINCH,YINCH,NDIV)
      DIMENSION Y(NN),X(NN)
      X(1)=0.0
      DO 1 I=2,NN
    1 X(I)=X(I-1)+1.0
      YMAX=Y(1)
      YMIN=Y(1)
      DO 2 I=2,NN
      YMAX=AMAX1(YMAX,Y(I))
    2 YMIN=AMIN1(YMIN,Y(I))
      YINCR=(YMAX-YMIN)/((YINCH-0.5)/0.25)
      XINCR=(X(NN)-X(1))/((XINCH-0.5)/0.25)
      CALL PLOT(XDISP,YDISP,-3)
      CALL GRAFF(NN,X,Y,XINCR,YINCR,XINCH,YINCH,NDIV)
      RETURN
      END
$IBFTC GRAPH   DECK
      SUBROUTINE GRAPH(NN,X,Y,XINCR,YINCR,XINCH,YINCH,NDIV)
      DIMENSION X(NN),Y(NN)
      LOGICAL XAXIS,YAXIS
      XP=0.0
      YP=0.0
      XMARG=0.5
      YMARG=0.5
      XMAX=0.0
      YMAX=0.0
      XMIN=0.0
      YMIN=0.0
      XAXIS=.TRUE.
      YAXIS=.TRUE.
      ALMT=(XINCH-XMARG)/0.005+1.0
      LMT=ALMT
      IF(NN.GT.LMT)NN=LMT
C     INITIALIZE PLOT
      CALL FACTOR(NN,X,Y,XINCH,YINCH,XMARG,YMARG)
C     DETERMINE MAX. AND MIN. VALUES OF X AND Y
      DO 1 I=1,NN
      XMAX=AMAX1(XMAX,X(I))
      YMAX=AMAX1(YMAX,Y(I))
      XMIN=AMIN1(XMIN,X(I))
```

```
    1 YMIN=AMIN1(YMIN,Y(I))
      WRITE(6,70)YMAX,YMIN,XMAX,XMIN
   70 FORMAT(1H0,6HYMAX =,E15.10,3X,6HYMIN =,E15.10,3X,6HXMAX =,E15.10,3
     1X,6HXMIN =,E15.10)
      YSCALE=(YMAX-YMIN)/(YINCH-YMARG)
      XSCALE=(XMAX-XMIN)/(XINCH-XMARG)
      WRITE(6,71)YSCALE,XSCALE
   71 FORMAT(1H0,8HYSCALE =,E12.6,19HDATA UNITS PER INCH/1H0,8HXSCALE =,
     1E12.6,19HDATA UNITS PER INCH)
      IF(XMAX.LT.0.0.OR.XMIN.GT.0.0)XAXIS=.FALSE.
      IF(YMAX.LT.0.0.OR.YMIN.GT.0.0)YAXIS=.FALSE.
      IF(.NOT.YAXIS)GO TO 20
      CALL PLTLN(0.0,YMIN,0.0,YMAX)
   20 IF(.NOT.XAXIS)GO TO 21
      CALL PLTLN(X(1),0.0,X(NN),0.0)
   21 IF(NDIV.NE.0)GO TO 23
      IF(XINCR.EQ.0.0.OR.YINCR.EQ.0.0)GO TO 23
      AM=(YMAX-YMIN)/YINCR+1.0
      M=AM
      IF(M.GT.201)GO TO 53
      IF(YMAX.LT.0.0.OR.YMIN.GT.0.0)GO TO 22
      AMP=YMAX/YINCR
      MP=AMP
      AMN=ABS(YMIN)/YINCR
      MN=AMN
      IF(MP.LT.1)GO TO 101
      YIN=YINCR
      DO 2 I=1,MP
      CALL UNITTO(0.0,YIN,XP,YP)
      CALL PLOT(XP-0.05,YP,3)
      CALL PLOT(XP+0.05,YP,2)
    2 YIN=YIN+YINCR
  101 IF(MN.LT.1)GO TO 51
      YIN=-YINCR
      DO 22 I=1,MN
      CALL UNITTO(0.0,YIN,XP,YP)
      CALL PLOT(XP-0.05,YP,3)
      CALL PLOT(XP+0.05,YP,2)
   22 YIN=YIN-YINCR
   51 AN=(X(NN)-X(1))/XINCR+1.0
      N=AN
      IF(N.GT.201)GO TO 24
      IF(XMAX.LT.0.0.OR.XMIN.GT.0.0)GO TO 23
      AMP=X(NN)/XINCR
      MP=AMP
      AMN=ABS(X(1))/XINCR
      MN=AMN
      IF(MP.LT.1)GO TO 102
      XIN=XINCR
      DO 3 I=1,MP
      CALL UNITTO(XIN,0.0,XP,YP)
      CALL PLOT(XP ,YP-0.05,3)
      CALL PLOT(XP ,YP+0.05,2)
    3 XIN=XIN+XINCR
  102 IF(MN.LT.1)GO TO 23
      XIN=-XINCR
      DO 33 I=1,MN
      CALL UNITTO(XIN,0.0,XP,YP)
```

```
      CALL PLOT(XP ,YP-0.05,3)
      CALL PLOT(XP ,YP+0.05,2)
   33 XIN=XIN-XINCR
   23 CALL UNITTO(X(1),Y(1),XP,YP)
      CALL PLOT(XP,YP,3)
      DO 6 I=2,NN
      CALL UNITTO(X(I),Y(I),XP,YP)
      CALL PLOT(XP,YP,2)
    6 CONTINUE
      RETURN
   53 WRITE(6,52)
   52 FORMAT(1H0,70HCALLS FOR MORE THAN 200 DIVISIONS,Y-AXIS DIVISION MA
     1RKS ARE SUPPRESSED)
      GO TO 51
   24 WRITE(6,25)
   25 FORMAT(1H0,70HCALLS FOR MORE THAN 200 DIVISIONS,X-AXIS DIVISION MA
     1RKS ARE SUPPRESSED)
      GO TO 23
      END
```

CD TOT 0890

```
$JOB            003506 JWMARK
$PAUSE          PLEASE MOUNT 300 FT MINI REEL ON TC2 FOR B-L PLOTTER
$IBJOB
$IBFTC ADAPT2  NODECK
C      A SELF-SYNCHRONYZED ADAPTIVE SYSTEM FOR THE DETECTION OF MULTIPLE
C      TARGETS IN A RANDOMLY FADING ENVIRONMENT
       DIMENSION SHRG(4),ATAPS(3),TAPS(4),SIG1(15),SIG2(7),BUFF1(15),BUFF
      12(105),BUFF3(105),BUFF4(75)
       DIMENSION X(366)
       DIMENSION AVC1(366),AUTOP1(366),AUTOQ1(366),PSIG(540),QSIG(540)
       DIMENSION PFMEM(291),QFMEM(291),IDLY(6),TGTST(6),TGTPH(6),PMN(6),
      1QMN(6),VRP(6),VRQ(6)
       DIMENSION PCHAN(75),QCHAN(75),ALPHA(75)
       DATA TAPS/0.0,0.0,1.0,1.0/
       DATA ATAPS/1.0,0.0,1.0/
       DATA FCTR,ISAMP/1.0,5/
       DATA STA,STQ,STD/0.0,0.0,0.751/
       DATA ISWCH,JSWCH/0,1/
       DATA ICDLTH,MCDLTH,LL,ML/1,15,3,4/
       NN=MCDLTH*ICDLTH
       MN=ISAMP*NN
       CALL CCGEN(SIG1,SIG2,MCDLTH,ICDLTH,BUFF1,BUFF2,NN,ISWCH,JSWCH,BUFF
      14,MN,FCTR,TAPS,ML,ATAPS,LL,SHRG,ISAMP)
       DATA STR,SD/0.0,0.001/
       DATA PMEAN,QMEAN,VARP,VARQ/0.0,0.0,0.0,0.0/
       DATA ANOP,ANOQ,PVAR,QVAR/0.0,0.0,0.0,0.0/
       DATA AMEAN,AVAR/0.0,0.0/
       DATA IASPCT/180/
       DATA MTGT,IDLY/6,0,54,84,92,142,180/
       DATA TGTST/0.54,0.70,0.57,1.00,0.48,0.61/
       DATA TGTPH/1.0,1.0,1.0,1.0,1.0,1.0/
       CALL LETTER(10,5,90,0.0,1.0,10HJ. W. MARK)
       CALL PLOT(3.0,0.0,-3)
       MDLAY=IDLY(MTGT)
       MI=MN+MDLAY
       DSTD=0.25
       DO 301 JKM=1,4
       DO 41 II=1,MTGT
       THETA=TGTPH(II)
       IDLAY=IDLY(II)
       TGT=TGTST(II)
       WRITE(6,98)II
    98 FORMAT(1H0,42HTHE FOLLOWING ARE STATISTICS OF TARGET NO.,I3)
       CALL MNOISE(ALPHA,PCHAN,QCHAN,MN,STR,SD,PMEAN,QMEAN,VARP,VARQ,II,T
      1HETA,TGT)
       WRITE(6,109)II,TGT,THETA,IDLAY
   109 FORMAT(1H0,10HTARGET NO.,I3/1H0,17HTARGET STRENGTH =,F10.5/1H0,25H
      1TARGET PHASE IN RADIANS =,F10.5/1H0,65HDIFFERENTIAL TARGET DELAY W
      2.R.T. FIRST TARGET IN NO. OF SAMPLES =,I4)
       PMN(II)=PMEAN
       QMN(II)=QMEAN
       VRP(II)=VARP
       VRQ(II)=VARQ
       DO 40 JN=1,MN
       PCHAN(JN)=PCHAN(JN)*BUFF4(JN)
    40 QCHAN(JN)=QCHAN(JN)*BUFF4(JN)
       CALL MULTGT(PFMEM,QFMEM,PCHAN,QCHAN,MN,MI,IDLAY,1.0)
    41 CONTINUE
       INTL=MN
```

```
      IFNL=2*MN-1+MDLAY
      IDMM=3*MN+MDLAY
      IDMN=IDMM-ISAMP
      CALL RANGAU(PSIG,IDMM,STA,STD)
      CALL RANGAU(QSIG,IDMM,STQ,STD)
      CALL VARCE(PSIG,IDMM,ANOP,PVAR,1)
      CALL VARCE(QSIG,IDMM,ANOQ,QVAR,1)
      DO 42 JM=1,MTGT
      WRITE(6,98)JM
      PNSNR=10.0*ALOG10(PMN(JM)**2/(VRP(JM)+PVAR))
      QNSNR=10.0*ALOG10(QMN(JM)**2/(VRQ(JM)+QVAR))
      WRITE(6,10)PNSNR,QNSNR
   10 FORMAT(1H0,21HPCHANNEL SIR IN DBS =,E15.10/1H0,21HQCHANNEL SIR IN
     1DBS =,E15.10)
      CNSNR=10.0*ALOG10(PMN(JM)**2/(VRP(JM)+PVAR)+QMN(JM)**2/(VRQ(JM)+QV
     1AR))
      WRITE(6,21)CNSNR
   21 FORMAT(1H0,21HCOMBINED SIR IN DBS =,E15.10)
      PSNR=10.0*ALOG10(PMN(JM)**2/PVAR)
      QSNR=10.0*ALOG10(QMN(JM)**2/QVAR)
      CSNR=10.0*ALOG10(PMN(JM)**2/PVAR+QMN(JM)**2/QVAR)
      WRITE(6,9)PSNR,QSNR,CSNR
    9 FORMAT(1H0,21HPCHANNEL SNR IN DBS =,E15.10/1H0,21HQCHANNEL SNR IN
     1DBS =,E15.10/1H0,21HCOMBINED SNR IN DBS =,E15.10)
      PMTAN=10.0*ALOG10(VRP(JM)/PVAR)
      QMTAN=10.0*ALOG10(VRQ(JM)/QVAR)
      WRITE(6,11)PMTAN,QMTAN
   11 FORMAT(1H0,62HPCHANNEL MULTIPLICATIVE NOISE TO ADDITIVE NOISE RATI
     1O IN DBS =,E10.6/1H0,62HQCHANNEL MULTIPLICATIVE NOISE TO ADDITIVE
     2NOISE RATIO IN DBS =,E10.6)
   42 CONTINUE
      DO 8 I=INTL,IFNL
      J=I-INTL+1
      QSIG(I)=QSIG(I)+QFMEM(J)
    8 PSIG(I)=PSIG(I)+PFMEM(J)
      MM=2*MN+MDLAY
      WRITE(6,108)IASPCT
  108 FORMAT(1H-,I4,15H  DEGREE ASPECT)
      DATA PEAK,IPOSN,TRNG,SNR1,SNR2,VAR,SW,NNT,ICNTL,ISIDE/0.0,0,0.0,0.
     10,0.0,0.0,1.0,87,30,30/
      CALL RECVR(AVC1,AUTOP1,AUTOQ1,BUFF1,IDMM,NN,PSIG,QSIG,ISAMP,MM)
      XDISP=0.0
      YDISP=0.0
      XINCH=3.0
      YINCH=2.0
      CALL CGRAPH(MM,AVC1,X,XDISP,YDISP,XINCH,YINCH,1)
      YDISP=2.5
      CALL CGRAPH(MM,AUTOQ1,X,XDISP,YDISP,XINCH,YINCH,1)
      CALL CGRAPH(MM,AUTOP1,X,XDISP,YDISP,XINCH,YINCH,1)
      CALL PLOT(9.0,-5.0,-3)
      STD=STD-DSTD
  301 CONTINUE
      CALL PLOT(0.0,0.0,999)
      STOP
      END
```

CD TOT 0114

## REFERENCES


1. Woodward, P. M.

   "Probability and Information Theory with Applications to Radar"

   McGraw-Hill, New York, 1953.

2. Turin, L.

   "Communication Through Noisy, Random-Multipath Channels"

   1956 IRE Convention Record, Pt. 4, PP. 154-166.

3. Stewart, J. L., and Westerfield, E. C.

   "Theory of Active Sonar Detection"

   Proc. IRE, Vol. 47, PP. 872-881, May 1959.

4. Rice, S. O.

   "Mathematical Analysis of Random Noise"

   Bell System Technical Journal, 24:46 (1945), Section 3. 10.

5. Davenport, W. B., and W. L. Root

   "An Introduction to the Theory of Random Signals and Noise"

   McGraw-Hill, 1958.

6. Helstrom, Carl W.

   "Statistical Theory of Signal Detection"

   Pergamon Press, 1960.

7. Middleton, David

"An Introduction to Statistical Communication Theory"

McGraw-Hill, 1960.

8. Schwartz, M.

"Abstract Vector Spaces Applied to Problems in Detection and Estimation Theory"

IEEE Trans. On Information Theory - July 1966, Vol. IT-12, PP. 327-336.

9. Van Trees, H. L.

"Analog Communication Over Randomly-Time-Varying Channels"

IEEE Trans. On Information Theory, Jan. 1966, Vol. IT-12, PP. 51-63.

10. Wozencraft, J. M., and I. M. Jacobs

"Principles of Communication Engineering"

Wiley, 1965.

11. Mark, J. W., and G. J. G. Hicks

"On the Detection of A Coded Signal in A Gaussian Environment"

Presented at the IEEE 4th Canadian Symposium on Communications, Montreal, Canada, October 13, 1966. (Canadian Westinghouse)

12. Peterson, W. W.

"Error Correcting Codes"

MIT Press, Wiley, 1961.

13. Titsworth, R. C.

"Correlation Properties of Cyclic Sequences"

Technical Report No. 32-388, JPL, 1963.

14. Mark, J. W.

"Signal Coding with Binary Sequences"

Canadian Westinghouse Company Technical Note No. 3444, June 1966.

15. Mark, J. W.

"Optimal Adaptive Filtering for Sampled Systems with Random and Deterministic Excitations"

Canadian Westinghouse Company Technical Note No. 3476, May 1967.

16. Mark, J. W. and G. J. G. Hicks

"A Generalized Computer Program for Data Reduction"

Canadian Westinghouse Company Technical Note No. 3481, June 1967.